

11-2016

Study of Surface Tension, Natural Evaporation, and Subcooled Boiling Evaporation of Aqueous Surfactant Solutions

Matthew John Lehman

Follow this and additional works at: <https://commons.erau.edu/edt>



Part of the [Aerospace Engineering Commons](#)

Scholarly Commons Citation

Lehman, Matthew John, "Study of Surface Tension, Natural Evaporation, and Subcooled Boiling Evaporation of Aqueous Surfactant Solutions" (2016). *Dissertations and Theses*. 305.
<https://commons.erau.edu/edt/305>

This Thesis - Open Access is brought to you for free and open access by Scholarly Commons. It has been accepted for inclusion in Dissertations and Theses by an authorized administrator of Scholarly Commons. For more information, please contact commons@erau.edu.

STUDY OF SURFACE TENSION, NATURAL EVAPORATION,
AND SUBCOOLED BOILING EVAPORATION
OF AQUEOUS SURFACTANT SOLUTIONS

A Thesis

Submitted to the Faculty

of

Embry-Riddle Aeronautical University

by

Matthew John Lehman

In Partial Fulfillment of the

Requirements for the Degree

of

Master of Science in Aerospace Engineering

November 2016

Embry-Riddle Aeronautical University

Daytona Beach, Florida

STUDY OF SURFACE TENSION, NATURAL EVAPORATION,
AND SUBCOOLED BOILING EVAPORATION
OF AQUEOUS SURFACTANTS SOLUTIONS

by

Matthew John Lehman

A Thesis prepared under the direction of the candidate's committee chairman, Dr. Birce Dikici, Department of Mechanical Engineering, and has been approved by the members of the thesis committee. It was submitted to the School of Graduate Studies and Research and was accepted in partial fulfillment of the requirements for the degree of Master of Science in Aerospace Engineering.

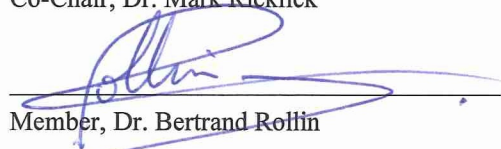
THESIS COMMITTEE



Chair, Dr. Birce Dikici



Co-Chair, Dr. Mark Ricklick



Member, Dr. Bertrand Rollin



Graduate Program Coordinator, Dr. Magdy Attia

11.22.2016

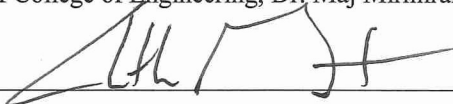
Date



Dean of College of Engineering, Dr. Maj Mirmirani

11/28/16

Date



Vice Chancellor, Academic Support, Dr. Christopher Grant

11/29/16

Date

Acknowledgements

Thank you to all who supported this endeavor! A debt of gratitude is owed to my thesis advisor, Dr. Birce Dikici, for her guidance and support in the research and writing of this thesis. Thank you to my co-advisor, Dr. Mark Ricklick, for his advice concerning the thesis work and write up. Thanks to Dr. Bertrand Rollin for his feedback on experimental procedure. Thank you to all who assisted in the laboratory work including Qayyum Mazumder and Remelisa Esteves who helped with the surface tension measurements. Finally, I would like to express my gratitude to my parents for their encouragement and support through both undergraduate and graduate studies.

Abstract

Researcher: Matthew John Lehman
Title: Study of Surface Tension, Natural Evaporation, and Subcooled Boiling Evaporation of Aqueous Surfactant Solutions
Institution: Embry-Riddle Aeronautical University
Degree: Master of Science in Aerospace Engineering
Year: 2016

The relation between surface tension and surfactant concentration and its effect on solution evaporation under natural convection and subcooled pool boiling is examined through experimental methods. Aqueous solutions of sodium lauryl sulfate (SLS), ECOSURF™ EH-14, and ECOSURF™ SA-9 are used in this study. SLS is an anionic surfactant while EH-14 and SA-9 are environmentally-friendly nonionic surfactants.

Surfactants, surface active agents, are known to affect evaporation performance of solutions and are studied in relation to water loss prevention and heat dissipation. Surfactants could be useful under drought conditions which present challenges to water management on a yearly basis in arid areas of the world. Recent water scarcity in the greater Los Angeles area, south eastern Africa nations, eastern Australia and eastern Mediterranean countries has highlighted the cost of water loss by evaporation. Surfactants are studied as a potential effective method of suppressing evaporation in water reservoirs and lowering associated human suffering and costs. Surfactants are also studied as performance enhancers for the working fluid of heat dissipation devices, such as pulsating heat pipes used for electronics cooling. Some surfactants have been shown to lower thermal resistances and friction pressure in such devices and thereby increase their efficiency.

The static surface tensions of the aqueous-surfactant solutions are measured by Wilhelmy plate method. The surfactants are shown to lower surface tension significantly from pure water. The surface tension values found at the Critical Micelle Concentration are 33.8 mN/m for SLS, 30.3 mN/m for EH-14, and 30.0 mN/m for SA-9. All three surfactants reduced natural convection water loss over 5 days with SLS showing the greatest effect on evaporation rates. The maximum evaporation reduction by each surfactant from distilled water with no surfactants after 5 days is 26.1% for SLS, 20.8% for EH-14, and 18.4% for SA-9. Surfactant caused less than 15% change in total mass evaporation during solution boiling and caused either increase or decrease in mass evaporation depending on surfactant and its concentration.

Table of Contents

Acknowledgements.....	iii
Abstract.....	iv
Table of Contents.....	vi
List of Tables.....	ix
List of Figures.....	x
Symbols.....	xiii
Abbreviations.....	xvi
Nomenclature.....	xvii
Chapter 1.....	1
Introduction.....	1
1.1 Introduction to Surfactants and Surface Tension.....	1
1.1.1 Surfactants.....	1
1.1.2 Surface Tension.....	6
1.1.3 Measuring Surface Tension.....	8
1.2 Natural Evaporation Suppression.....	12
1.2.1 Significance of Evaporation Suppression.....	12
1.2.2 Surfactant Monolayers and Natural Evaporation.....	15
1.2.3 Health Effects of Surfactants.....	20
1.2.4 Theory of Monolayers.....	21
1.2.5 Calculating Natural Evaporation Mass Transfer.....	23
1.3 Evaporation at Boiling.....	26
1.3.1 Surfactants and Boiling.....	26
1.3.2 Previous Studies on Current Surfactants.....	29
1.3.3 Calculating Boiling Mass Transfer.....	33
1.4 Summary.....	33
1.5 Hypothesis.....	34
1.6 Significance of the Study.....	35
1.7 Statement of the Problem.....	35
1.8 Purpose Statement.....	36
1.9 Delimitations.....	36
1.10 Limitations and Assumptions.....	36
Chapter 2.....	37
Methodology.....	37

2.1 Surfactant Solution Preparation	37
2.2 Surface Tension Measurement.....	38
2.3 Natural Evaporation Tests.....	40
2.4 Subcooled Boiling Evaporation Tests.....	41
2.5 Surfactants Analyzed	42
2.6 Equipment	43
2.7 Treatment of the Data	47
2.7.1 Normalizing Natural Evaporation Measurements	47
2.7.2 Repeatability Testing	48
2.7.3 Hypothesis Testing.....	50
Chapter 3.....	51
Results and Discussions	51
3.1 Surface Tension Measurements	51
3.1.1 Sodium Lauryl Sulfate	53
3.1.2 ECOSURF™ EH-14.....	54
3.1.3 ECOSURF™ SA-9	54
3.1.4 Discussion of Surface Tension Measurements	54
3.1.5 Comparison of SLS Measurements to Literature Data	55
3.2 Natural Evaporation Measurements.....	56
3.2.1 Sodium Lauryl Sulfate	56
3.2.2 ECOSURF™ EH-14.....	64
3.2.3 ECOSURF™ SA-9	70
3.2.4 Further Discussion of Natural Evaporation Results.....	76
3.3 Subcooled Boiling Evaporation Measurements.....	78
3.3.1 Sodium Lauryl Sulfate	78
3.3.2 ECOSURF™ EH-14.....	79
3.3.3 ECOSURF™ SA-9	80
3.3.4 Further Discussion of Subcooled Boiling Evaporation Results.....	81
Chapter 4.....	83
Conclusions and Recommendations	83
4.1 Conclusions.....	83
4.1.1 Surface Tension Suppression.....	83
4.1.2 Natural Evaporation Suppression	83
4.1.3 Subcooled Boiling Evaporation Suppression.....	84

4.2 Recommendations.....	85
4.2.1 Natural Evaporation Further Studies	86
4.2.2 Subcooled Boiling Evaporation Further Studies.....	86
References.....	87
Appendix A.....	91
Appendix B.....	97
Appendix C.....	99

List of Tables

Table.....	Page
Table 2.1 Solutions tested in natural evaporation.	40
Table 2.2 Solutions tested in boiling evaporation tests.....	42
Table 2.3 Information on surfactants used in current study (Dikici & Al-Sukaini, 2016; Dow, 2013; Dow, 2012; Frey Scientific, 2014).....	43

List of Figures

Figure	Page
Figure 1.1 Molecular structure representation for nonionic, anionic, cationic, and amphoteric surfactants (Salager, 2002).....	2
Figure 1.2 Surfactant concentration increasing from low to above CMC (Kyowa, 2015).	3
Figure 1.3 Micelle orientation and potential structure forms (Rosen, 2004).....	4
Figure 1.4 Solution properties in relation to CMC (Schramm et al., 2003).	5
Figure 1.5 Imbalance of molecular forces at surface (Kyowa, 2015).....	6
Figure 1.6 Schematic of Pendant Drop Method and important dimensions (Kyowa, 2015).	9
Figure 1.7 Schematic of Du Nouy ring measurement (Kyowa, 2015).	10
Figure 1.8 Wilhelmy plate method technique (L.G., 1999).....	10
Figure 1.9 Schematic of Wilhelmy plate measurement (Kyowa, 2015).....	11
Figure 1.10 Precipitation data for California in 2016 up to June 24 (Seager et al., 2015).	13
Figure 1.11 Rainy season rainfall deficiencies in southern Africa (Di Liberto, 2016).....	14
Figure 1.12 Rainfall deficiencies in Australia from 2012-2016 (Australian Bureau of Meteorology 2016).....	14
Figure 1.13 Sandia National Laboratories test results and testing pools (Hightower & Brown, 2004).	18
Figure 1.14 Boiling at heat flux 30.38 kW/m^2 no SLS and with SLS (Dikici & Al-Sukaini, 2016).....	28
Figure 1.15 Shift of boiling curves with increasing SLS (Wasekar & Manglik, 2000). ..	30
Figure 1.16 Boiling curves for aqueous solution: SLS (Dikici & Al-Sukaini, 2016).....	31
Figure 1.17 Boiling curves for aqueous solution: EH-14 (Dikici & Al-Sukaini, 2016)...	32
Figure 1.18 Boiling curves for aqueous solution: SA-9 (Dikici & Al-Sukaini, 2016).	32
Figure 2.1 Stirring of solution with rotating magnet.	38
Figure 2.2 Wilhelmy plate surface tension measurement method used (L.G., 1999).....	39
Figure 2.3 Solutions covered with muslin gauze for natural evaporation test.....	41
Figure 2.4 Boiling evaporation test setup.	42
Figure 2.5 A&D GF-300 Digital Scale Balance.	44

Figure 2.6 Benchmark Scientific H4000-HS Hotplate and Stirrer.	44
Figure 2.7 Automatic surface tensiometer used in surface tension measurements.....	45
Figure 2.8 Transformer used to convert wall outlet voltage to the required voltage.....	46
Figure 2.9 Omega 4-Channel Portable Thermometer/ Data Logger used in study.	46
Figure 2.10 CASIO Exilim EX-FH20 camera used in study.....	47
Figure 2.11 Laboratory environment effects on evaporation test results.....	49
Figure 3.1 Surface tension measurements of aqueous SLS solutions.....	52
Figure 3.2 Surface tension measurements of aqueous EH-14 solutions.....	52
Figure 3.3 Surface tension measurements of aqueous SA-9 solutions.	53
Figure 3.4 Surface tension measurements SLS aqueous solutions found in literature.	55
Figure 3.5 Natural evaporation losses for 0, 500, 1000, 1500, 2000, 2500 PPM SLS.	57
Figure 3.6 Natural evaporation losses for 3000 and 3500 PPM SLS.	58
Figure 3.7 Average mass loss measurements over all SLS natural evaporation tests.	59
Figure 3.8 Normalized natural evaporation for 500 to 3000 PPM SLS.....	60
Figure 3.9 Normalized natural evaporation for 3500 PPM SLS.....	61
Figure 3.10 Natural evaporation suppression by SLS monolayers over 120 hours.....	61
Figure 3.11 Maximum natural evaporation suppression versus surface tension for SLS.	63
Figure 3.12 Natural evaporation mass losses for 0 and 500 PPM EH-14.....	64
Figure 3.13 Natural evaporation mass losses for 1500 to 6500 PPM EH-14.	65
Figure 3.14 Average mass loss measurements for EH-14 natural evaporation tests.	66
Figure 3.15 Normalized evaporation mass loss measurements: 500 to 5500 PPM EH-14	67
Figure 3.16 Normalized evaporation mass loss measurements: 6500 PPM EH-14.	68
Figure 3.17 Natural evaporation suppression by EH-14 over 120 hours.....	68
Figure 3.18 Maximum natural evaporation suppression versus surface tension for EH-14.	69
Figure 3.19 Natural evaporation mass loss measurements: 0 and 20 PPM SA-9.....	70
Figure 3.20 Natural evaporation mass loss measurements: 40 to 100 PPM SA-9.	71
Figure 3.21 Average mass loss by SA-9 aqueous solutions in natural evaporation tests.	72
Figure 3.22 Normalized natural evaporation mass losses: 20, 40, 60, 80 PPM SA-9.	73
Figure 3.23 Normalized natural evaporation mass losses: 100 PPM SA-9.....	74

Figure 3.24 Natural evaporation suppression of water by SA-9 after 120 hours.	75
Figure 3.25 Maximum natural evaporation suppression versus surface tension for SA-9.	76
Figure 3.26 Subcooled boiling mass evaporation measurements for SLS solutions.	78
Figure 3.27 Subcooled boiling mass evaporation measurements for EH-14 solutions. ...	79
Figure 3.28 Subcooled mass evaporation measurements for SA-9 solutions.	80

Symbols

A	Surface area (m^2)
C	Concentration (kg/m^3)
c_p	Specific heat ($\text{J}/\text{kg}\cdot\text{K}$)
C_{sf}	Experimental constant
d	Diameter (m)
D	Diffusion coefficient (m^2/s)
F	Force (N)
g	Gravitational acceleration (m/s^2)
G	Gibbs free energy (J)
h	Transfer coefficient ($\text{W}/\text{m}^2\cdot\text{K}$ for heat or m/s for mass)
H	Dimensionless correction coefficient
h_{fg}	Enthalpy of vaporization (J/kg)
k	Thermal conductivity ($\text{W}/\text{m}\cdot\text{K}$)
K	Constant coefficient
L	Wetted perimeter (m)
L_c	Characteristic length (m)
\dot{m}	Mass transfer rate (kg/s)
n	Constant
N	Rate of vapor nuclei formation
P	Pressure (atm)
Pr	Prandtl number
r	Radius (m)
R	Universal Gas Constant ($\text{J}/\text{mol}\cdot\text{K}$)

Ra_L	Rayleigh number
Re_L	Reynolds number
T	Temperature (K or °C)
V	Velocity (m/s)
x	Distance (m)

Greek Symbols

σ	Surface tension (mN/m)
Γ	Surface excess concentration (mol/1000*m ²)
μ	Chemical potential (J/mol)
μ_l	Viscosity (kg/m*s)
ρ	Density (kg/m ³)
θ	Wetting or contact angle (radians)
α	Thermal diffusivity (m ² /s)
∞	At a distance from interface
β	Coefficient of thermal expansion (1/K)
ν	Thermal diffusivity (m ² /s)

Subscripts

A	Species A
AB	From species A to species B
b	Bubble
conv	Convection
diff	Diffusion
e	Droplet

f	Film
H ₂ O-Air	From water to air
heat	Related to heat
l	Liquid
mass	Related to mass
s	Surface
sat	Saturation
v	Vapor

Superscripts

s	Surface
---	---------

Abbreviations

CMC	Critical micelle concentration
CNRFC	California Nevada River Forecast Center
NOAA	National Ocean and Atmosphere Administration
PPM	Parts per million
SLS	Sodium lauryl sulfate

Nomenclature

CMC	Concentration at which surfactant solutions form micelles
Distilled	Processed by steam distillation, micron filtration, ultraviolet light, and ozonation
Micelles	Surfactant aggregates suspended in solution body
Monolayer	A layer that is one molecule thick
Subcooled boiling	Boiling with the solution bulk temperature not at boiling temperature
Surface Tension	Measure of a surface's resistance to expansion and contraction
Surfactants	Surface active agents
Tensiometer	Surface tension measurement apparatus

Chapter 1

Introduction

Sodium lauryl sulfate, ECOSURF™ EH-14, and ECOSURF™ SA-9 are studied in aqueous solutions in order to see their effects on surface tension, natural evaporation, and subcooled boiling evaporation. Relevant literature concerning surfactants, surface tension, and surfactants effect on the evaporation of water in natural and boiling conditions is reviewed here. Description of the significance and purpose of the current study follow the review of literature.

1.1 Introduction to Surfactants and Surface Tension

1.1.1 Surfactants

Surfactants, surface active agents, are unique chemicals with many engineering applications. The most common use of surfactants is cleaning detergents such as body wash and dish soap. The surfactants are the ingredient that removes stains and debris from clothes and dishes. This application accounts for over half of surfactants produced. A few other common applications of surfactants are petroleum production, paints, and paper processing. All applications use the unique nature of surfactants to alter the attraction between the solvent and a given gas, solid, or liquid (Schramm et al., 2003).

Surfactants are composed of an amphipathic molecular structure meaning one end of the molecular chain is lyophobic, repelled by the solvent, and the other end is lyophilic, attracted to the solvent (Rosen, 2004). For example, when used in water, the ends are hydrophobic and hydrophilic. Surfactants are classified by the charge of the lyophilic section as depicted in Figure 1.1. Nonionic surfactants have no charge on the lyophilic molecular chain section, anionic surfactants have a negative charge, cationic have a

positive charge, and amphoteric surfactants have both positive and negative charges on the lyophilic end. The charges on the amphoteric surfactants can offset and leave the surfactant with no net charge or, for specified conditions, can form either a net negative or net positive charge (Myers, 2006).

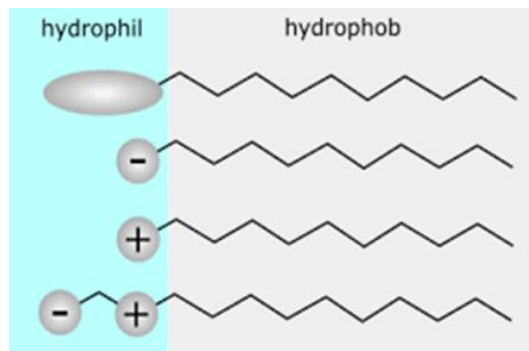


Figure 1.1 Molecular structure representation for nonionic, anionic, cationic, and amphoteric surfactants (Salager, 2002).

An example of the use of these charges is making natural surfaces hydrophobic. Surfaces are usually negatively charged (Rosen, 2004). Thus, using a cationic surfactant would cause the hydrophilic end of the surfactant to be oriented towards the surface leaving the hydrophobic end oriented away from the surface. The surface will now have a hydrophobic nature due to the surfactants aligned there. Figure 1.2 shows a schematic of increasing concentration of surfactants and their alignment at the interface.

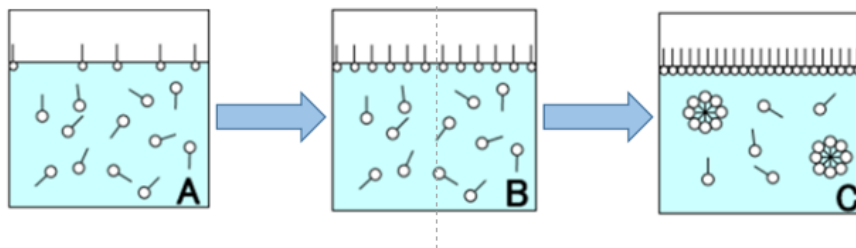


Figure 1.2 Surfactant concentration increasing from low to above CMC (Kyowa, 2015).

The lyophobic nature of the surfactants causes a distortion in the solvent molecular structure (Rosen, 2004). To remedy this distortion, the surfactants move to the interfaces of the solution and orient the lyophobic end away from the solution interior. At lower concentrations, most of the surfactant mass resides at the interfaces of the solution as this is the main method of energy reduction for surfactants (Myers, 2006). However at a given concentration, the surfactants will begin to form spherical clusters with the lyophobic end oriented to the interior of the cluster. These clusters, called micelles, are another method the system uses to lower the distortion caused by the lyophobic nature of surfactants. Figure 1.3 shows a schematic of micelle formation and some possible formation structures. The number of surfactant molecules that can aggregate into a single micelle for SLS at 23°C is 71 (Myers, 2006).

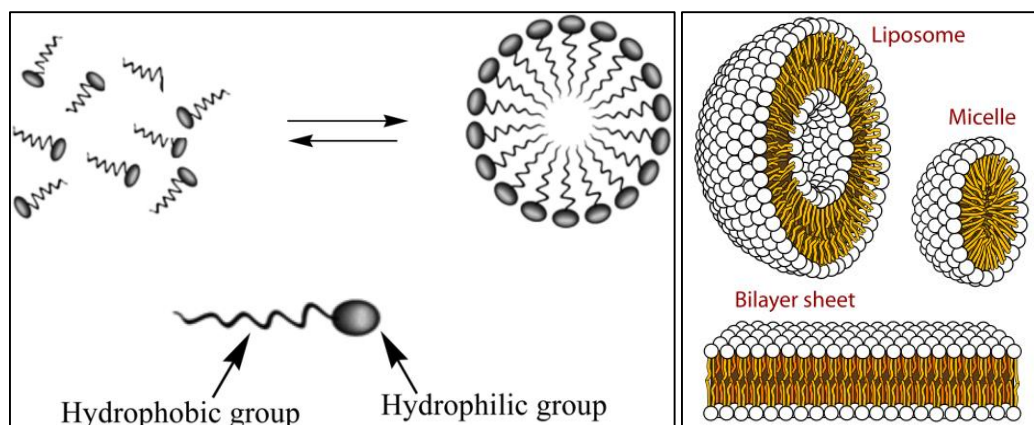


Figure 1.3 Micelle orientation and potential structure forms (Rosen, 2004)

The onset concentration at which these clusters form is called the Critical Micelle Concentration (CMC). CMC in surfactant solutions is a changing point of the relation between several physical attributes and surfactant concentration. These attributes include, among others, solution charge, surfactant solubility, and surface tension as exemplified in Figure 1.4. Micelles increase surfactant solubility and are the “predominant form of surfactant” present above CMC (Myers, 2006, p.110). Thus, above CMC surfactants begin to affect activity within the body of the solution in addition to affecting activity at the interfaces. Additional surfactant mass above CMC goes almost exclusively into micelle formation (Myers, 2006, p.124).

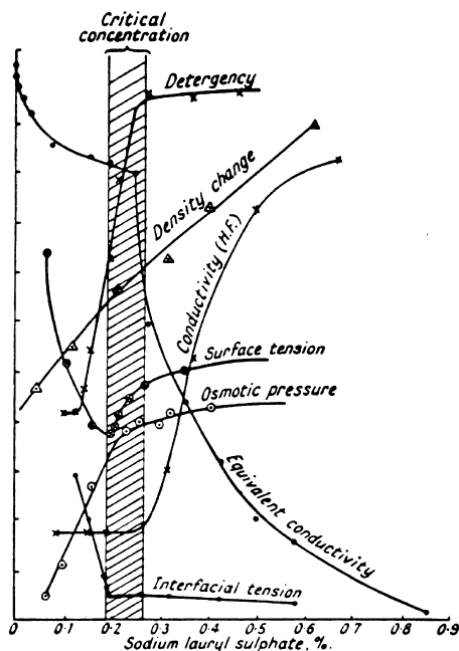


Figure 1.4 Solution properties in relation to CMC (Schramm et al., 2003).

Many factors can affect the CMC value for surfactants. For hydrocarbon surfactants, the CMC will decrease with increasing number of carbons in the molecular chain. Polar atoms in the hydrocarbon chain increase the CMC. The CMC decreases with increasing hydrophobicity. The ionic, or hydrophilic, end of the surfactant has significantly less effect on the CMC as compared to the hydrophobic end (Myers, 2006).

Other characteristics significant to surfactant performance include Krafft point and cloud point. Krafft point is the temperature at which the solubility increases due to the ability for the surfactants to aggregate in micelles (Schramm et al., 2003). Cloud point is the temperature at which an aqueous surfactant solution separates into 2 phases. At the cloud point, the surfactant becomes insoluble in the water and the solution becomes turbid (Myers, 2006). This separation is reversed when the solution is cooled below cloud point (Rosen, 2004).

1.1.2 Surface Tension

The accumulation of surfactants at the interface has a large effect on surface tension, a measurement of energy needed to expand the area of the surface. Surface tension causes the surface of a liquid to contract to the smallest area possible and originates from a molecular attraction imbalance at the surface. The molecules at the surface have stronger molecular bonding with interior solution molecules as compared with the external phase. The resulting imbalance, which is visually represented in Figure 1.5, explains the shape of water droplets and the ability of flies to rest on a water surface. In general, surfactants lower surface tension. Surfactants are thus useful when the surface area of the system is large compared to the volume or when the activity at the boundaries has strong influence on the system (Rosen, 2004).

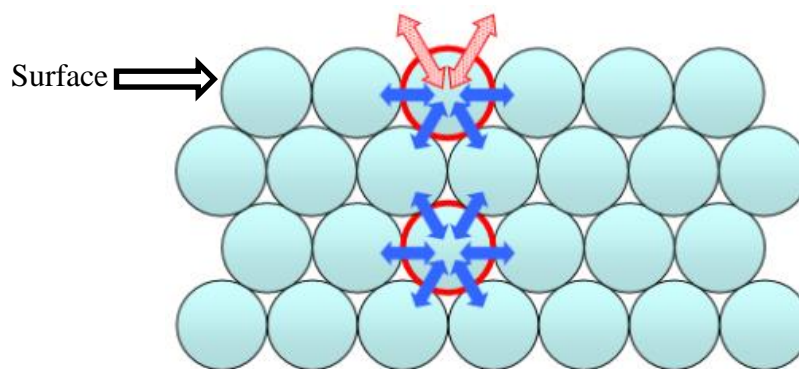


Figure 1.5 Imbalance of molecular forces at surface (Kyowa, 2015).

Important factors in the ability of surfactants to reduce surface tension are concentration of the surfactant at the surface, orientation and packing, adsorption rate, and energy changes including Gibbs free energy. Two common values used to quantify the capabilities of surfactants are efficiency and effectiveness. Efficiency is the amount of

change a given amount of surfactant will affect a system characteristic such as surface energy, and effectiveness is the maximum amount of change a surfactant can cause to a system characteristic (Rosen, 2004). For example, to quantify the effect of a surfactant on surface tension, the efficiency might be 10 mN/m per 500 PPM, if the relation was linear, whereas the effectiveness might be 30 mN/m if 30 mN/m is the most the surfactant can lower the surface tension. In dilute surfactant solutions the efficiency is determined by the ratio of the interface concentration ($C_{interface}$) to the bulk concentration (C_{bulk}) and this ratio is related to free energy (G) by the following relation (Rosen, 2004, p.35):

$$\frac{C_{interface}}{C_{bulk}} = e^{(-\Delta G/RT)} \quad (1-1)$$

Where R is the universal gas constant and T is the absolute temperature. This relation arises from the fact that interior (bulk) molecule need energy to move to the surface (Rosen, 2004).

Adsorption at liquid-gas interfaces is governed by the Gibbs adsorption equation (Rosen, 2004, p.61):

$$d\sigma = -\sum_i \Gamma_i d\mu_i \quad (1-2)$$

Where $d\sigma$ is the change in surface tension (mN/m), Γ_i is the surface excess concentration for i^{th} component of the system (moles/1000*m²), $d\mu_i$ is the change in chemical potential of the i^{th} component. For solutions of one surfactant and one solvent, this equation becomes:

$$d\sigma = -RT\Gamma_1 d(\ln C_1) \quad (1-3)$$

Where R is the universal gas constant (8.31 J/mol*K), T is the solution temperature (K), Γ_1 is the surface excess concentration (mol/1000*m²), C_1 is the surfactant molar concentration (mol/liter).

The effectiveness of surface tension reduction can be based on the ratio of surface concentration to bulk concentration. Surface excess concentration will reach its maximum value at Critical Micelle Concentration. The efficiency in surface tension reduction is highest below CMC. The surface concentration (C_1^s) in moles per liter is related to surface excess concentration (Γ_1) in moles per cm^2 by the following relation (p.212):

$$C_1^s = \frac{1000\Gamma_1}{d} + C_1 \quad (1-4)$$

Where d is the thickness of the inter-facial region (cm). For surfactants, the inter-facial region is 50×10^{-8} cm or less. Because C_1 is 0.01M or less it can be ignored in the equation above without significant error. The effectiveness of surfactants in lowering surface tension depends on the number of ions involved at the surface, effectiveness of the surfactant adsorption, and the relation between CMC and the effectiveness (Rosen, 2004).

1.1.3 Measuring Surface Tension

Several methods of measuring surface tension exist. Pendant drop method is a manual method. The solution is pressed through a needle. A droplet forms at the end of the capillary as depicted in Figure 1.6. The maximum droplet size before gravity breaks the droplet from the needle is measured. Surface tension is then calculated by the following relation:

$$\sigma = \Delta\rho g d_e^2 \frac{1}{H} \quad (1-5)$$

Where $\Delta\rho$ is density difference (kg/m^3), g is gravitational acceleration (m/s^2), $1/H$ is a dimensionless correction coefficient, and d_e is droplet diameter (m) (Kyowa, 2015, p.11).

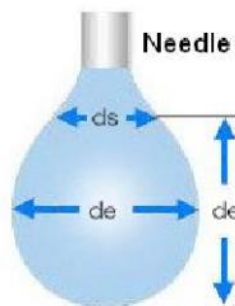


Figure 1.6 Schematic of Pendant Drop Method and important dimensions (Kyowa, 2015).

Du Nouy Ring Method is a more precise surface tension measurement and is widely used. The ring is pulled slowly through the surface. As the ring breaks away from the surface a meniscus is formed by the attraction between the surface and ring as shown in Figure 1.7. The tensiometer, the surface tension measurement device, will then measure the force required to break the meniscus. Surface tension is found from the force measurement by the following relation (Kyowa, 2015, p.10):

$$\sigma = \frac{F}{4\pi r} k \quad (1-6)$$

Where F is the force required to break the meniscus (N), r is the ring radius (m), and k is the correction factor. Du Nouy method keeps the surface in a non-equilibrium state during measurement by expanding and contracting the surface. To make an accurate measurement with a surfactant solution, there must not be motion in the surface or the surface concentration and surfactant orientation will be affected. Therefore, using Du Nouy method with surfactant solutions may yield measurements erring to a higher value (L.G, 1999).

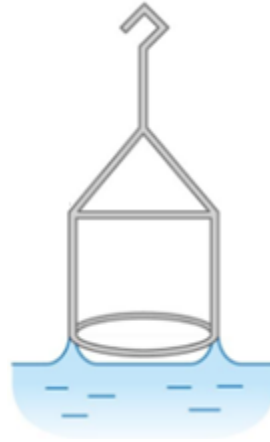


Figure 1.7 Schematic of Du Nouy ring measurement (Kyowa, 2015).

Wilhelmy plate method can measure surface tension of a surface in equilibrium and is thus useful for surfactant solutions (L.G., 1999). A plate, usually platinum, is dipped into the solution and then raised until it is just in contact with the surface. This action is usually performed by raising and lowering the platform on which the specimen rests as shown in Figure 1.8.

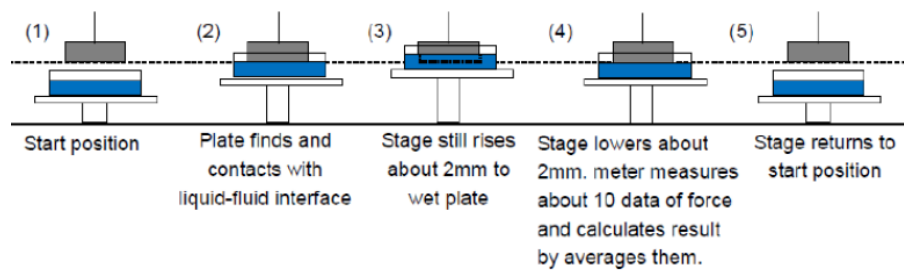


Figure 1.8 Wilhelmy plate method technique (L.G., 1999).

The tensiometer measures the force the surface applies to the plate. Tension is calculated from the following relation:

$$\sigma = \frac{F}{L \cdot \cos\theta} \quad (1-7)$$

Where F is the force measured (N), L is wetted perimeter which is the perimeter of the bottom of the plate (m), θ is the angle at which the solution wets the plate (Kruss, 2016). For most solutions, $\theta = 0$ is assumed (Kyowa, 2015). A schematic of a Wilhelmy plate measurement and the important parameters is shown in Figure 1.9.

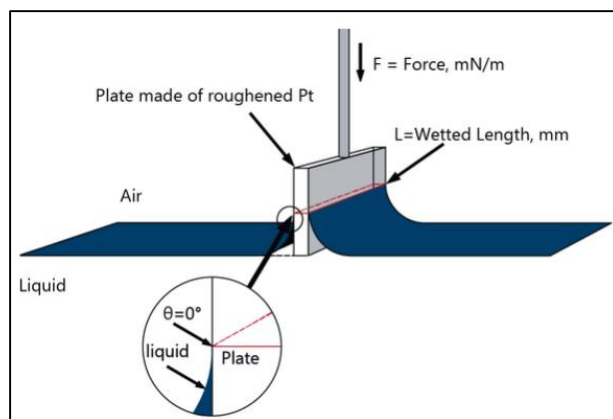


Figure 1.9 Schematic of Wilhelmy plate measurement (Kyowa, 2015).

The Wilhelmy method is more accurate than the pendant drop method and Du Nouy for surfactants but cannot be used for cationic surfactants. The platinum surface has a negative charge that attracts the positive charge of the cationic lyophilic end to the surface. The plate surface is then lyophobic which affects the interaction of the solution and the plate and hence the surface tension measurements (C.R., 2004). For the current study with nonionic and anionic surfactants, the Wilhelmy plate represents the most accurate method for determining the equilibrium surface tension of the aqueous solutions.

1.2 Natural Evaporation Suppression

1.2.1 Significance of Evaporation Suppression

Drought conditions are afflicting many parts of the world with the potential for worsening conditions due to climate change. According to data acquired by the National Ocean and Atmosphere Administration (NOAA), the average winter precipitation in California for 2011 through 2014 was the second lowest on record since 1895. This low rainfall lead to water storage levels 56% of the average levels for previous winter months according to the California Department of Water Resources (Seager et al., 2015). Precipitation in the greater Los Angeles area was below 60% of normal for 2016 up to June 24 according to the California Nevada River Forecast Center as shown in Figure 1.10 (CRNFC, 2016).

These conditions are seen in other arid areas of the world. Australia has seen slight to severe rainfall deficiencies in Queensland and Victoria since October 2012 according to the Australian Government's Bureau of Meteorology website (2016). Some areas have seen the lowest rainfall on record over a 43 month period as shown in Figure 1.12. Many nations in southeastern Africa are experiencing lower than normal precipitation during the rainy season with parts of Mozambique, Zimbabwe and South Africa receiving less than half their normal rainfall. In 2015, South Africa had the lowest annual rainfall total since 1904. Some areas recorded precipitation 20% of normal for the winter of 2015 to 2016 as shown in Figure 1.11 (Di Liberto, 2016). A recent tree ring study conducted by NASA showed that the eastern Mediterranean Levant region (Cyprus, Israel, Jordan, Lebanon, Syria, and Turkey) has experienced a drought from 1998-2012 that is the driest period in the past 500 years (Gray, 2016).

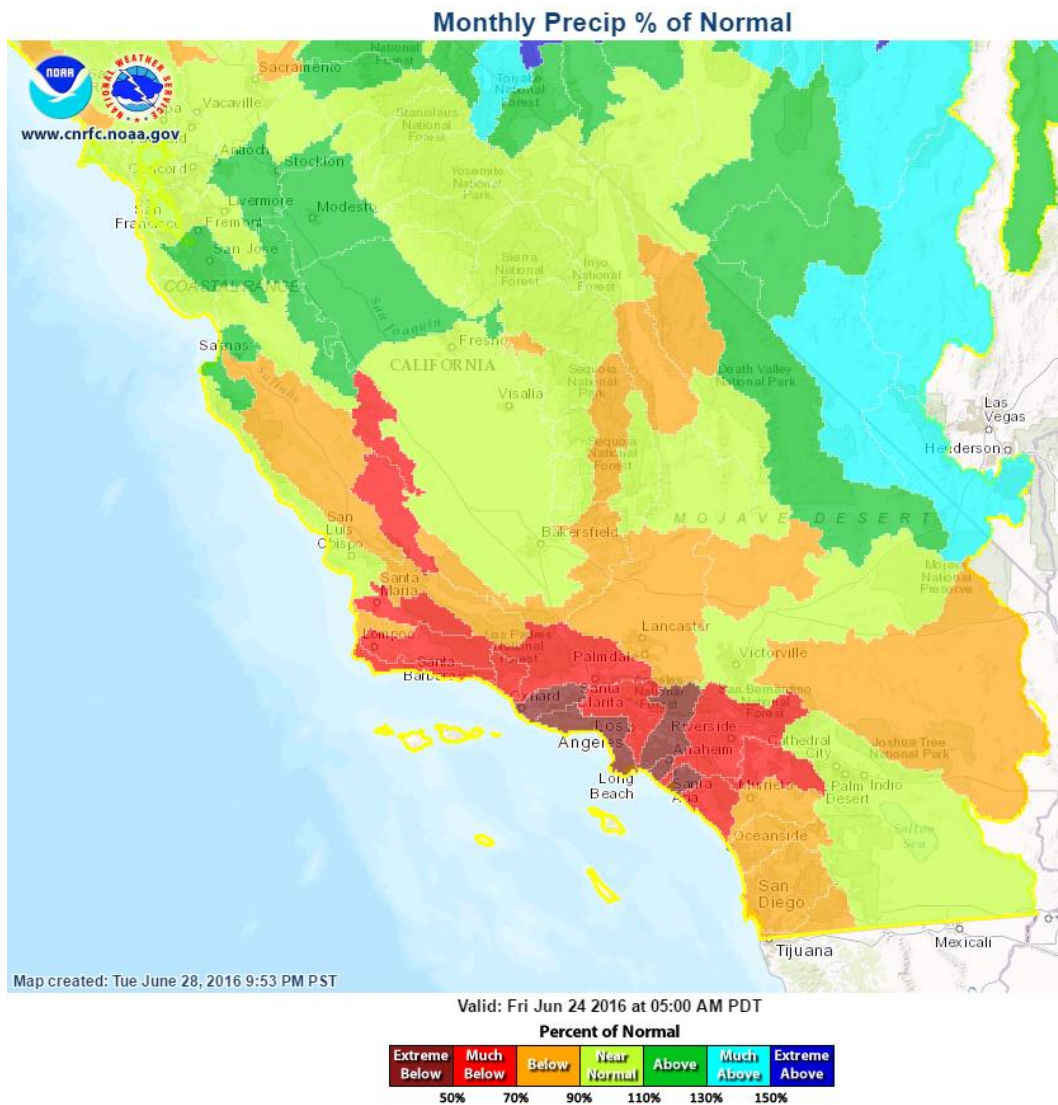


Figure 1.10 Precipitation data for California in 2016 up to June 24 (Seager et al., 2015).

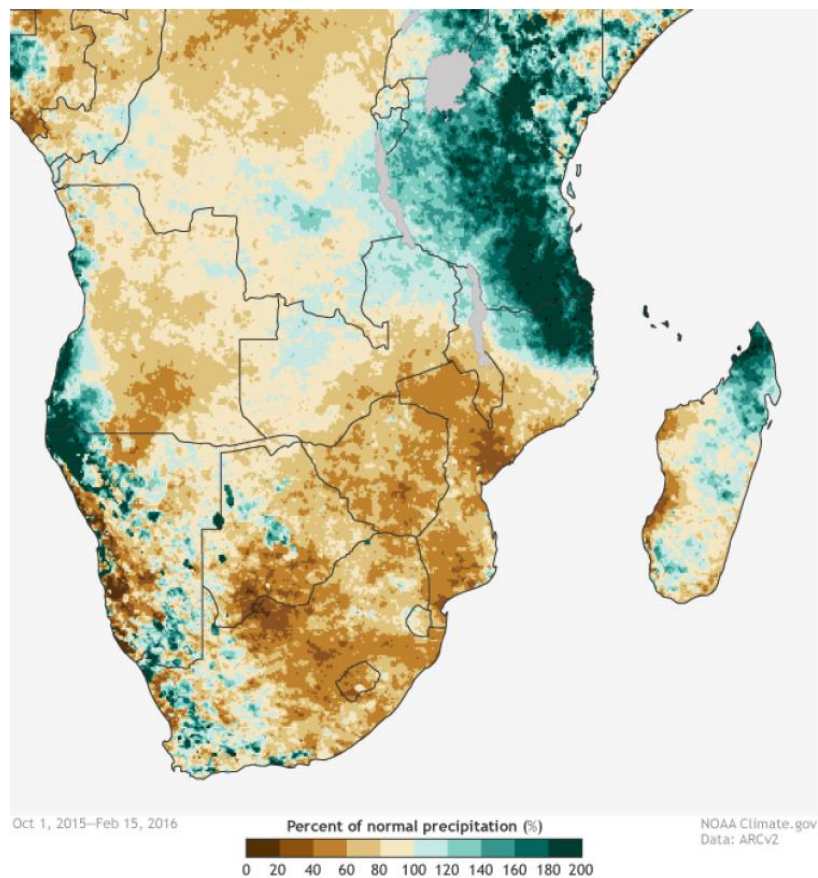


Figure 1.11 Rainy season rainfall deficiencies in southern Africa (Di Liberto, 2016).

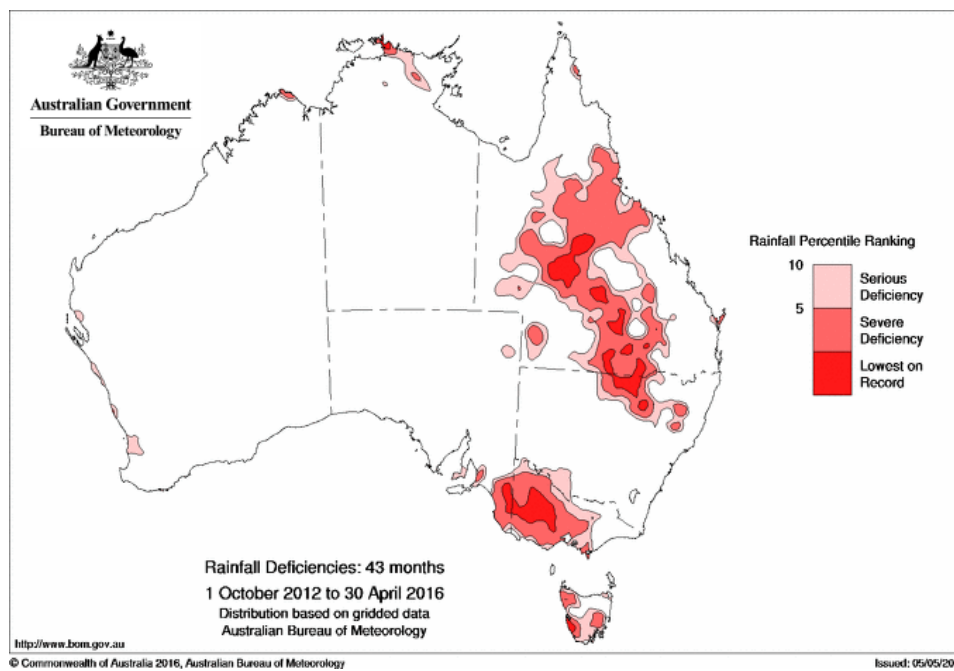


Figure 1.12 Rainfall deficiencies in Australia from 2012-2016 (Australian Bureau of Meteorology 2016).

These worldwide drought conditions make water evaporation a major issue. In arid regions, water evaporation often accounts for 25 to 30% of water use (Hightower & Brown, 2004). Water loss from storage can exceed 40% (Dawood et al., 2013) and often does in the agricultural regions of Australia (Prime E. et al., 2012). In a 1958 U.S. Geological Survey Press Release, the water evaporation lost by an area including several states was 11.5 million acre-feet as compared to the total water use 111 million acre-feet (Magin & Randall, 1960). A similar study in 1956 found that a single lake in Oklahoma lost, by evaporation, the amount of water used by 80000 people over the same time span (Manges & Crowe, 1965).

Reduction of the evaporation rates from reservoirs would help alleviate human suffering and financial costs associated with droughts. Methods of reducing evaporation from reservoirs include reducing exposed surface area per volume by increasing the depth of the reservoir or using mechanical covers such as roofs or floating rafts but the most economical and effective appear to be surface films (Magin & Randall, 1965). Ultra-thin chemical layers are also the only potentially cost-effective method of evaporation reduction for irrigation channels (Prime E. et al., 2012). Water savings by these films have been shown to be 20 times greater than the cost of application (Roberts, 1957). A study in Illinois indicated that a 33% reduction of water evaporation would be equal to a 17% increase in reservoir storage capacity (Roberts, 1957). Surface films can provide this level of cost-effective evaporation reduction.

1.2.2 Surfactant Monolayers and Natural Evaporation

Included in the surface film classification are surfactant monolayers which have been shown to lower evaporation of water by up to 50% (Zhang et al., 2003). Monolayers

are one molecule thick films that form at a phase boundary such as the air-water interface (Barnes, 2008). Some surfactants that form well compressed monolayers useful in evaporation suppression are long-chain fatty acids, long-chain alcohols, alkoxy ethanols, some methyl and ethyl esters of fatty acids, and calcium salts of long-chain fatty acids (Barnes, 2008). Studies indicate that surfactant films effects on surface tension are a significant contributor to evaporation reduction (Hightower & Brown, 2004). This relation is explored in the current study.

The most common molecule that forms condensed monolayers has a long, linear, fully saturated alkyl chain with a polar group at one end (Barnes, 2008). “Compounds with 12 or more carbon atoms in the aliphatic chain and with a hydrophilic headgroup can form stable and insoluble monolayers” (Prime E.L. et al., 2012, p.48). Increasing the length of the hydrocarbon chain of the fatty acids and long chain alcohols decreases the permeability of the monolayer (Magin & Randall, 1960). Increasing the alkyl chain length lowers evaporation rates but reduces spreading rate, which is the rate at which a surfactant can reform a disrupted monolayer (Prime E.L. et al., 2012). Increasing the chain length gives an exponential increase in evaporation resistance (Barnes, 2008). The effects of changes to the hydrophilic end on evaporation reduction are not known (Prime E.L. et al., 2012).

In “Review of Literature on Evaporation Suppression,” George B. Magin, Jr. and Lois E. Randall (1960) reported that an extensive amount of research had been done prior to 1960 in both in the laboratory and the field. Several different types of surfactants were shown to lower water evaporation rates. In 1950’s evaporation reduction studies, the long chain alcohols, cetyl alcohol and stearyl alcohol, showed the most promise with evaporation losses reduced by up to 60% (Barnes, 1997). Cetyl alcohol ($C_{16}OH$) and stearyl

alcohol (C₁₈OH) are composed of a hydrophilic hydroxyl group and a hydrophobic hydrocarbon chain (Prime E. et al., 2012). A cetyl alcohol monomolecular film in one study was found to have 65000 units of resistance (cm²*s/g, a reciprocal of an evaporation rate) to evaporation as compared to the 3 units of a clean water surface (Magin & Randall, 1960). A thin film of cetyl alcohol on a pond reduced evaporation from 50 to 70 percent and was shown to be harmless to fish and other wildlife except for mosquito larvae (Magin & Randall, 1960). In field tests, cetyl alcohol (C₁₆OH) and stearyl alcohol (C₁₈OH) reduced evaporation by up to 40% but did not show good long term performance under dynamic conditions with "rapid loss from the water surface and lack of stability to wind and wave action" (Prime E. et al., 2012, p.3). Winds above 10 km/hr broke up these monolayers (Prime E. et al., 2012).

Cetyl alcohol and stearyl alcohol are well known in literature as evaporation suppressants. However, many other surfactants have been studied in relation to evaporation suppression. Fatty acids were shown to decrease evaporation rate by a factor of 10⁴ (Magin & Randall, 1960). A freshly-formed thin film of n-docosanol almost completely eliminated evaporation but became increasingly permeable as the film age increased (Magin & Randall, 1960). Environmentally-friendly surfactant monolayers have been shown to reduce evaporation by 40-70% (Hightower & Brown, 2004).

Despite early results showing the depression of evaporation, field test results had high variability and because of this monomolecular films have not been exploited at a commercial level (Fellows et al., 2015). Many field tests have shown promise though. A Canadian product based on cetyl alcohol has been tested on several dams in Australia. The evaporation reduction ranged from 0 to 40% with indicated savings overall of 20% (Barnes,

2008). Fatty alcohols, mostly stearyl and cetyl, were applied to a lake near Jaipur, India. Results showed up to a 30% reduction in water loss (Barnes, 2008). A recent study at Sandia National Laboratories in Albuquerque, New Mexico set pools of water 8 foot in diameter outside with alcohol-functionalized straight chain hydrocarbons. Results showed a 60-70% evaporation reduction over a week time with the monolayer evaporation resistance decreasing over time (Hightower & Brown, 2004).

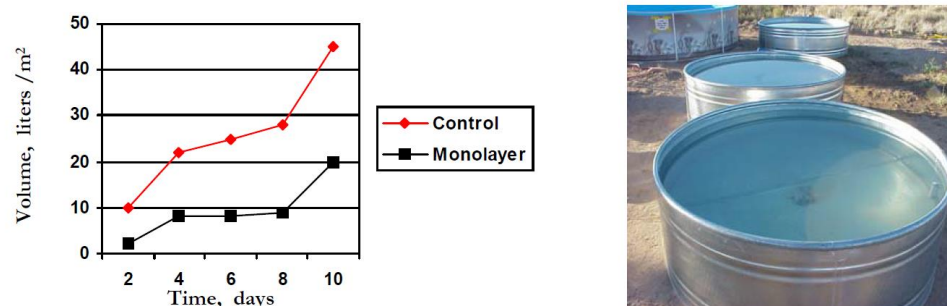


Figure 1.13 Sandia National Laboratories test results and testing pools (Hightower & Brown, 2004).

Other surfactants have been tested in the field as well. On outdoor test ponds, Mages and Crow (1965) found that a continuous surfactant monolayer yielded an evaporation reduction of 36%, a similar effect to a mesh suspended six inches above the water surface. A blend of straight-chain saturated higher alcohols (5% C₁₄, 44% C₁₆, 46% C₁₅, and 5% C₃₀) reduced evaporation in an outdoor testpan by 70% (Manges & Crow, 1965). Testing of 1 mg of hexadeconal in 55 gallon drums showed water savings of 27% during months of July, August, and September of 1956 (Roberts, 1957).

A thorough testing of a novel surfactant was performed by Prime E. et al. including laboratory and field testing. Three surfactant application techniques were used. In the first method, the unnamed (under patent application) surfactant was completely dissolved in the water. In the second, the surfactant was suspended in the water without completely dissolving. In the third, the surfactant was applied as a fine powder on the surface. Water savings in wind tunnel for horizontal wind by this unnamed surfactant ranged from 67% to 84%. The completely dissolved surfactant solutions performed the best and the solid formulations performed better than suspended formulations. Field trials of the novel surfactants showed savings ranging from 20% to 60% across multiple small reservoirs and bodies of water. Field trials show that surfactants need more than CMC to form evaporation suppressing monolayers. Prime E. et al. found through field trials that the best performing dosage of the surfactant was 18 times the amount needed to form a complete monolayer with a daily reapplication of 2 to 3 times the monolayer amount (Prime E. et al., 2012).

Field testing of surfactants has had high variability (Fellows, 2015). Several issues encountered in field tests include impurities and contaminants, vaporization of the film, displacement by wind, bacterial decomposition, organic material accumulation on the surface, and photo-degradation from irradiation (Barnes, 2008). Winds are known to be a major issue for monomolecular film stability in the field (Prime E.L. et al., 2012). The wind shear creates waves which have been shown to break up monolayers and thereby reduce effectiveness (Hightower & Brown, 2004).

Based off these issues, an ideal monolayer has high evaporation resistance, high equilibrium spreading pressure, high spreading rate, stability under wind shear, slow vaporization rate, resistance to solar degradation, resistance to bacterial decomposition,

and negligible environmental and ecological effects (Barnes, 2008). Only tightly packed surface films are useful evaporation suppressants (Prime E. et al., 2012). The optimal methods of spreading and reapplication of monolayers have yet to be determined (Barnes, 2008). Laboratory tests are the first step for selecting new monomolecular layers for evaporation reduction in reservoirs that meet all the requirements mentioned (Prime E.L. et al., 2012). The resistance of a monolayer to evaporation can be found by measuring the difference between two surfaces one with a monolayer and one without (Barnes, 1997). This technique is especially important in field tests or wherever there is variability in testing conditions.

1.2.3 Health Effects of Surfactants

Surfactants can exhibit toxicity towards organisms. Effects of surfactants on aquatic organisms can include “membrane disruption and protein denaturation” (Schramm et al., 2003, p.37). However, this toxicity is reasonably predictable in surfactants and can be determined by tests before application (Schramm et al., 2003). A test of hexadecyl (or cetyl alcohol) for evaporation suppression on a large pond showed that the only ecological effects were an increase in surface temperature and suffocation of mosquito larvae (Hightower & Brown, 2004). Some surfactants may reduce the solution or reservoirs access to oxygen which could have an effect on decaying organic matter. (Magin & Randall, 1960). However, most surfactants have been shown to have small effects on temperature of the water and negligible effects on the oxygenation of the water but may have some effects on ultraviolet penetration (Prime E. et al., 2012). Biodegradability of surfactants and the potential dangers posed by the results of the decomposition must also be taken into account but are also predictable (Schramm et al., 2003).

1.2.4 Theory of Monolayers

The Hertz-Knudsen equation, shown below, indicates that the mass flux is relatively insensitive to temperature of the vapor in contact with the surface and the temperature of the liquid surface.

$$J = \eta_e \sqrt{\frac{M}{2\pi R}} \left(\frac{P_{Sat}}{\sqrt{T_L}} - \frac{P_V}{\sqrt{T_V}} \right) \quad (1-8)$$

The commanding factor seems to be the vapor pressure of the water near the interface which in turn depends on motion of the vapor above the interface and the roughness of the surface. The surfactant monolayers provide additional roughness to the surface as well as providing dampening to waves on the surface through surface elasticity (Fellows et al., 2015). Surfactants can add elasticity to air-water surfaces and dampen turbulence near the surface (Kou et al., 2011).

Surfactant monolayers also introduce compressibility to the air-water interface which would otherwise be absent. In a study on oleic acid and cetyl alcohol monolayers, the surface temperature was held below the bulk temperature due to this compressed layer that retarded convective motion of a thin layer of water limited to near the surface. A study on the natural evaporation effects of cetyl alcohol and stearic acid showed that evaporation resistance increased with increasing surface pressure. However, the same study showed contradictory results as to the abilities of monolayers to inhibit natural convection. Heat transfer and motion in the solution can be inhibited by a surfactant monolayer. Bower and Saylor (2011) investigated oleyl alcohol, stearic acid, and stearyl alcohol versus a clean surface in glass tanks in a laboratory. The monolayers were subjected to natural convection. They concluded that convective heat transfer was more efficient without a monolayer because the shear-yielding surfactant layers inhibited convection near the

surface. The monolayers decreased the mobility of the air-water interface and dampened any turbulence of the water under the surface. They also found that the Nusselt number (the ratio of convective to conductive heat transfer across the surface) and Rayleigh number (the ratio of buoyancy and viscosity forces multiplied by the ratio of momentum and thermal diffusivities) the relationship was significantly different between the clean surface and the monolayer surfaces but the relation showed little change between different surfactant monolayers (Bower & Saylor, 2011).

Several theories on surfactant monolayers evaporation suppression effects exist. On layers no thicker than a few molecules, the surfactant monolayers have been theorized to act as impermeable hydrophobic barriers (Fellows et al., 2015). When air movement is minuscule or the water surface is too small to sustain any wave movement, the evaporation reduction is explained by the hydrogen-bonding at the surface which creates a “structure that is thermodynamically less favorable to evaporation than a clean water surface” (Fellows et al., 2015, p.40). The dependence of evaporation resistance on temperature and chain lengths is consistent with an energy barrier theory (Barnes, 2008). The Energy Barrier Theory explains the dependence of evaporation suppression efficiency on temperature, chain length, and surface pressure. It is unable to predict evaporation resistance values or explain the effects of impurities on evaporation (Barnes, 1997).

The Density Fluctuation Theory claims that the evaporation only occurs through holes in the monolayer large enough to allow water molecules to escape. The holes are assumed to arise from local fluctuations in the monolayer structure or forced to open by the kinetic energy of interior molecules moving into the surface. This theory can predict resistance values accurately. However, the theory requires an evaporation coefficient to

be known and it does not explicitly explain the effects of temperature, alkyl chain length, chain length, or impurities (Barnes, 1997).

The Accessible Area Theory claims that solutions will evaporate through naturally occurring holes, with sum of the areas of these holes being the “accessible area” in the monolayer, at the same rate as a clean surface. This theory provides reasonable predictions for resistance values while taking into account the concentrations of the surfactant on the surface. The theory does not account for the effects of the alkyl chain lengths, temperature, or impurities and requires a known value for an evaporative coefficient (Barnes, 1997).

Barnes concludes in “Permeation through Monolayers” that Energy Barrier Theory and Accessible Area Theory are not applicable to monolayers as a whole but rather “interdomain regions” where the structure of the film is less ordered and more loosely packed (Barnes, 1997, p.157). Another theory attempted to account for the additional elasticity added to air-water surfaces that dampens turbulence near the surface and thus convection (Kou et al., 2011). However, the Inhibition of Convection Theory was shown to be ineffective for many surfactants including octadecanol and cholesterol (Barnes, 1997).

1.2.5 Calculating Natural Evaporation Mass Transfer

For an air-water interface without surfactants where water and air are still, mass transfer is governed by diffusion of the water into air. This can be quantified with Fick’s Law of Diffusion (Cengel & Ghajar, 2011, p.798):

$$\dot{m}_{diff} = D_{H2O-Air} * A * \frac{dC_A}{dx} \quad (1-9)$$

Where \dot{m}_{diff} is the mass transfer rate by diffusion (kg/s), A is the surface area (m²), dC_A/dx is the change in concentration as the distance from the surface increases. The diffusion

coefficient in Fick's Law above is calculated with the following relation (Cengel & Ghajar, 2011, p.803):

$$D_{H_2O-Air} = (1.87 * 10^{-10}) * \frac{T^{2.072}}{P} \text{ (m}^2\text{/s)} \quad (1-10)$$

Where T is the temperature of the surface (K) and P is the total pressure (atm). The monolayers effect on this relation is significant but not yet quantified in literature and varies depending on surfactant type.

Natural and forced convective evaporation from an air-water interface without surfactants can be quantified using a mass transfer coefficient (h_{mass}) which is similar in concept to a heat transfer coefficient (h_{heat}). The mass transfer coefficient has a unit of meters-per-second (m/s) and can be related to heat transfer coefficient for the same control volume by the Chilton-Colburn Analogy (Cengel & Ghajar, 2011, p.836):

$$\frac{h_{heat}}{h_{mass}} = \rho c_p \left(\frac{\alpha}{D_{AB}} \right)^{2/3} \quad (1-11)$$

Where ρ is density of air (kg/m³), c_p is the specific heat of air (J/kg*K), α is the thermal diffusivity of air (m²/s), and D_{AB} is the mass diffusivity at the interface (m²/s). For air-water interfaces, the ratio of thermal diffusivity to mass diffusivity (also known as the Lewis Number) is close to unity and thus the correlation can be reduced to the following with little loss in accuracy (Cengel & Ghajar, 2011, p.837):

$$h_{mass} = \frac{h_{heat}}{\rho c_p} \left(\frac{m}{s} \right) \quad (1-12)$$

The mass flux (\dot{m}_{conv}) is then calculated with the following equation (Cengel & Ghajar, 2011, p.833):

$$\dot{m}_{conv} = h_{mass} A_s (\rho_{A,s} - \rho_{A,\infty}) \left(\frac{kg}{s} \right) \quad (1-13)$$

Where the A_s is the surface area (m^2), $\rho_{A,s}$ is the mass concentration of species A at the surface (kg/m^3), $\rho_{A,\infty}$ is the mass concentration of species A in the air (kg/m^3). For the current study, species A is water vapor.

The heat transfer coefficient for natural convection may be found by the following relations (Cengel & Ghajar, 2011, p.527):

$$h_{heat,natural\ convection} = \frac{kKRa_L^n}{L_c} \left(\frac{W}{m^2 * K} \right) \quad (1-14)$$

Where n is a constant equal to $\frac{1}{4}$ for laminar flow, L_c is $\frac{1}{4}$ of the diameter and is the characteristic length (m), K is a constant coefficient less than unity which is dependent on geometry, and k is thermal conductivity of air ($W/m * K$). Ra_L is the Rayleigh number for a horizontal surface given by the following equation (Cengel & Ghajar, 2011, p.526):

$$Ra_L = \frac{g\beta(T_s - T_\infty)L_c^3}{\nu\alpha} \quad (1-15)$$

Where g is gravitation acceleration (m/s^2), $\beta = 1/T_f$ is the coefficient of thermal expansion ($1/K$), $T_f = (T_s + T_{\infty})/2$ is film temperature (K), T_s is surface temperature (K), T_∞ is temperature of flow (K), ν is kinematic viscosity of air (m^2/s), and α is thermal diffusivity of air (m^2/s).

The heat transfer coefficient for forced convection can be found by the following relations for laminar flow over a flat horizontal plate (Cengel & Ghajar, 2011, p.424):

$$h_{heat,forced\ convection} = 0.664Re_L^{0.5}Pr^{\frac{1}{3}}\frac{k}{L_c} \left(\frac{W}{m^2 * K} \right) \quad (1-16)$$

Where L_c is characteristic length (m), $Re_L = L_c * V / \nu$ is Reynolds number, $Pr = \nu / \alpha$ is Prandtl number, k is thermal conductivity of air ($W/m * K$), d is the diameter of the circular surface (m), ν is kinematic viscosity of air (m^2/s), α is thermal diffusivity of air (m^2/s), and V is the velocity of the air flow (m/s).

Summary of Mass Transfer Calculation

The air just above the water surface is saturated quickly due to molecules escaping through the interface. The water vapor is then dispersed by diffusion, buoyancy (natural convection), or air currents (forced convection) (Shah, 2014). The values calculated using the equations enumerated for these mass fluxes are respectively: 0.015 g/hr, 0.34 g/hr, and 1.7 g/hr. (See Appendix C for calculations.) The effects from forced and natural convection on the current study are lowered considerably but not eliminated by the muslin gauze covering. Thus, the actual mass flux from the solutions should be higher than the 0.015 g/hr and significantly lower than 0.34 g/hr.

1.3 Evaporation at Boiling

1.3.1 Surfactants and Boiling

Nucleate boiling is a very efficient mode of heat transfer (Cheng et al., 2007). Boiling has many applications in energy conversion systems, heat exchange systems, air conditioning and refrigeration (Cheng et al., 2007). Boiling is also used in industry for steam production in turbines or for high heat transfer coefficients in electronics cooling (Dikici & Al-Sukaini, 2016). Surfactants can greatly enhance boiling performance. This can be accomplished at such low concentrations that no significant changes in physical properties other than surface tension are made (Cheng et al., 2007).

The main factors assessed to be contributing to enhanced heat transfer are heat flux, surfactant concentration, surface tension, and molecular weight (Dikici & Al-Sukaini, 2016). Surfactant type is also important as the ionic nature and molecular weight have an effect on boiling phenomena (Wasekar & Manglik, 2000). For example, the accessible area and the hydrophobic interaction of alkyl chains can have significant effects on

evaporation suppression in boiling mechanisms (Zhang & Wang, 2003). Nucleate pool boiling heat transfer has been seen to increase with increasing surfactant concentration with this increase slowing after the critical micelle concentration (Cheng et al., 2007). Although seen in some boiling tests, this peak at CMC in boiling enhancement has not been established as a common correlation (Wasekar & Manglik, 2000). Some surfactants enhance boiling heat transfer while others do not but the reason for this is unclear (Cheng et al., 2007).

Surface tension and viscosity are known to affect the boiling phenomena. The depression of surface tension increases in surfactant types from nonionic to anionic to cationic (Cheng et al., 2007). Increase in heat transfer could be related to increase of vapor nuclei formation shown in Figure 1.14. Improvement in boiling heat transfer by surfactants is associated with lowering of interfacial tension at the heated surface which allows smaller bubbles to release from the surface (Elghanam, 2011). This increases the formation rate of the vapor nuclei which causes increased convection near the surface (Wasekar & Manglik, 2000). Heat transfer coefficient (h_{heat}) has been found to have the following relation to surface tension (σ) (Dikici & Al-Sukaini, 2016):

$$h_{heat} \propto \sigma^n \quad (1-17)$$

Experimental values for n have ranged from -2.5 to +1.275 with surfactant solutions which indicates surfactant type is very important (Cheng et al., 2007). The rate of vapor nuclei formation increases with decreasing surface tension by the relation (Dikici & Al-Sukaini, 2016):

$$N \propto e^{-\sigma^3} \quad (1-18)$$

The Fritz equation also suggests that the bubble departure diameter is directly proportional to surface tension (Wasekar & Manglik, 2000). The Fritz equation is shown below (Yang et al., 1999, p. 203):

$$D_b = 0.0208 * \theta * \sqrt{\frac{\sigma}{g * (\rho_l - \rho_v)}} \quad (1-19)$$

Where D_b is bubble diameter (m), θ is contact angle (radians), g is gravitational acceleration (m/s^2), ρ_l is the liquid density (kg/m^3), ρ_v is the vapor density (kg/m^3), and σ is the surface tension (N/m). The increase of vapor nuclei formation and decrease in bubble diameter with the addition of sodium lauryl sulfate to boiling water is shown in the images of Figure 1.14 from the Dikici & Al-Sukaini (2016) boiling studies.

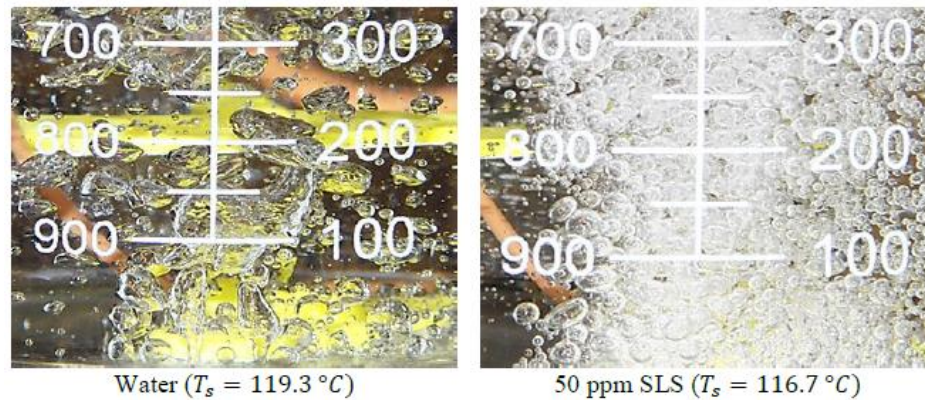


Figure 1.14 Boiling at heat flux 30.38 kW/m^2 no SLS and with SLS (Dikici & Al-Sukaini, 2016).

Some studies indicate that dynamic surface tension (instead of equilibrium surface tension) and surfactant adsorption is important to the boiling phenomenon (Cheng et al., 2007). The dynamic surface tension is related to the ability of the surfactant to reabsorb at the heated surface as the monolayer is repeatedly broken by vapor nuclei formation.

Dynamic surface tension rises with increasing concentration and increasing vapor nuclei formation rate (Cheng et al., 2007). Heat transfer enhancement does not always relate to either equilibrium or dynamic surface tension (Wasekar & Manglik, 2000). Viscosity increases with increasing concentration for all surfactants and may affect boiling phenomena at higher concentrations (Dikici & Al-Sukaini, 2016).

Subcooled boiling heat transfer is also increased by addition of surfactants but boiling hysteresis has been witnessed (Cheng et al., 2007). Subcooled boiling occurs when the liquid temperature is below saturation temperature but boiling is still occurring at the heated surface (Cengel & Ghajar, 2011). The current study explores the surfactant effect on subcooled boiling.

Another surfactant characteristic that could affect boiling is cloud point, the temperature at which an aqueous surfactant solution separates into two phases and becomes turbid. Cloud points for anionic surfactants are higher than nonionic and thus are not generally encountered in boiling of aqueous anionic surfactant solutions. The turbidity is reversed by cooling the solution back to a temperature below the cloud point (Dikici & Al-Sukaini, 2016).

1.3.2 Previous Studies on Current Surfactants

Some studies have been performed on sodium lauryl sulfate effects on the boiling of water. Elghanam (2011) studied several surfactants including SLS effects on boiling. SLS was tested in nucleate pool boiling with a stainless steel heating element. Results for SLS showed an increase in heat transfer coefficient from a clean surface of 170% at 200 PPM, 200% at 500 PPM, 280% at 1000 PPM, 330% at 1500 PPM (Elghanam, 2011).

Wasekar and Manglik (2000) found in a study with SLS that boiling curves were moved left indicating an increase in heat transfer coefficient as shown in Figure 1.15.

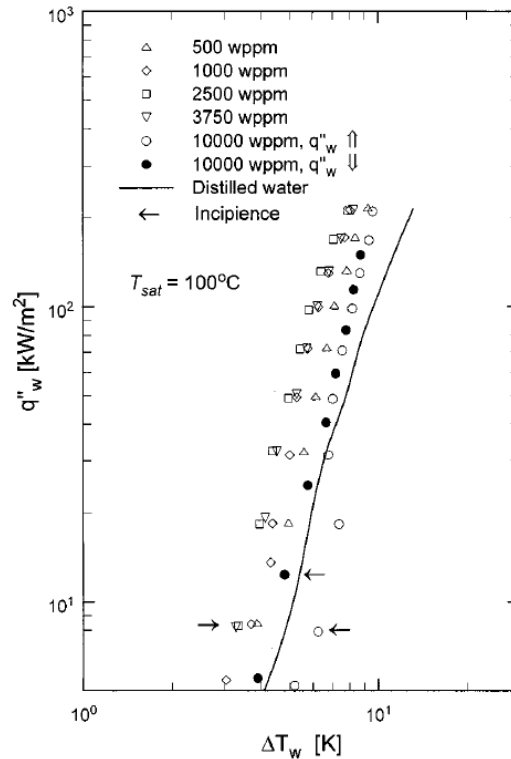


Figure 1.15 Shift of boiling curves with increasing SLS (Wasekar & Manglik, 2000).

Sodium lauryl sulfate, ECOSURFTM EH-14, and ECOSURFTM SA-9 were studied by graduate students under Dr. Birce Dikici. The boiling curves were observed to shift to left with the addition of all three surfactants with respect to water. Boiling heat transfer enhancement for SLS was higher than that of ECOSURFTM EH-14 and ECOSURFTM SA-9 for aqueous solutions. Maximum increases in heat transfer coefficients from pure water were 46% for SLS at 400 PPM, 30% for EH-14 at 800 PPM, and 21% for SA-9 at 200 PPM. Enhancement of heat transfers at lower concentrations is due to surfactants depression of interfacial tension at the heated surface but is due to increases in viscosity at

higher concentrations. Surfactant solutions boiled more vigorously than water without surfactants (Dikici & Al-Sukaini, 2016). The boiling curves for the Dikici & Al-Sukaini study are shown in Figures 1.16, 1.17, and 1.18.

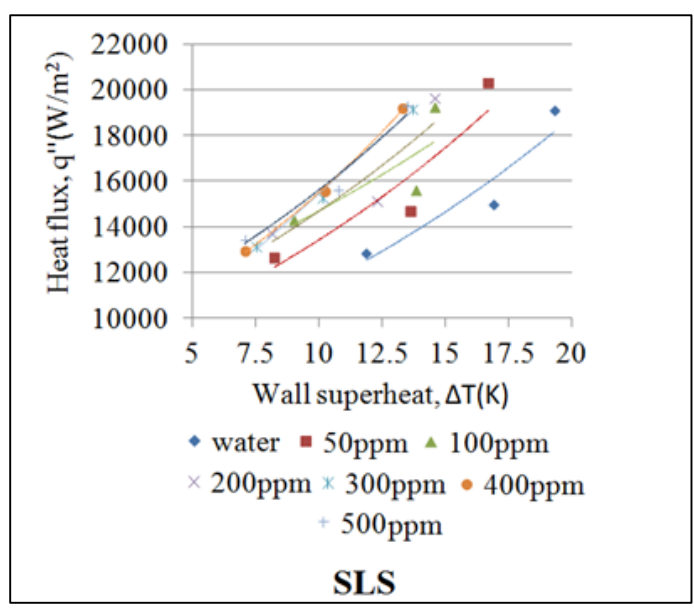


Figure 1.16 Boiling curves for aqueous solution: SLS (Dikici & Al-Sukaini, 2016).

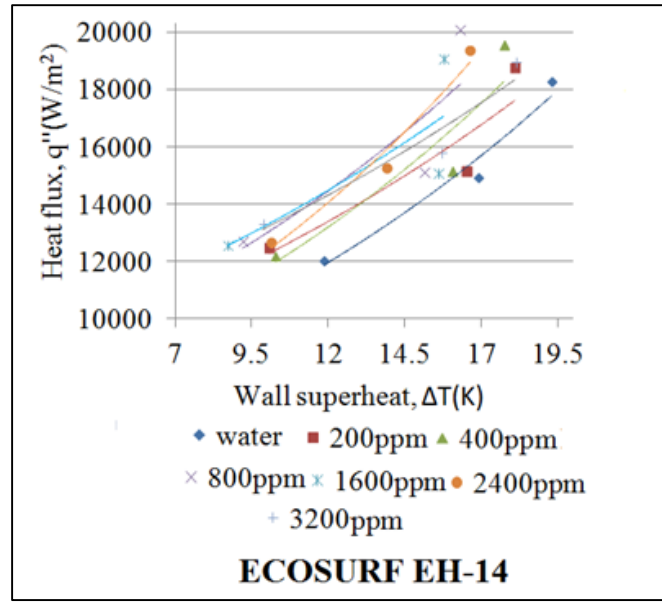


Figure 1.17 Boiling curves for aqueous solution: EH-14 (Dikici & Al-Sukaini, 2016).

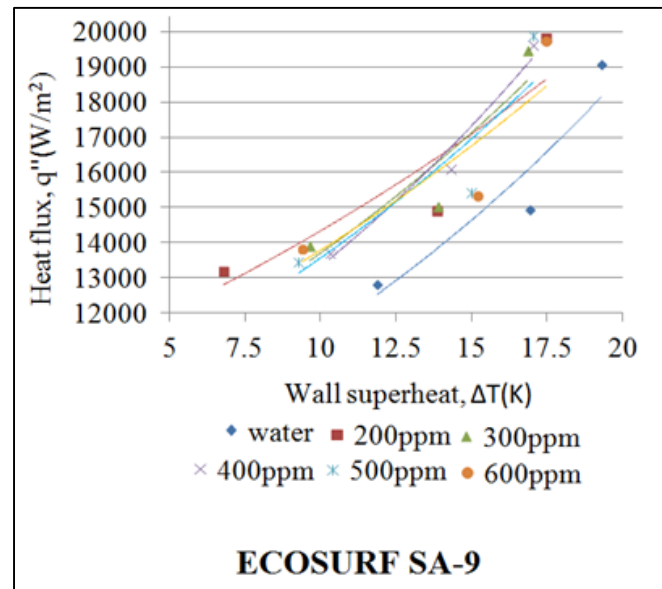


Figure 1.18 Boiling curves for aqueous solution: SA-9 (Dikici & Al-Sukaini, 2016).

1.3.3 Calculating Boiling Mass Transfer

Boiling mass transfer for the current study of water without surfactants can be estimated by the following equations for nucleate pool boiling (Cengel & Ghajar, 2011, p.588):

$$\dot{q}_{nucleate} = \mu_l h_{fg} \left[\frac{g(\rho_l - \rho_g)}{\sigma} \right]^{\frac{1}{2}} \left[\frac{c_{pl}(T_s - T_{sat})}{C_{sf} h_{fg} Pr_l^n} \right]^3 \quad (1-20)$$

Where $\dot{q}_{nucleate}$ is nucleate boiling heat flux (W/m²), μ_l is viscosity of the liquid (kg/m*s), h_{fg} is enthalpy of vaporization (J/kg), g is gravitational acceleration (m/s²), ρ_l is density of the liquid (kg/m³), ρ_g is density of the vapor (kg/m³), σ is surface tension of the vapor-liquid interface (N/m), c_{pl} is specific heat of the liquid (J/kg*C), T_s is the surface temperature of the heater (°C), T_{sat} is saturation temperature of the fluid (°C), C_{sf} is experimental constant that depends on surface-fluid combination, Pr_l is Prandtl number of the liquid, and n is an experimental constant that depends on the fluid.

The evaporation rate ($\dot{m}_{evaporation}$) in kg/s is then found by the following equation (Cengel & Ghajar, 2011, p.597):

$$\dot{m}_{evaporation} = \frac{A \dot{q}_{nucleate}}{h_{fg}} \quad (1-21)$$

Where A is surface area of the heated surface (m²).

For the current study, equations 1-20 and 1-21 predict an evaporation rate of 35.5 g/min which is a general estimate because this study deals with subcooled boiling. (See Appendix C: Subcooled Boiling Evaporation Calculations for complete calculations.)

1.4 Summary

Surfactants are known to lower surface tension of solutions due to their surface activity. The use of surfactants in evaporation suppression has yielded varying results.

Surface tension may not directly relate to evaporation suppression but may be used as an indicator of surface excess concentration and thus the compactness of the surfactant monolayer. The surfactant monolayer then acts as a barrier to evaporation with several theories as to why this occurs including energy barrier theory, density fluctuation theory, and accessible area theory. Each theory fails to explain some aspect of the monolayer evaporation suppression phenomena.

Surfactants have been shown to increase nucleate boiling heat transfer and vapor nuclei formation. SLS, ECOSURF™ EH-14, and ECOSURF™ SA-9 were shown to increase nucleate boiling heat transfer and vapor nuclei formation. However, subcooled boiling behavior is markedly different from nucleate boiling and surfactants effect on subcooled boiling evaporation has not been widely explored. The studies done have seen enhancement of heat transfer and large vapor cluster formation before subcooled boiling begins.

For the current study, evaporation rates for natural evaporation tests should range between 0.015 g/hour to 1.7 g/hour with the average rate being closer to the low end of this range. For subcooled boiling, the mass loss for the current study should be close to but less than 35.5 g/min for the solution without surfactants. Aqueous-surfactant solutions are expected to have lower mass losses than the 0 PPM solutions for natural evaporation and higher mass losses for the subcooled boiling evaporation.

1.5 Hypothesis

Based on literature, the sodium lauryl sulfate and ECOSURF™ EH-14 and SA-9 are expected to lower surface tension considerably. The surfactants are expected to lower natural evaporation rates due to the monolayer they form at the air-water interface.

Evaporation by subcooled pool boiling evaporation of the aqueous surfactant solutions is expected to increase due to increases in heat transfer coefficient seen by Dikici & Al-Sukaini (2016). Some difference in performance is expected between the anionic (SLS) and nonionic (EH-14 and SA-9) surfactants in subcooled boiling tests as this charge will affect interaction with the heated glass beaker surface. A relation between surface tension, CMC, and evaporation suppression is expected for both natural evaporation and subcooled boiling evaporation.

1.6 Significance of the Study

Water usage is a growing issue due to global warming. Drought conditions are seen annually in locations worldwide. Surfactants could be used to lower evaporation rates thus cutting water loss from reservoirs and increasing efficiency of engineering boiling water usage. The unique behavior of the amphiphilic surfactant molecules could be the answer to managing the loss of water that has plagued humanity across the world since the origin of humans. The use of surfactants to prevent water loss could be the next step in humanity's endeavor to tame the world that it calls home. The use of surfactants to increase heat transfer of boiling water could increase the ability of devices using this mode of heat transfer to help engineers cope with an ever increasing challenge to improve performance of devices. The study of surfactants capabilities and applications could potentially affect a span of engineering and scientific fields.

1.7 Statement of the Problem

Many studies have been performed on sodium lauryl sulfate and its effect on surface tension and various engineering applications. No studies observe its effect on natural

evaporation or subcooled boiling evaporation. No literature data exists related to ECOSURF™ EH-14 and SA-9 surface tension or evaporation suppression studies as these are new surfactants. The current study explores the capability of surfactants to lower water loss by natural evaporation and to increase water loss by subcooled boiling evaporation and examines EH-14 and SA-9 as eco-friendly alternatives to SLS.

1.8 Purpose Statement

The purpose of the current study is to obtain the surfactant concentrations most effective at lowering water loss of aqueous solutions under natural evaporation and increasing water loss under subcooled boiling evaporation and obtain a relation between the evaporation effects and surface tension.

1.9 Delimitations

Three surfactants studied are sodium lauryl sulfate (SLS), ECOSURF™ EH-14, ECOSURF™ SA-9. The concentrations studied range from 0 to 3500 parts per million (PPM) for SLS, 0 to 6500 PPM for EH-14, and 0 to 100 PPM for SA-9. The surface tension was measured with Wilhelmy plate method.

1.10 Limitations and Assumptions

Changes in the laboratory environment in which evaporation tests are conducted are assumed to be small enough to allow comparison between tests run at different times.

Chapter 2

Methodology

Aqueous solutions with various concentrations of sodium lauryl sulfate, ECOSURF™ EH-14, and ECOSURF™ SA-9 are tested to determine the surfactants' effects on surface tension, natural evaporation and subcooled boiling evaporation.

2.1 Surfactant Solution Preparation

The surfactants were mixed with distilled (processed by steam distillation, micron filtration, ultraviolet light, and ozonation) water to form dilute aqueous solutions. The 100 mL glass beaker was first cleaned with isopropyl alcohol. The surfactant mass was measured into the beaker. After measuring out the surfactant mass, 100.0 grams of distilled water was added to the beaker. The solutions were then mixed with a magnetic stirrer for 5 minutes at setting of 3 as shown in Figure 2.1. The magnet was removed from the solution with a plastic spoon immediately after stirring ended. The two highest concentrations of the EH-14 and SLS solutions were mixed for an additional minute to ensure complete mixing.



Figure 2.1 Stirring of solution with rotating magnet.

2.2 Surface Tension Measurement

The surface tensiometer is set on a countertop and the legs are adjusted to ensure the platform is level. The tensiometer is plugged into a transformer which is plugged into a wall outlet. The transformer converts the 120 V wall outlet voltage to the 220 V required by the tensiometer. The Wilhelmy plate is checked to verify the plate bottom surface will be perpendicular on all faces to a solution surface when hung from the tensiometer balance hook. The plate is rinsed with water and then flame cleansed. Flame cleansing is completed by immersing the plate in a 99.9% isopropyl alcohol-lamp flame until the plate begins turning red. The plate is then hung on the balance.

The solutions are mixed and allowed to sit for 30 minutes before measurements so that equilibrium surface tension is measured. After calibration, the beaker of solution is set on the tensiometer platform. The platform is raised manually until the plate surface has been mostly wetted. The platform is then lowered until the meniscus formed between the plate and the solution surface is about to break. Once the measurement displayed on the digital screen comes to a set value, it is recorded. The platform is lowered until the plate and solution separate and then the dip and raising to point of meniscus break is repeated. This last procedure evaluates the measurement repeatability.

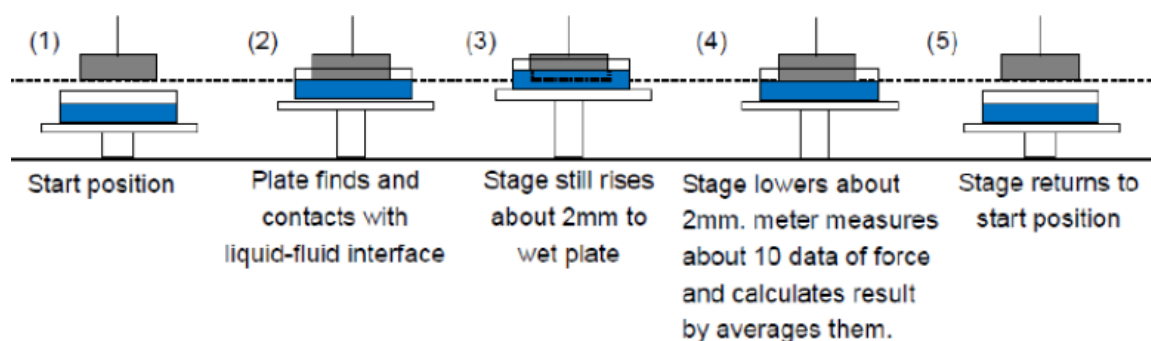


Figure 2.2 Wilhelmy plate surface tension measurement method used (L.G., 1999).

The plate is adjusted, rinsed and flame cleansed before every measurement. The tensiometer is calibrated before each measurement. Every measurement session is started by measuring pure water to make sure the tensiometer reads the correct value known from literature at room temperature. Pure water has a surface tension of 72.75 mN/m at 20°C and 1 atmosphere with an uncertainty of 0.36 mN/m (Vargaftik et al., 1983, p.819).

2.3 Natural Evaporation Tests

Solutions are mixed in 100 mL glass beakers and set on a cabinet top in the corner of the lab. The beakers are covered with cotton muslin gauze as shown in Figure 2.3 to prevent debris from affecting the surfactant monolayers and damp any random breezes over the beakers. The gauze covering allows an assumption of natural convection. The solutions sit for 5 days undisturbed except for mass measurements taken at 24, 48, 72, 96, and 120 hours from initial measurements. These initial measurements are taken after all the concentrations have been mixed for the specific surfactant. The concentrations of the surfactants in the aqueous solutions are seen in the table below. The concentration intervals were chosen to include the critical micelle concentration. The units used for concentration are parts per million (PPM) which is defined as (Dikici & Al-Sukaini, 2016, p.4):

$$PPM = \frac{1,000,000 \text{ mass of surfactant}}{\text{mass of solution}} \quad (2-1)$$

Table 2.1 Solutions tested in natural evaporation.

Surfactant	Concentrations Tested (PPM)	Water Mass (g)
Sodium Lauryl Sulfate	0, 500, 1000, 1500, 2000, 2500, 3000, 3500	100.0
ECOSURF™ EH-14	0, 500, 1500, 2500, 3500, 4500, 5500, 6500	100.0
ECOSURF™ SA-9	0, 20, 40, 60, 80, 100	100.0



Figure 2.3 Solutions covered with muslin gauze for natural evaporation test.

2.4 Subcooled Boiling Evaporation Tests

Each solution is prepared and allowed to sit for 30 minutes to reach an equilibrium state. Table 2.2 shows the concentrations tested for each surfactant. The total initial mass is measured and the beaker is set on the Benchmark hotplate. Two thermocouples are immersed into the solution. The thermocouples are attached to the Omega SD Card Data Logger and temperature is measured versus time for the experiment. A subcooled boiling test setup is shown in Figure 2.4. The heat on the hotplate is set to 9 (the highest setting) and the solution is brought to boiling temperature of water. After solution reaches boiling temperature, the heat is shut off and the beaker sits on the hotplate for 5 minutes. The remaining total mass is measured precisely five minutes after the hotplate is shutoff. As the solution and beaker are still near 100 Celsius, thermal protection is used for both hands and the mass scale. The solutions are tested one at a time and hotplate surface is allowed to cool to room temperature before each test run.

Table 2.2 Solutions tested in boiling evaporation tests.

Surfactant	Concentrations Tested (PPM)	Solution Water Mass (g)
Sodium Lauryl Sulfate	0, 500, 1000, 1500, 2000, 2500	100.0
ECOSURF™ EH-14	0, 500, 1500, 2500, 3500, 4500	100.0
ECOSURF™ SA-9	0, 20, 40, 60, 80, 100	100.0



Figure 2.4 Boiling evaporation test setup.

2.5 Surfactants Analyzed

The surfactants used in this study were sodium lauryl sulfate, ECOSURF™ EH-14, and ECOSURF™ SA-9. SLS is used in detergents, cosmetics, and pharmaceutical products. EH-14 is used in agrochemicals, cleaning detergents, paints, and textile processing. SA-9 is used in hard surface cleaners, detergents, paper processing, textile

processing, and paints. Relevant data for these surfactants is found in Table 2.3 (Dikici & Al-Sukaini, 2016; Dow, 2013; Dow, 2012; Frey Scientific, 2014).

Table 2.3 Information on surfactants used in current study (Dikici & Al-Sukaini, 2016; Dow, 2013; Dow, 2012; Frey Scientific, 2014).

Surfactant	Sodium Lauryl Sulfate (SLS)	ECOSURF™ EH-14	ECOSURF™ SA-9
Manufacturer	Frey Scientific	Dow	Dow
Type	<u>Anionic</u>	<u>Nonionic</u>	<u>Nonionic</u>
Other Name	Sodium Dodecyl Sulfate	Alcohol Alkoxyate	Seed Oil Surfactant
Chemical Formula	$\text{CH}_3(\text{CH}_2)_{11}\text{OSO}_3\text{Na}$	-	-
CMC (PPM)	2365	4018	22
Molar Mass (g/mol)	288.38	1036	668
Density (g/cm ³)	1.05	1.0538	0.9831
Appearance	White Powder	Clear Slippery Liquid	Pale Yellow Liquid

2.6 Equipment

Masses were measured with A&D GF-300 Digital Scale Balance. This scale uses a Super Hybrid Sensor to weigh the mass. The weighing capacity is 310 gram maximum and 0.001 gram minimum. The standard deviation is 0.001 grams. The scale has a sensitivity drift of +/- 0.002 g per degree Celsius.



Figure 2.5 A&D GF-300 Digital Scale Balance.



Figure 2.6 Benchmark Scientific H4000-HS Hotplate and Stirrer.

Mixing was performed with the magnetic stirring function of the Benchmark Scientific H4000-HS Hotplate and Stirrer. The H4000-HS has white ceramic surface that is 18cm (7.1 in) by 18cm (7.1 in). The surface temperature range is 80 Celsius to 380 Celsius with 9 potential heat settings. The magnetic stirrer has a speed range of 60 RPM to 1500 RPM with 9 potential stir speed settings. The hotplate and stirrer draws 120 volts at 60 hertz.

Surface tension measurements were conducted using the BZY-101 Automatic Surface Tensiometer. The tensiometer's measuring range is 0 milli-newton per meter (mN/m) to 600 mN/m. The minimum resolution is 0.1 mN/m and the standard deviation is +/- 0.1 mN/m.

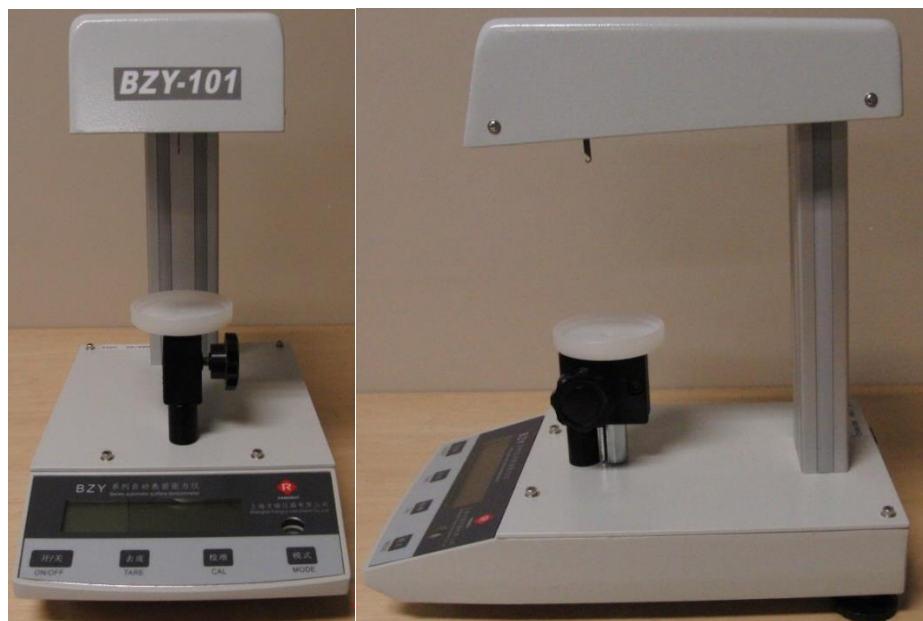


Figure 2.7 Automatic surface tensiometer used in surface tension measurements.

The tensiometer was purchased from a Chinese company Shanghai Fangrui Instrument Co., Ltd. The required supply voltage was 220 Volts (V) and thus a transformer was purchased to complete the required conversion. The Goldsource® Step Up & Down Transformer STU-300N converted the 120 V wall outlet to the 220 V required by the tensiometer.



Figure 2.8 Transformer used to convert wall outlet voltage to the required voltage.

The temperature data was recorded using the Omega 4-Channel Portable Thermometer/ Data Logger with SD Card Data Recorder. The Omega RDXL4SD runs off battery and displays the temperature measured by the attached thermocouples onto a digital display and records the data on an SD Card. Type K thermocouples were used. The response time of the thermocouples is 0.0002 seconds in still water (Dikici & Al-Sukaini, 2016).



Figure 2.9 Omega 4-Channel Portable Thermometer/ Data Logger used in study.

Photographs were taken with CASIO Exilim EX-FH20 camera. This camera has 9.1 megapixels clarity in normal mode and 7 megapixel clarity at a high-speed photo setting capable of 40 captures per second. The camera also has a 20X optical zoom and anti-shake mechanism. The camera is shown in Figure 2.10.



Figure 2.10 CASIO Exilim EX-FH20 camera used in study.

2.7 Treatment of the Data

2.7.1 Normalizing Natural Evaporation Measurements

The measurements for natural evaporation are normalized by the following ratio (Prime, E. et al., 2012, p.23):

$$\text{Normalized Mass Loss} = \frac{(\text{Mass Loss})_{\text{control}} - (\text{Mass Loss})_{\text{sample}}}{(\text{Mass Loss})_{\text{control}}} * 100 \quad (2-2)$$

The ratio will show the effectiveness of monolayers in lowering evaporation and allows comparison between testing despite the range of the control mass loss. (Explanation of laboratory environment effects on natural evaporation tests was tested and is explained in the Reliability Testing section). The control sample is the solution consisting of distilled water with no surfactant. For example, a natural evaporation test of an aqueous solution of 1000 PPM SLS loses 4 grams of water and the solution with no surfactant loses 5 grams of water. The normalized mass loss for the 1000 PPM SLS solution is equal to:

$$\text{Normalized Mass Loss} = \frac{5g - 4g}{5g} * 100 = 20\% \quad (2-3)$$

2.7.2 Repeatability Testing

The reliability of the surface tension measurements was tested by measuring the tension of a clean water surface at the beginning of every surface tension measurement session. The surface tension of water is known from literature to be 72.75 mN/m at 20°C and 1 atmosphere (Vargaftik et al., 1983, p.819).

The influence of the laboratory environment on natural evaporation tests was tested. The experiment to test these effects consisted in setting out 6 beakers of 100.0g of distilled water on the cabinet top and covering all 6 beakers with the muslin gauze. This set up was consistent with the natural evaporation tests run. The initial mass was measured and the final mass was measured after each part of this experiment. The experiment had three parts each lasting 1 hour. In part 1, all doors in the laboratory were closed and the lab had been closed for 8 hours or more. The mass loss from each beaker during this part 1 hour was measured. Part 2 was initiated by refilling the beakers to 100.0g of distilled water. All doors in the laboratory, this includes 2 bay doors and 1 personal door, were opened to the exterior atmosphere of 34.4 °C, 57% humidity, and wind speeds of 4.2 m/s (Time and Date AS, 2016). The part 2 hour long test was started immediately after doors were opened. The doors were left open for duration of the test. Immediately after the Part 2 hour elapsed, the doors were closed and the Part 3 hour was started. The mass loss during each part of the experiment was measured and the temperature of the lab was recorded with a type K thermocouple.

Thus, the mass evaporation rates of water under three laboratory conditions were tested. Part 1 tested the evaporation under equilibrium conditions. During Part 1 there was standard fluctuation of the lab temperature as AC unit cycled on and off. Part 2 tested the

evaporation as the room became exposed to the external weather. Part 3 tested the evaporation as AC units returned the room temperature to 20°C after the doors were closed. Results of this test are shown in Figure 2.11.

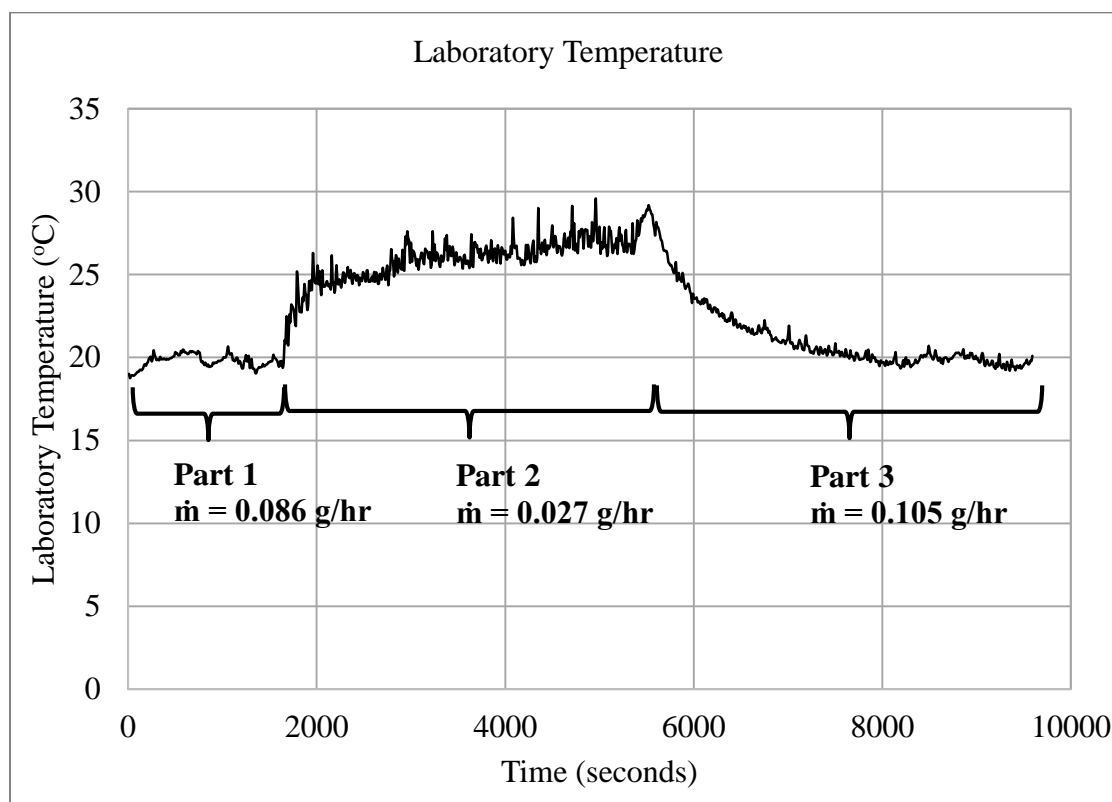


Figure 2.11 Laboratory environment effects on evaporation test results.

The results show that environment conditions significantly change evaporation rates of water. The open doors exposed the water to higher air temperatures and humidity and thus lowered evaporation rates despite wind causing significant air motion in the lab. The water evaporation increased significantly after the doors were closed. This indicates that the water warmed to the new room temperature over Part 2 and, as the AC returned

room temperature to the normal 20°C, natural and forced air convection was experienced by the air-water interface.

Due to these effects on natural evaporation testing, the mass loss measurements were normalized to control sample as discussed in Methodology: Treatment of the Data. The control sample is the distilled water solution that has no surfactant in it and thus has a clean surface. This allows comparison between testing even though activity in the laboratory prevented consistent conditions over the 5 day tests. This normalization is used for evaporation field tests of surfactants found in literature. The 5 day tests resemble field tests due to the lab environment changes.

2.7.3 Hypothesis Testing

The measurements taken for the tests show how the addition of surfactants affect the surface tension, natural evaporation rates, and subcooled boiling evaporation rates of distilled water.

Chapter 3

Results and Discussions

Sodium lauryl sulfate, ECOSURF™ EH-14, and ECOSURF™ SA-9 are studied in aqueous solutions for effects on surface tension, natural evaporation, and subcooled boiling evaporation. The results of the current study are presented and discussed in this section.

3.1 Surface Tension Measurements

The results of surface tension measurements for aqueous surfactant solutions with sodium lauryl sulfate, ECOSURF™ EH-14, and ECOSURF™ SA-9 are given in Figures 3.1, 3.2, and 3.3 respectively. Average surface tension of distilled water was measured as 70.0 (mN/m) for 20 °C as shown at the 0 PPM concentration measurements. The surface tension at 20°C found in literature is 72.75 mN/m (Vargaftik et al., 1983, p.819). Thus, the average distilled water surface tension measurement was 3.8% lower than literature data for water surface tension.

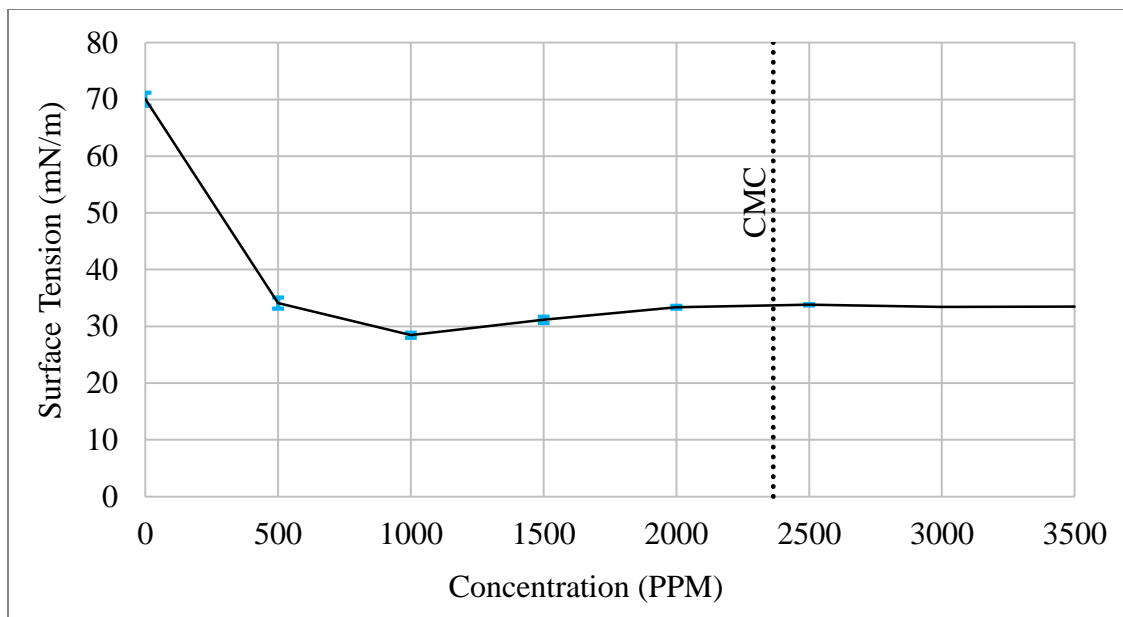


Figure 3.1 Surface tension measurements of aqueous SLS solutions.

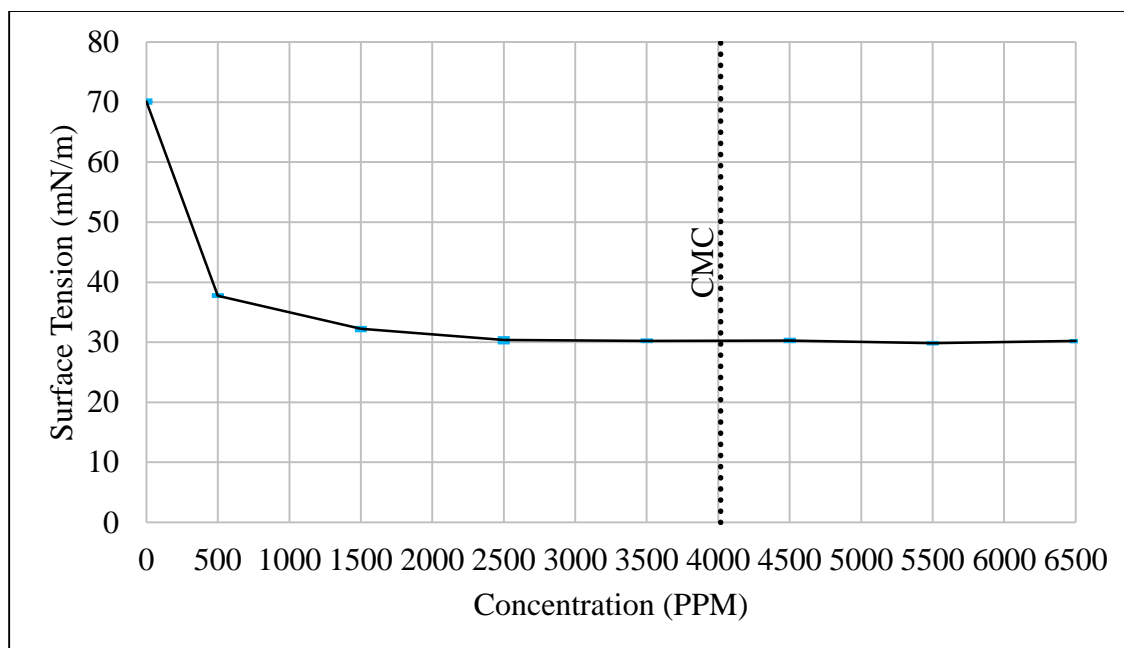


Figure 3.2 Surface tension measurements of aqueous EH-14 solutions.

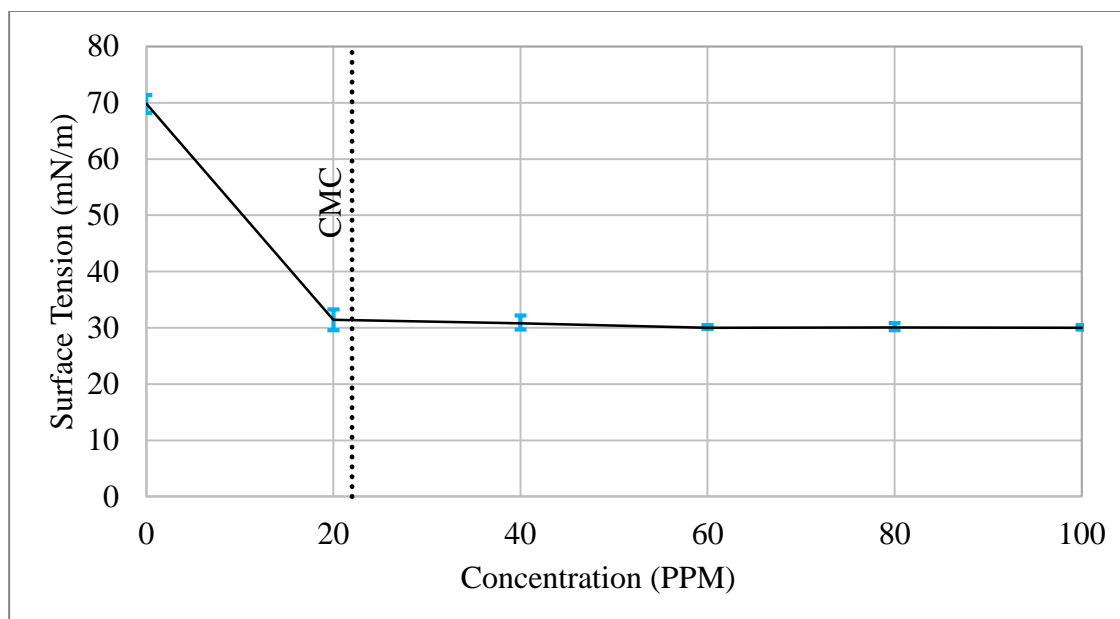


Figure 3.3 Surface tension measurements of aqueous SA-9 solutions.

3.1.1 Sodium Lauryl Sulfate

Aqueous SLS solution surface tension decreased as the solution concentration is increased to 1000 PPM as shown in Figure 3.1. The surface tension value obtained at 1000 ppm is 28.9 (mN/m) at 20°C. After exceeding the CMC of 2365 PPM, no considerable change in surface tension is observed. Surface tension value for concentrations near and exceeding CMC is 33.5 (mN/m) at 20°C.

The lowest surface tension for SLS was at 1000 PPM was below the CMC of 2365 PPM. The dip in surface tension may be due to molecular interaction between SLS molecules in the surface. At 1000 PPM, the SLS surface concentration may be low enough that surfactant molecules have not begun to interact with each other. The increase in surface tension with an increase in concentration from 1000 PPM may be the result of more interaction between surfactant molecules. The surface tension would then increase until the surface is saturated with surfactants at the CMC.

3.1.2 ECOSURF™ EH-14

Aqueous EH-14 solution surface tension showed a decrease as the solution concentration is increased to 2500 PPM as shown in Figure 3.2. The surface tension value obtained at 2500 ppm is 30.4 (mN/m) at 20°C. After exceeding the CMC of 4018 PPM, no considerable change in surface tension is observed. For concentrations near and exceeding CMC, the surface tension observed is 30.2 (mN/m).

3.1.3 ECOSURF™ SA-9

Aqueous SA-9 solution surface tension showed a decrease as the solution concentration is increased to 20 PPM as shown in Figure 3.3. The surface tension value obtained at 20 ppm is 31.4 (mN/m) at 20°C. After exceeding the CMC of 22 PPM, no considerable change in surface tension is observed. The surface tension observed for concentrations near or exceeding CMC is 30.0 (mN/m).

3.1.4 Discussion of Surface Tension Measurements

SLS, EH-14, and SA-9 all had similar trends in surface tension versus concentration as shown in Figures 3.1, 3.2, and 3.3. The surfactants' initial (i.e. lowest) respective concentrations of 500 PPM for SLS, 500 PPM for EH-14, and 20 PPM for SA-9 each reduced the surface tension of water by over 30 mN/m. Then increasing concentrations up to CMC lowered surface tension by less than 8 mN/m for EH-14 and less than 3 mN/m for SLS and SA-9. Increasing the concentrations above the respective CMCs did not have significant additional effects on the surface tension. The trend may be explained by the surfactants effect on inter-molecular bonding in the surface. Pure water has strong cohesion due to the attraction of the water molecules. The initial concentration of surfactant may interfere with this attraction at local levels enough to lower the overall cohesive force

of the surface, the surface tension, significantly. Addition of more surfactant mass above the initial concentrations would thus have little additional effect on surface tension because the cohesion of the pure water surface as a whole has already been broken by the initial surfactant concentration mass. Increase of concentrations above CMC does not significantly affect surface tension because this additional mass goes to micelles within the solution body and does not aggregate at the surface (Myers, 2006).

3.1.5 Comparison of SLS Measurements to Literature Data

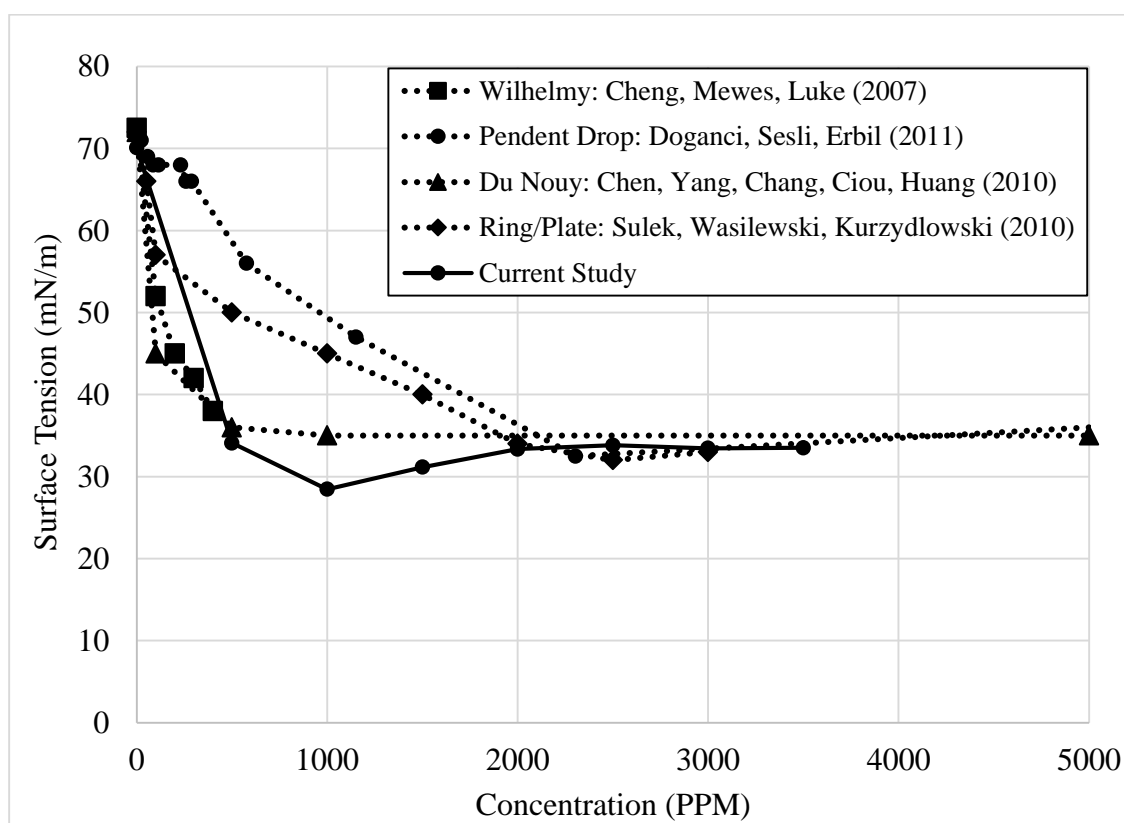


Figure 3.4 Surface tension measurements SLS aqueous solutions found in literature.

The SLS solution surface tension measurements from the current study are compared to literature in Figure 3.4. Literature showed a wide range of surface tension measurements under CMC (2365 PPM). This variation may be due to the different

techniques used for measuring surface tension. For example, the highest measurements for concentrations between 0 and 2000 PPM found in literature were done with the Pendant Drop Method (Doganci et al., 2011) and the lowest measurements found for the same range of concentrations were done with the Du Nouy (Ring) Method (Chen et al., 2010). The solution mixing techniques and other preparation techniques may affect measurements. For example, the current study procedure included cleaning the beakers with isopropyl alcohol before mixing solutions. Temperature of the solutions at time of measurement will also affect surface tension measurements as temperature changes can affect the hydrogen bonding occurring between surfactants and the water (Myers, 2006, p.202). If the bonding between molecules within the surface is weakened the overall cohesion of the surface will be changed and thus the surface tension will also be changed. A change in water temperature from 20°C to 25°C corresponds to a surface tension decrease of 0.76 mN/m (Vargaftik et al., 1983). The current study measurements agree with the Cheng et al. (2007) measurements for concentrations from 0 to 500 PPM which were completed with the Wilhelmy plate method and agree well with all literature measurements for concentrations of 2000 PPM and higher. Since EH-14 and SA-9 are new surfactants, no surface tension measurements for them are published in literature.

3.2 Natural Evaporation Measurements

3.2.1 Sodium Lauryl Sulfate

Mass loss measurements for the SLS natural evaporation tests are shown in Figures 3.5 and 3.6.

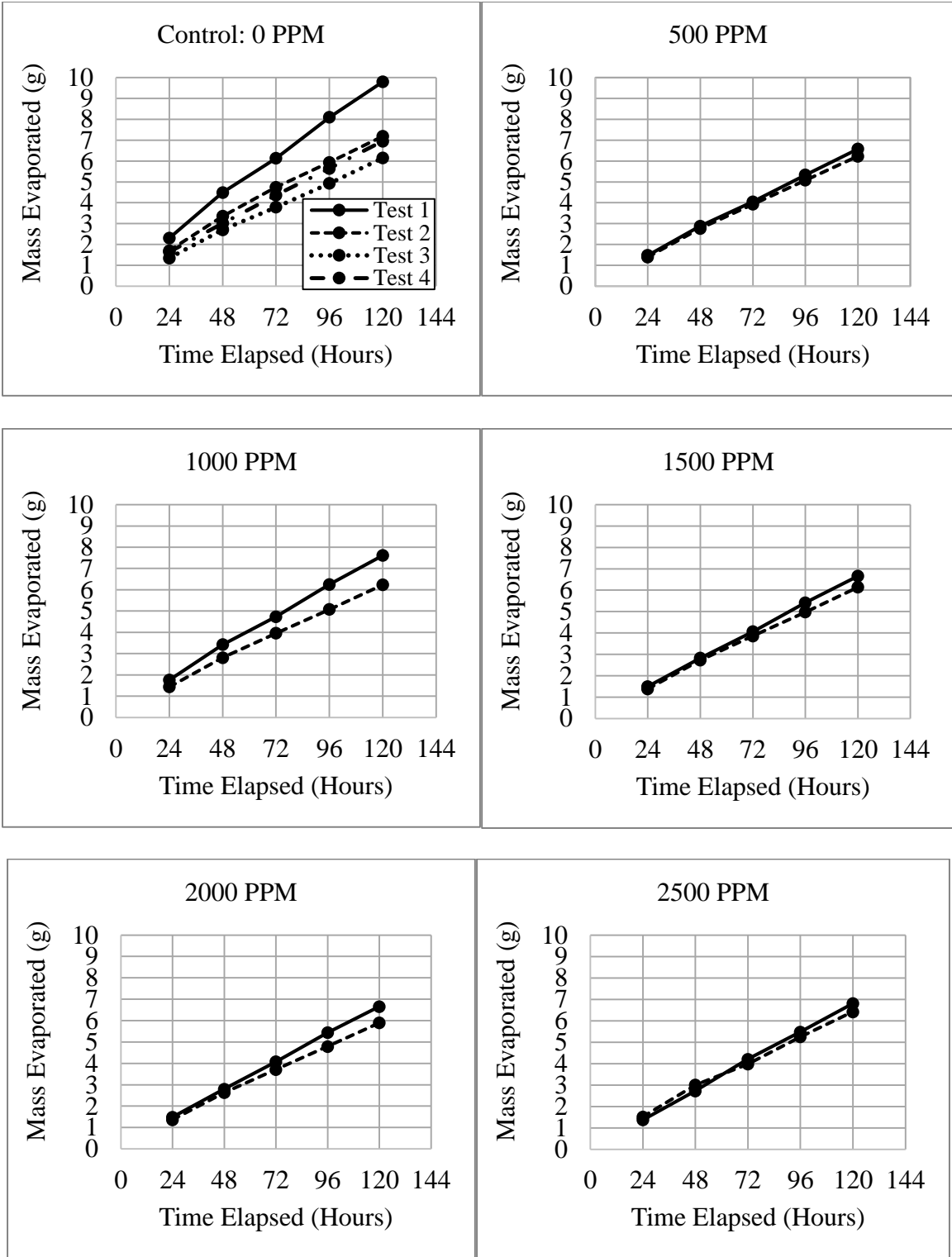


Figure 3.5 Natural evaporation losses for 0, 500, 1000, 1500, 2000, 2500 PPM SLS.

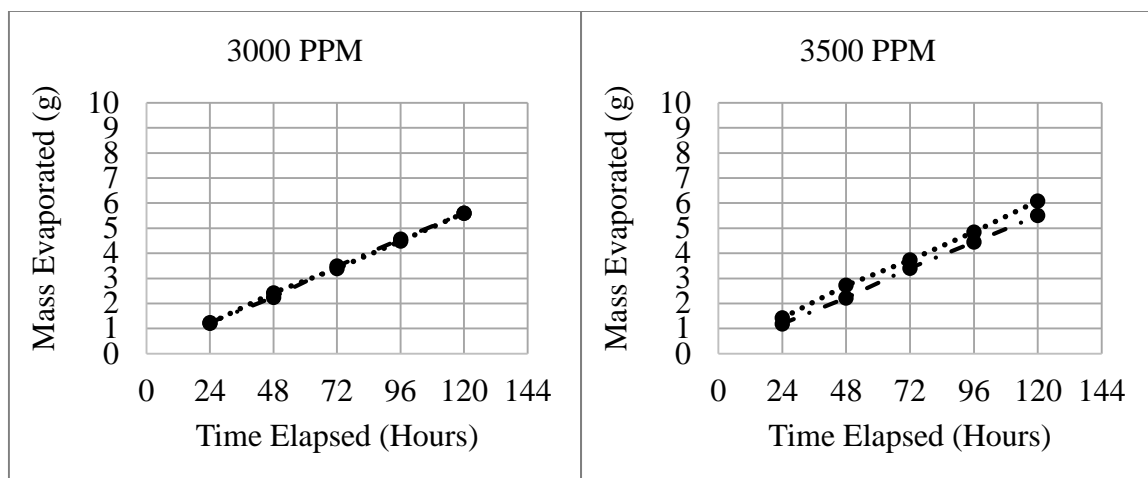


Figure 3.6 Natural evaporation losses for 3000 and 3500 PPM SLS.

The measurements of mass loss during natural evaporation testing of SLS solutions (Figures 3.5 and 3.6) show that SLS suppresses evaporation of water. The mass loss from SLS solutions showed consistency between test runs for all concentrations. The control (0 PPM) mass losses ranged from 6-10 g out of 100 g solutions (6-10%). The 3000 and 3500 PPM concentrations showed the least mass loss over 120 hours with mass loss in the 5-6 g range (5-6%). The average of the mass loss measurements from Figures 3.5 and 3.6 for each concentration are shown in Figure 3.7. Comparison of average mass losses per concentration over all tests shows that both concentrations well above the CMC of 2365 PPM had lower average mass losses than concentrations below CMC.

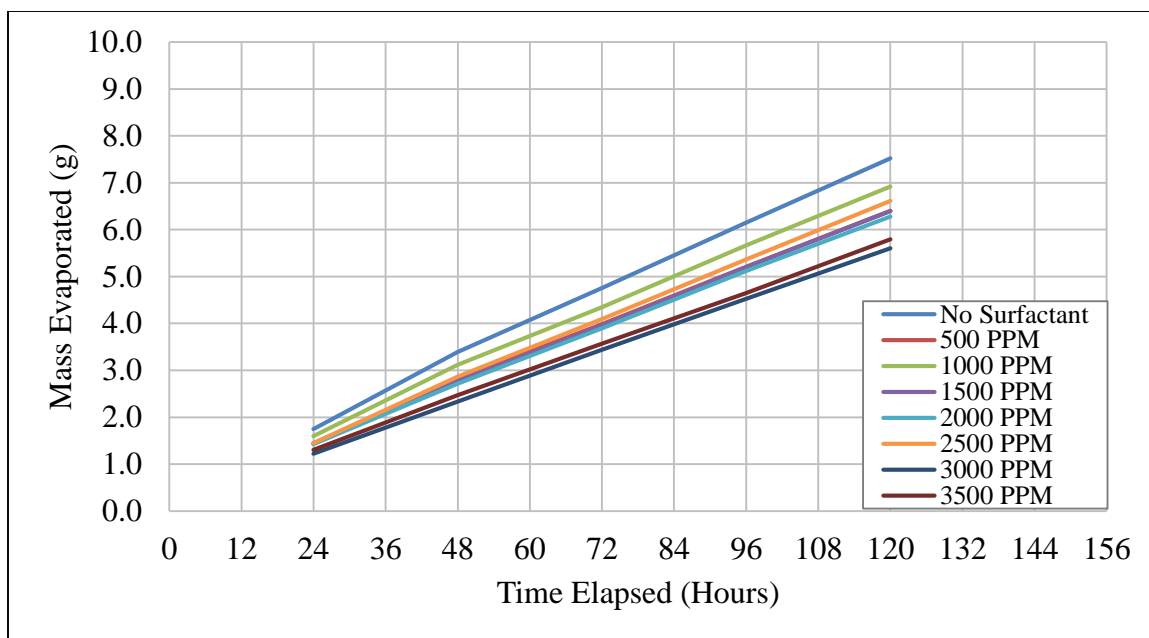


Figure 3.7 Average mass loss measurements over all SLS natural evaporation tests.

The normalized measurements for the SLS natural evaporation tests are shown in Figures 3.8 and 3.9. The measurements for natural evaporation are normalized by Equation 2-2 as previously discussed in Methodology: Treatment of the Data. The average evaporation suppression by SLS, shown in Figures 3.8 and 3.9, increased with increasing concentration in the aqueous solution up to CMC. The evaporation suppression decreased with time for all concentrations. The deterioration may be due to diffusion of the surfactant into the water or air or addition of contaminants, such as dust, from the environment (Barnes 1997). The largest deterioration in evaporation suppression from the beginning to the end of the test period was 14% for 2500 PPM. The 2000 PPM concentration yielded the best natural evaporation suppression effects over 120 hours for SLS ranging from 18% to 32%.

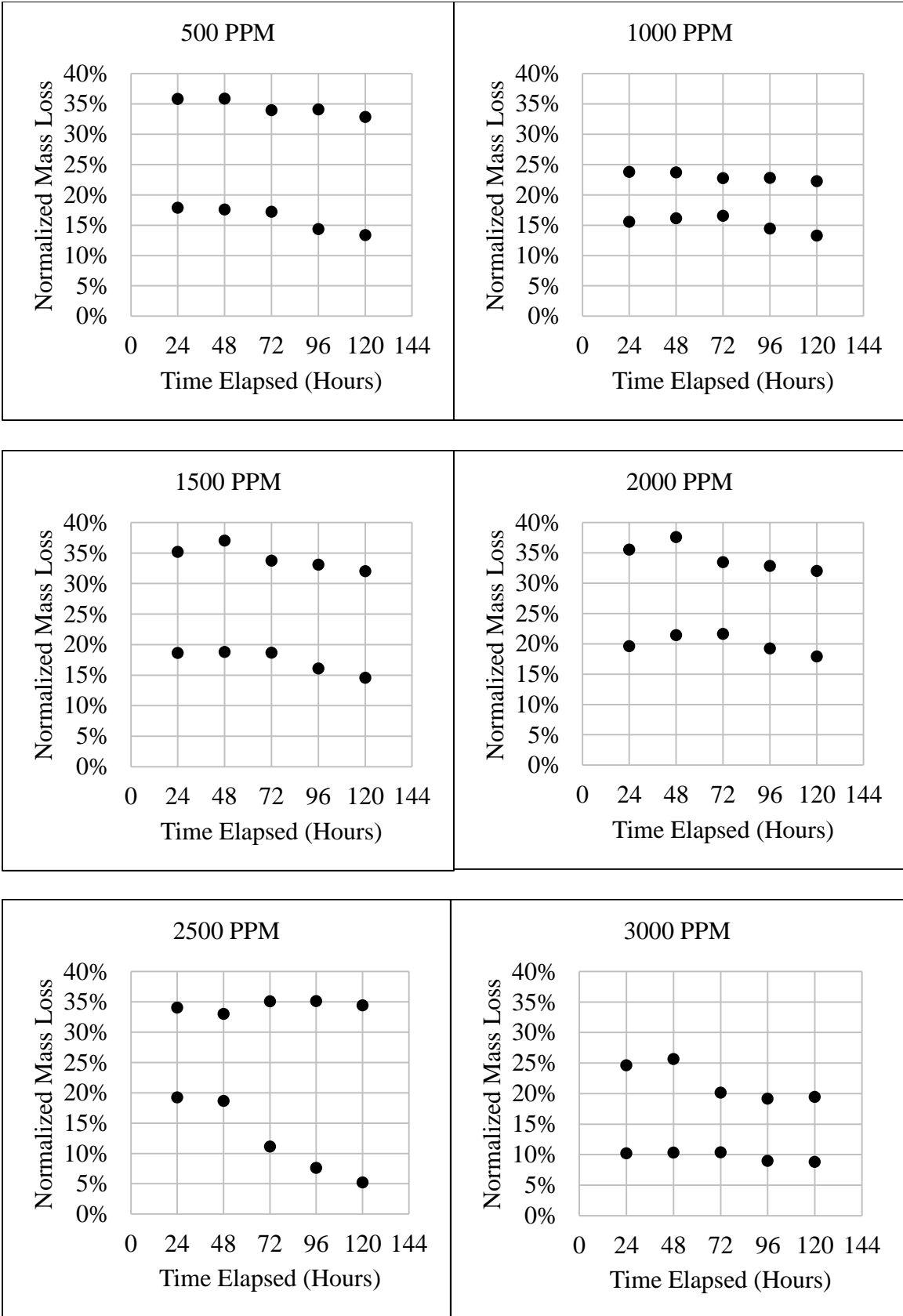


Figure 3.8 Normalized natural evaporation for 500 to 3000 PPM SLS.

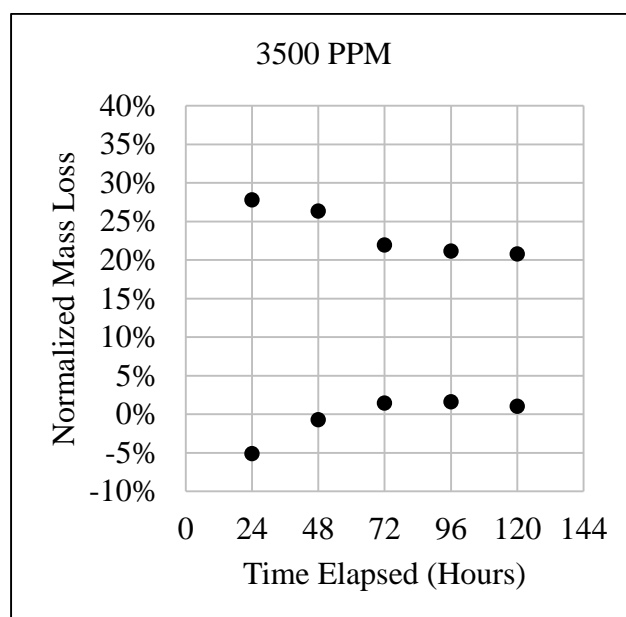


Figure 3.9 Normalized natural evaporation for 3500 PPM SLS.

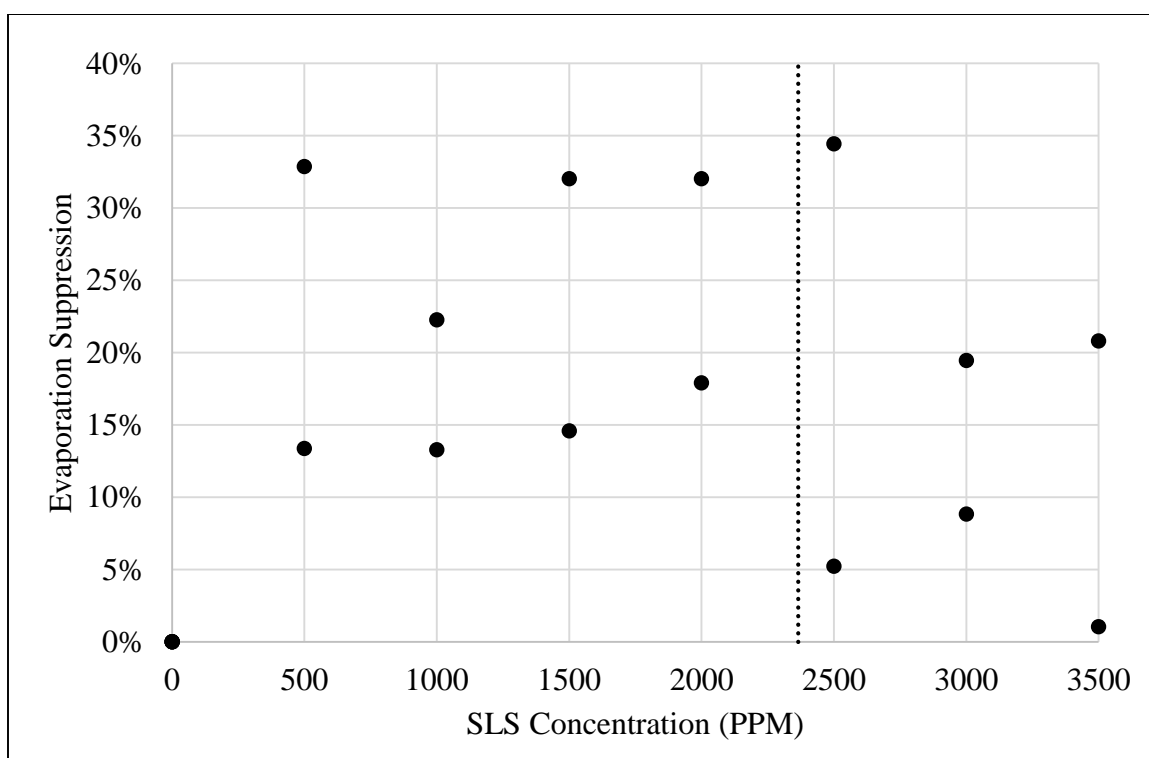


Figure 3.10 Natural evaporation suppression by SLS monolayers over 120 hours.

The evaporation suppression variation with increasing concentration at the air-water interface over 120 hours by SLS monolayers are shown in Figure 3.10. The average evaporation suppression increases slightly as concentration increases to CMC and then drops with increases in concentration above CMC.

Comparison between the measurements (Figures 3.5 and 3.6) and normalized measurements (Figures 3.8, 3.9, and 3.10) shows that variation in laboratory conditions may have some effect on experimental results. (This was discussed in a separate test explained in Methodology: Treatment of Data: Reliability Testing.) The measurements show that the concentrations of 3000 and 3500 PPM, which are much higher than CMC, performed the best as they had the lowest average mass losses. However, the control (0 PPM) solution measurements associated with tests of 3000 PPM and 3500 PPM show that the test conditions yielded lower evaporation effects for all solutions. The normalized measurements take into account the variation in conditions by comparison to the 0 PPM solution and shows that the 2000 PPM solutions performed better than the 3000 PPM and 3500 PPM solutions in evaporation suppression.

Surfactant monolayer theory suggests that the 2000 PPM should provide the highest evaporation suppression. Performance in laboratory setting should peak near the CMC (2365 PPM for SLS) because evaporation suppression is due to the monolayer formed at the air-water interface (Barnes, 1997) and CMC is an indication of surface saturation (Myers, 2006). Assuming the packing of the surfactant film is not adversely affected by the molecular structure, the film density should increase with increasing concentration up to CMC and then level off for concentrations exceeding CMC as additional surfactants

enter the body of the water in micelles (Myers, 2006). As the concentration of surfactant increases above CMC the free energy of the system will increase (due to increase of the structural distortion by additional surfactants) which may lead to an increase of evaporation (Vuglinsky, 2009). Micelles minimize this increase but do not eliminate the increase in system energy (Rosen, 2004).

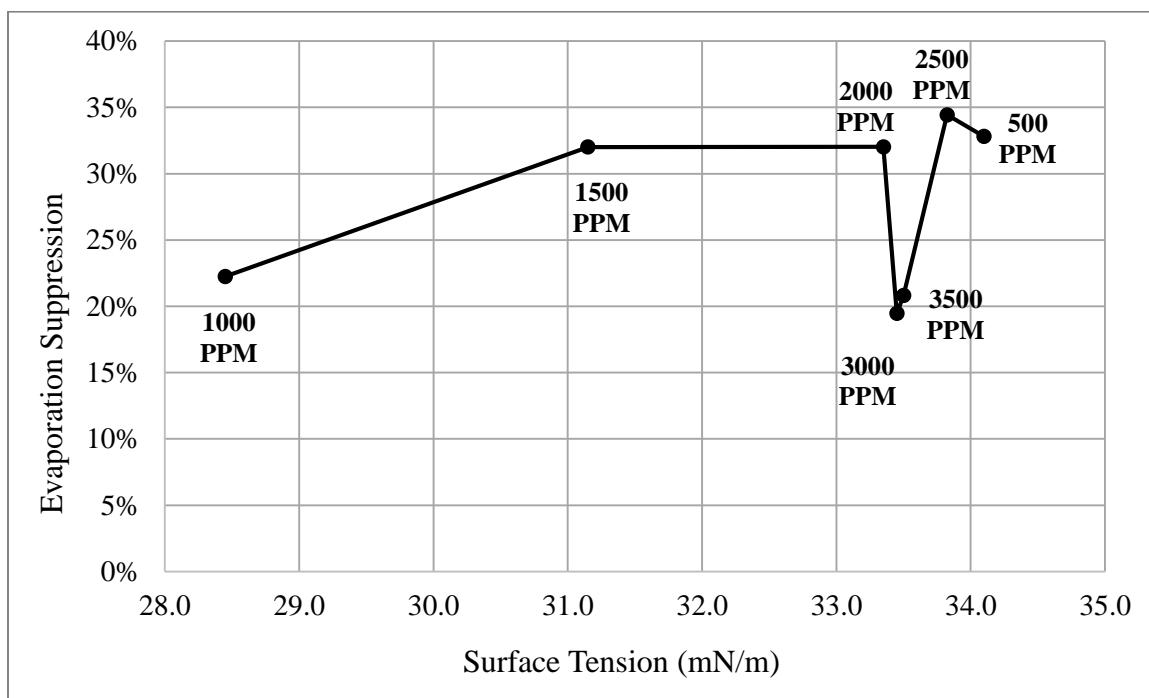


Figure 3.11 Maximum natural evaporation suppression versus surface tension for SLS.

The variation of the maximum evaporation suppression after 120 hours versus the measured surface tension for SLS natural evaporation tests is shown in Figure 3.11. Figure 3.11 shows that evaporation suppression is not directly related to the measured surface tension. The expected relation was an increase of natural evaporation suppression with decreasing surface tension. As the surface tension decreases, the surfactant concentration at the air-water interface increases which leads to closer molecular packing of the surfactant

monolayer. The close packing of the surfactant molecules may prevent permeation of water molecules through the surfactant monolayer, i.e. lower evaporation (Barnes, 1997). The increase in evaporation suppression associated with the surface tension increase from 1000 PPM to 1500 PPM is not witnessed for the surface tension increase from 1500 PPM to 2000 PPM. This discrepancy indicates that factors other than surface tension may be more relevant in determining the natural evaporation suppression performance of SLS for the concentrations tested.

3.2.2 ECOSURF™ EH-14

The mass loss measurements of ECOSURF™ EH-14 from the natural evaporation testing, shown in Figures 3.12 and 3.13, show that EH-14 suppresses evaporation of water. The results across tests varied slightly except for the 5500 PPM and 6500 PPM results which were more consistent across test runs. The control samples mass losses after 120 hours ranged from 6.5 to 9.5g from 100 g solutions (6.5-9.5%). The mass losses from the 5500 PPM and 6500 PPM were consistently the lowest staying near 6 g (6%).

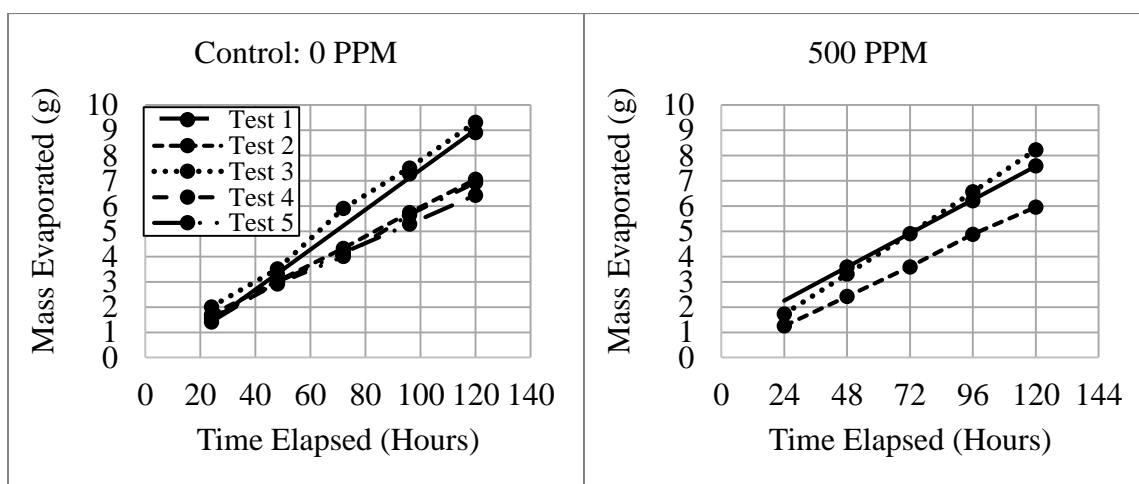


Figure 3.12 Natural evaporation mass losses for 0 and 500 PPM EH-14

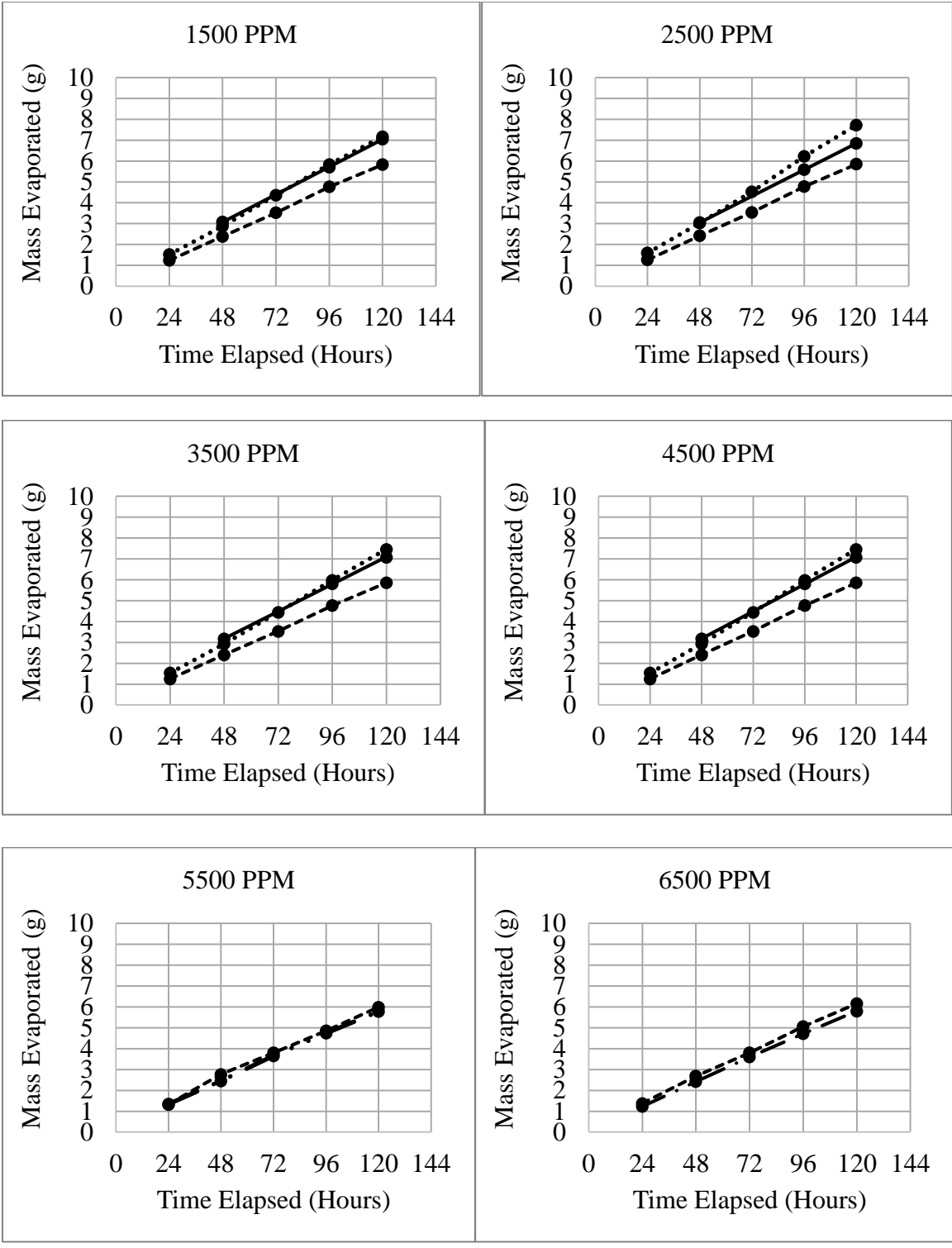


Figure 3.13 Natural evaporation mass losses for 1500 to 6500 PPM EH-14.

Average of the mass loss measurements for EH-14 natural evaporation tests from Figures 3.12 and 3.13 are shown in Figure 3.14. The average mass loss is lowest for the concentrations much higher than the CMC of 4018 PPM. The average mass loss after 120 hours did vary significantly for the concentrations from 1500 PPM to 4500 PPM.

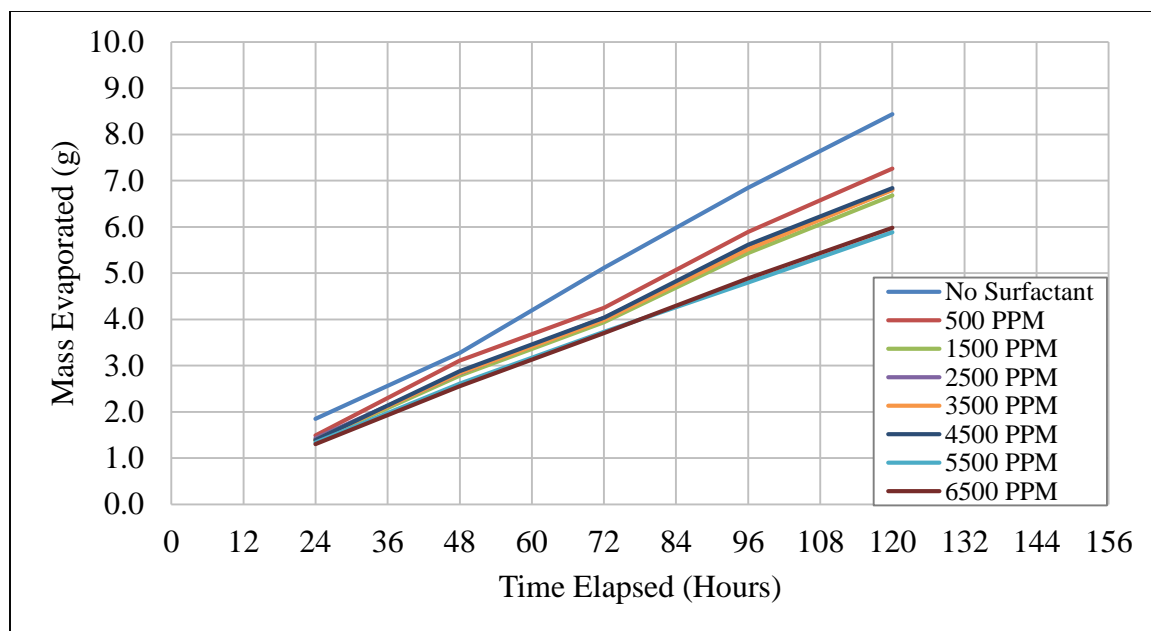


Figure 3.14 Average mass loss measurements for EH-14 natural evaporation tests.

Normalized mass loss measurements for EH-14 natural evaporation tests are shown in Figures 3.15 and 3.16. The evaporation suppression of water by ECOSURF™ EH-14, shown by the normalized mass loss measurements, generally decreased with time for all concentrations. The greatest decrease of suppression effects from the beginning to the end of the test period was 10% for 500 and 1500 PPM concentrations. The average suppression after 120 hours for the concentrations of 1500 PPM up to 4500 PPM was approximately 20%. The 500 PPM, 5500 PPM, and 6500 PPM concentrations had the lowest average suppression.

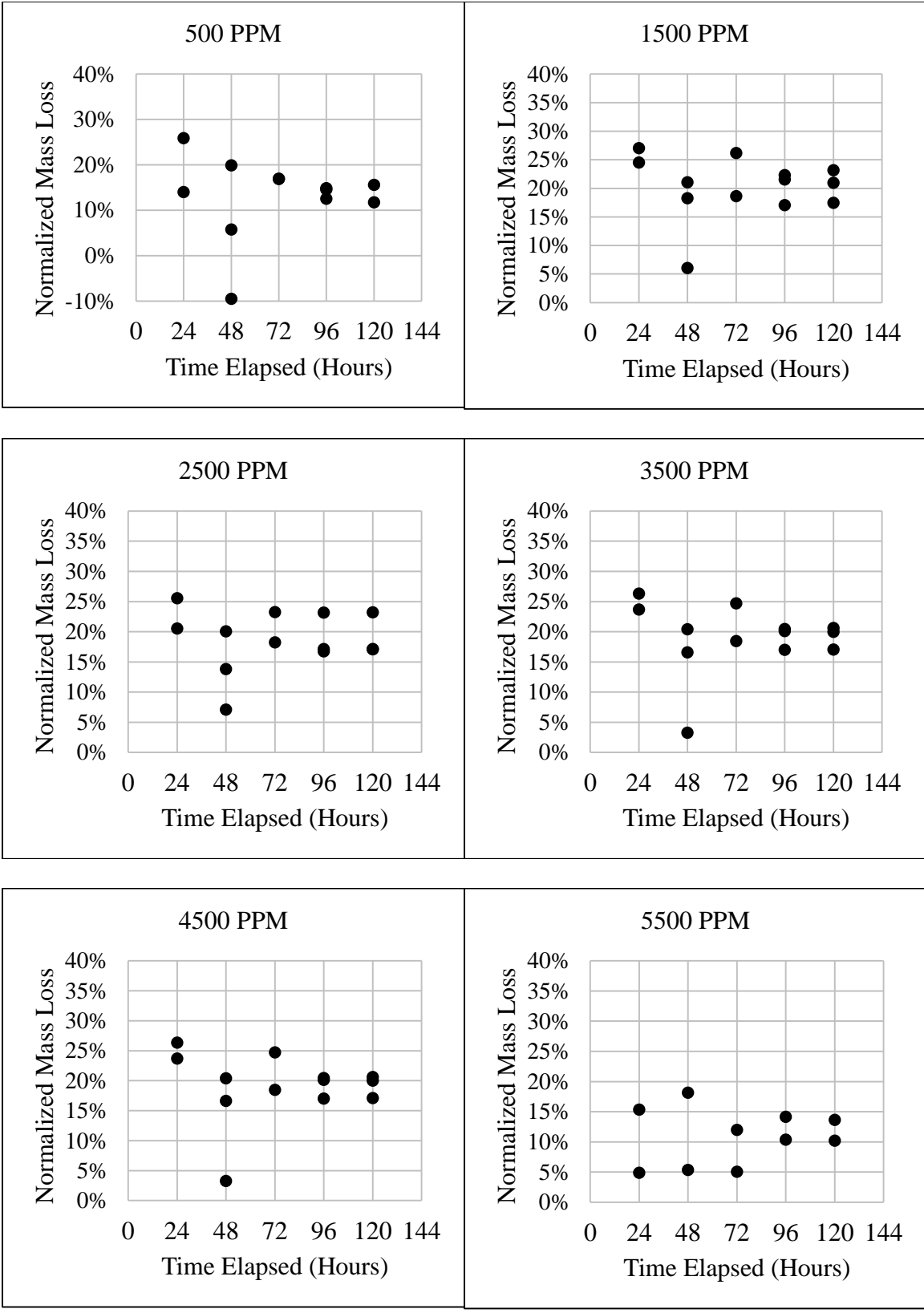


Figure 3.15 Normalized evaporation mass loss measurements: 500 to 5500 PPM EH-14

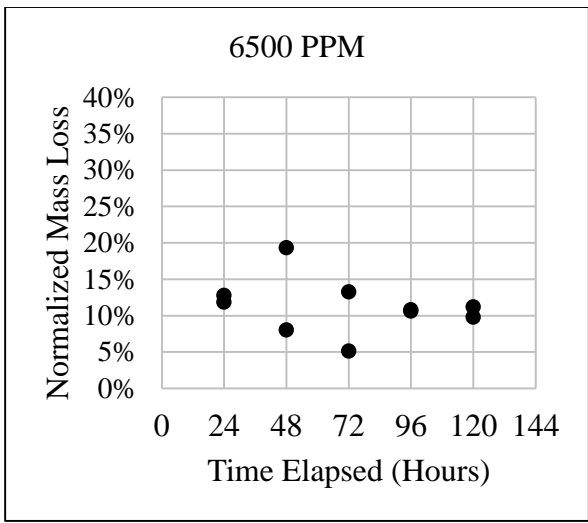


Figure 3.16 Normalized evaporation mass loss measurements: 6500 PPM EH-14.

The average evaporation suppression over the 120 hours of the natural evaporation tests are shown in Figure 3.17.

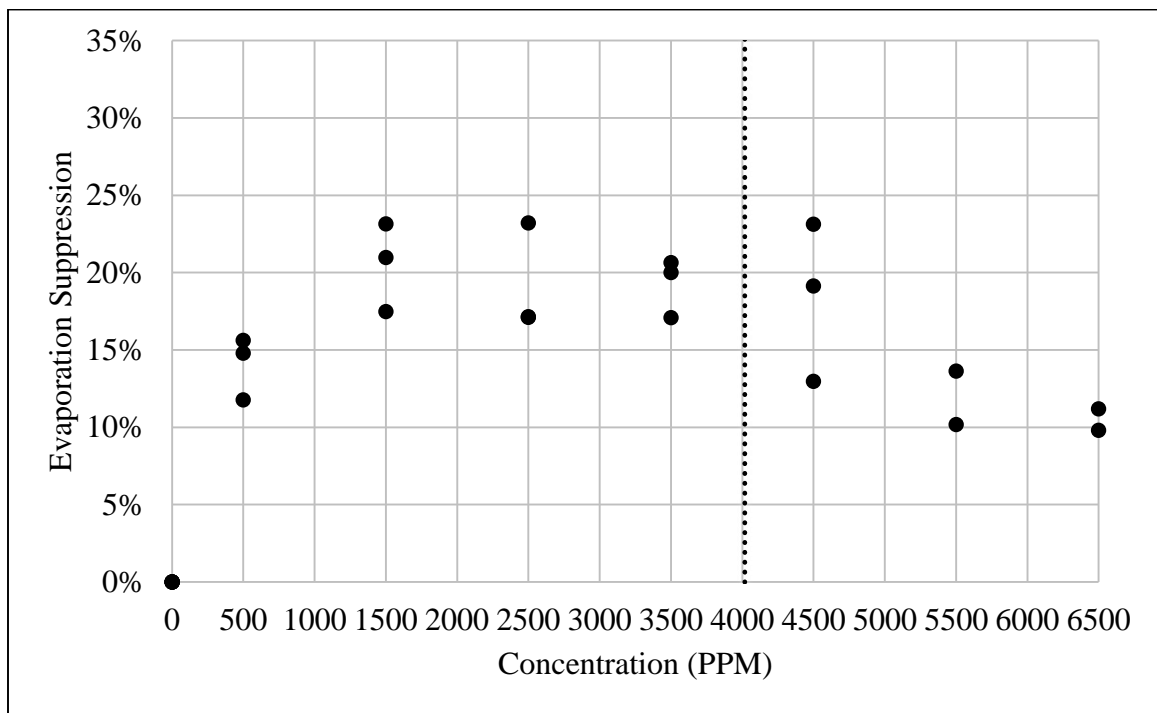


Figure 3.17 Natural evaporation suppression by EH-14 over 120 hours.

The average suppression after 120 hours increases with increasing concentration up to 1500 PPM, as shown in Figure 3.17. No significant change is observed in the average evaporation suppression with increasing concentration from 1500 PPM to the CMC of 4018 PPM. After CMC, the evaporation suppression decreases with increasing concentration.

The variation of the maximum evaporation suppression after 120 hours versus the measured surface tension for ECOSURF™ EH-14 natural evaporation tests is shown in Figure 3.18.

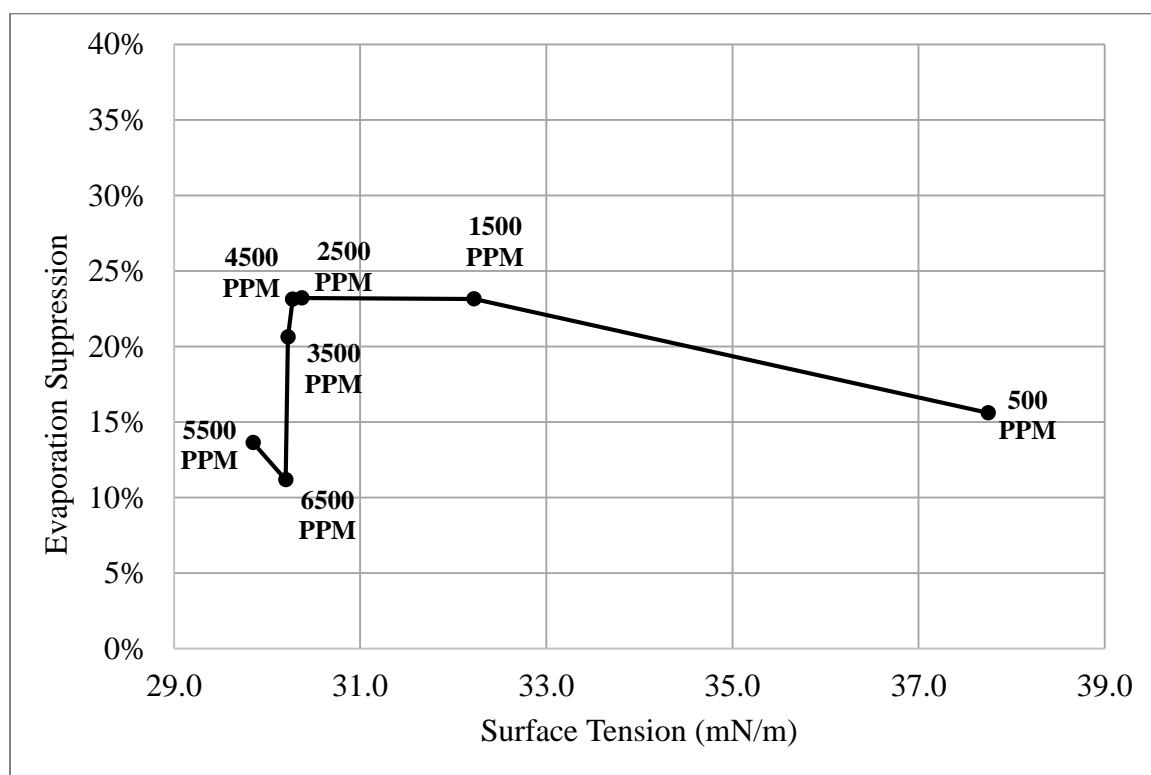


Figure 3.18 Maximum natural evaporation suppression versus surface tension for EH-14.

The EH-14 evaporation suppression showed some decrease with increasing surface tension, as shown in Figure 3.18. However, this trend was only seen between 37.8 mN/m

(500 PPM) and 32.2 mN/m (1500 PPM). The concentrations well above the CMC of 4018 PPM had the lowest evaporation suppression and the lowest surface tension. The expected relation is decreasing evaporation suppression with increasing surface tension as discussed in the SLS results. (See second from last paragraph in Section 3.2.1 for explanation.) This relation is not clearly shown by the current study results for ECOSURF™ EH-14.

3.2.3 ECOSURF™ SA-9

The measurements of mass loss by natural evaporation for ECOSURF™ SA-9, shown in Figures 3.19 and 3.20, show that SA-9 reduces evaporation of water. The mass loss across tests was consistent for the aqueous-surfactant solutions. The control mass losses after 120 hours ranged from just under 7 g to 8 g from 100 g solutions (7-8%). All surfactant solution mass losses ranged from 6 g to 7 g (6-7%) and showed little variation across concentrations.

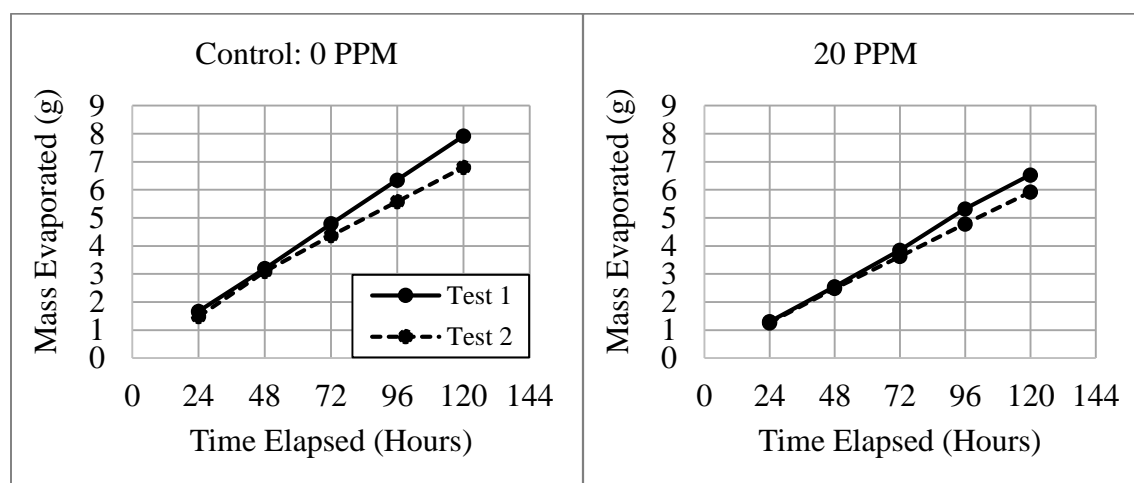


Figure 3.19 Natural evaporation mass loss measurements: 0 and 20 PPM SA-9.

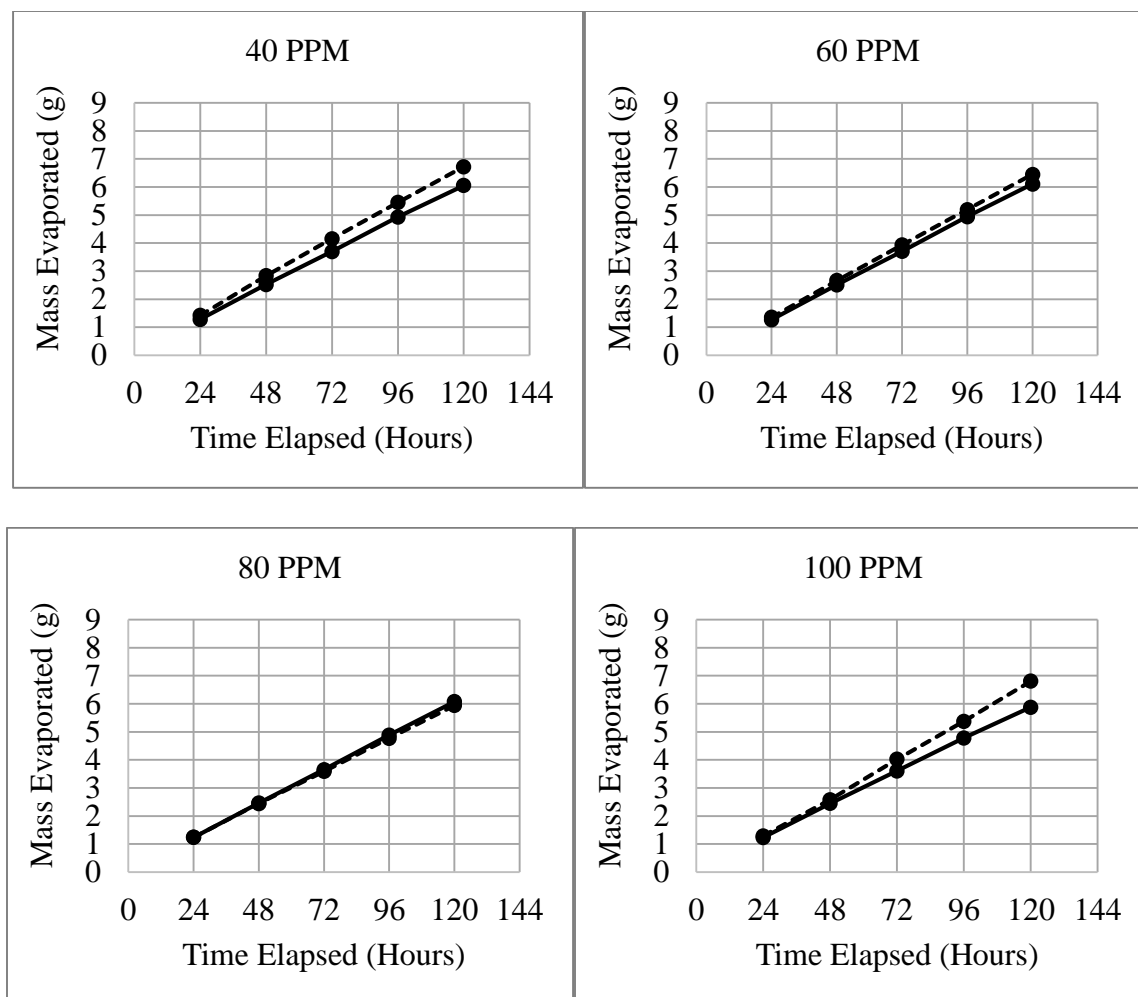


Figure 3.20 Natural evaporation mass loss measurements: 40 to 100 PPM SA-9.

The average of the mass loss measurements from Figures 3.19 and 3.20 are shown in Figure 3.21. The average mass loss from SA-9 solutions did not change significantly with changes in the surfactant solution concentration. This may result from all but one concentration being above CMC. Additional surfactant mass above CMC (22 PPM for SA-9) may go almost exclusively into micelle formation as the surfaces become saturated with surfactants (Myers, 2006). Thus, only the increase in concentration from 20 to 40

PPM would show an increase in the surfactant mass active at the air-water interface where the surfactant would have the most effect on evaporation.

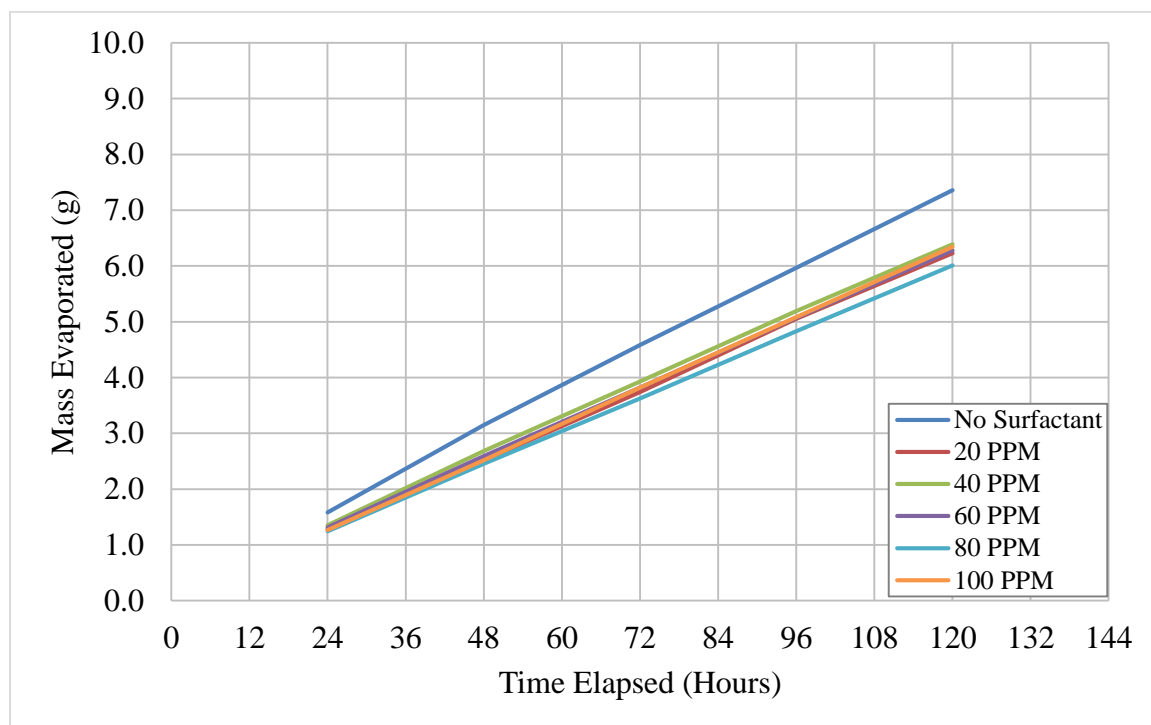


Figure 3.21 Average mass loss by SA-9 aqueous solutions in natural evaporation tests.

Normalized mass loss measurements for SA-9 aqueous solutions in natural evaporation tests are shown in Figures 3.22 and 3.23. Measurements are normalized as described in Methodology: Treatment of Data.

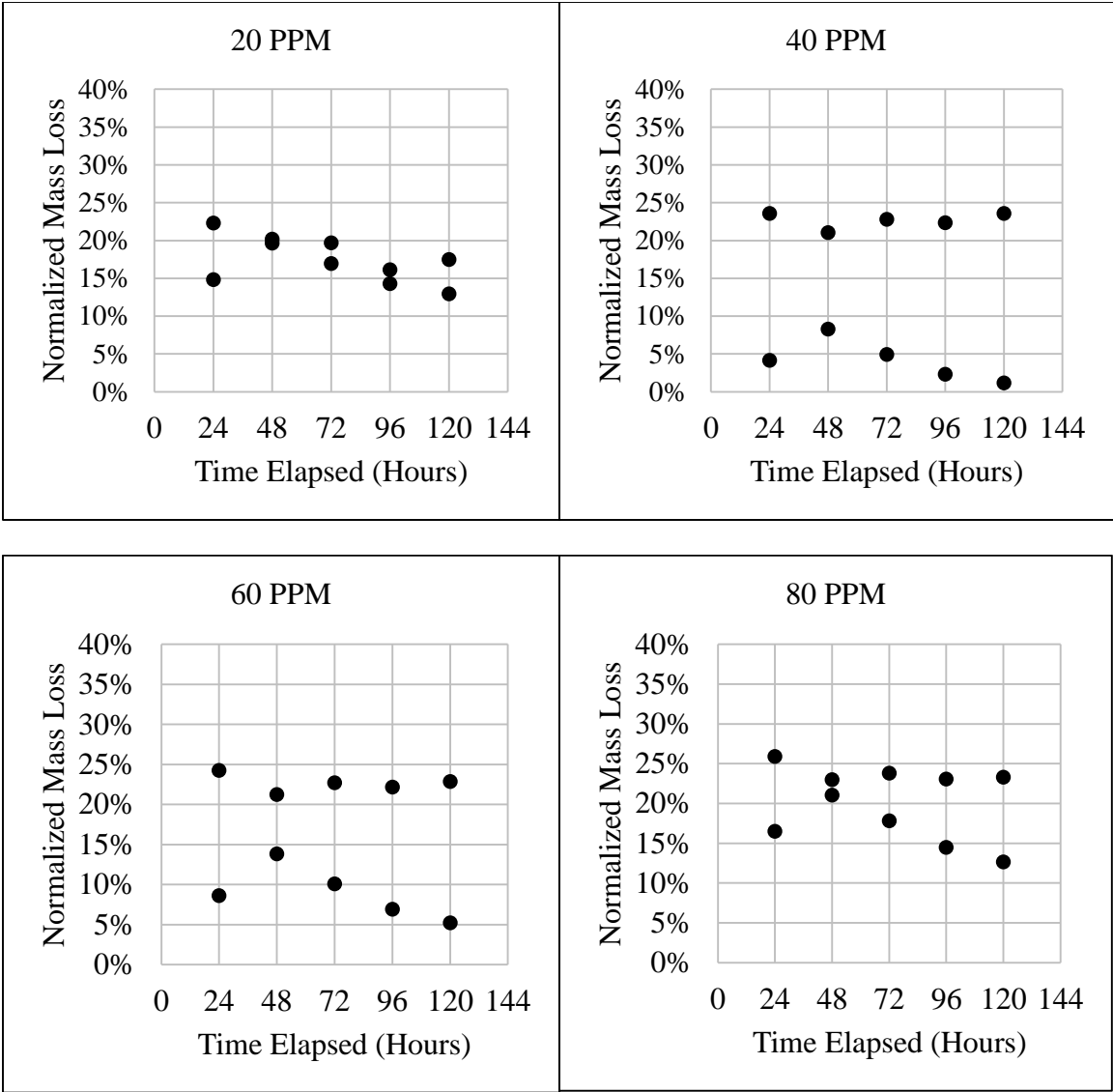


Figure 3.22 Normalized natural evaporation mass losses: 20, 40, 60, 80 PPM SA-9.

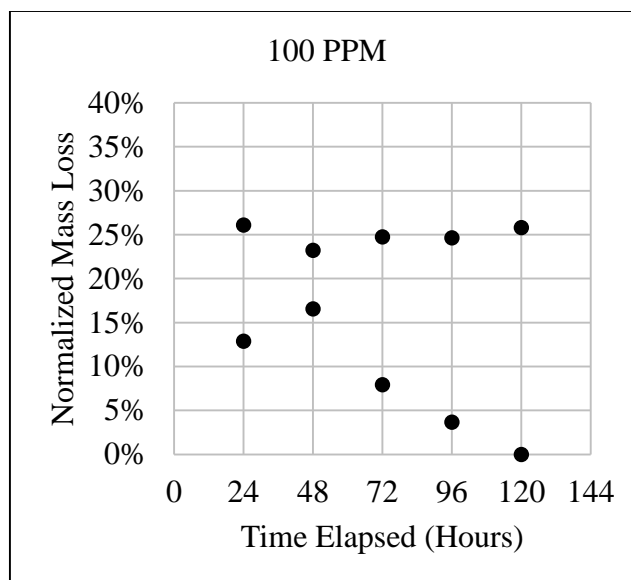


Figure 3.23 Normalized natural evaporation mass losses: 100 PPM SA-9.

The normalized measurements, Figures 3.22 and 3.23, show that SA-9 caused an evaporation suppression of up to 25%. The evaporation suppression deteriorates with time for all concentrations. The greatest deterioration in evaporation suppression from the beginning to end of the test period was 5% for the 20 PPM concentration. The average evaporation suppression for 20 PPM (the concentration just below the CMC of 22 PPM) was near 15%. The 80 PPM concentrations had the highest average evaporation suppression after 120 hours of 18%.

The evaporation suppression versus concentration in the natural evaporation tests of aqueous SA-9 solutions is shown in Figure 3.24. The evaporation suppression did not change significantly when concentration is increased above the 20 PPM concentration.

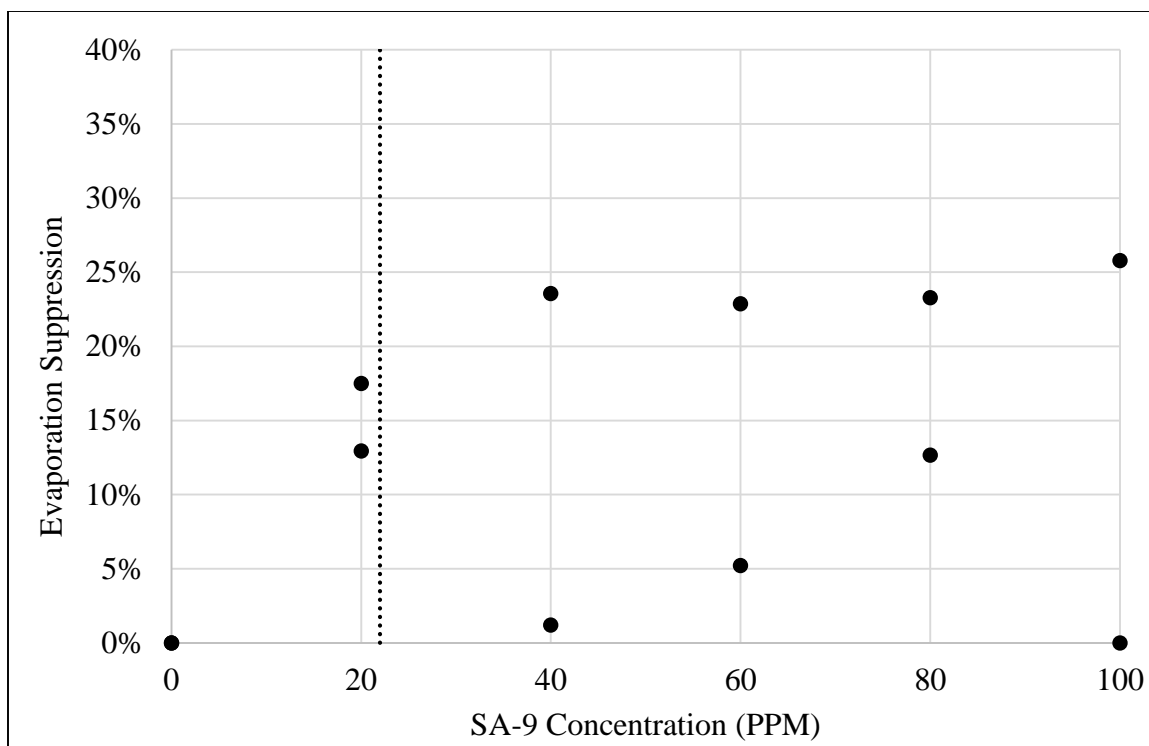


Figure 3.24 Natural evaporation suppression of water by SA-9 after 120 hours.

As discussed in the Sodium Lauryl Sulfate section, the concentration just below the CMC of 22 PPM should have the best evaporation suppression. The normalized mass loss measurements show that the 20 PPM solution had consistently high evaporation suppression as compared to other concentrations. The mass loss measurements show that the mass losses did not increase or decrease with increasing concentrations of SA-9. There is no disagreement between the conclusions drawn from mass loss measurements and the normalized measurements for ECOSURF™ SA-9.

The variation of the maximum evaporation suppression after 120 hours versus the measured surface tension for ECOSURF™ SA-9 natural evaporation tests is shown in Figure 3.25.

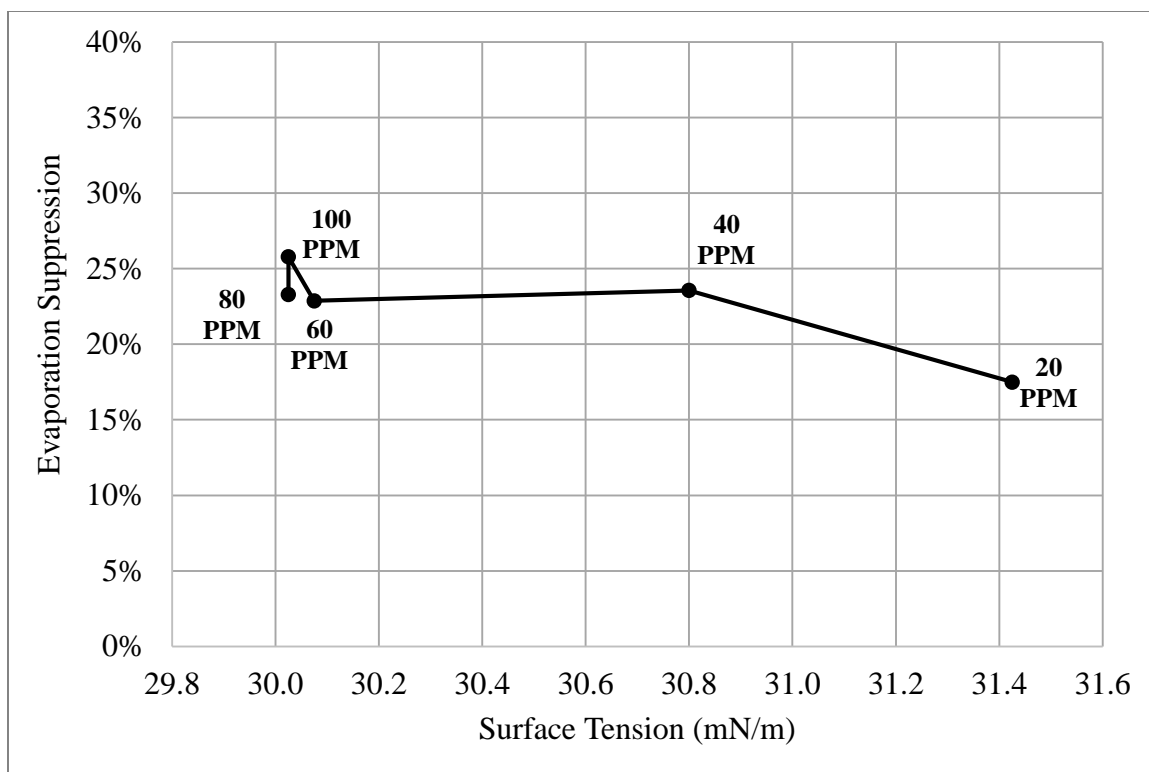


Figure 3.25 Maximum natural evaporation suppression versus surface tension for SA-9.

The evaporation suppression does not have a direct relation to surface tension. The expected decrease of evaporation suppression with increasing surface tension (see second from last paragraph in Section 3.2.1 for explanation) is seen between 30.8 mN/m (40 PPM) and 31.4 mN/m (20 PPM) but is not seen for other changes in surface tension between surfactant solutions. As all but 20 PPM are above the CMC, the surface tension for the current study solutions do not change significantly. Thus, surface tension may not be the only parameter affecting the surface evaporation.

3.2.4 Further Discussion of Natural Evaporation Results

Results from this study do not show a strong relation between surface tension and natural evaporation suppression for the surfactants and concentrations tested. The results

suggest that there may be other factors may more important than surface tension in determining surfactant ability to lower evaporation of water. Other surfactant characteristics which could affect the evaporation suppression include the density of packing at the air-water interface (Prime E. et al., 2012), the surface pressure (Barnes, 2008), and the elasticity of the surfactant monolayer (Bower & Saylor, 2011). These factors could affect the diffusion rates of water into air and also hinder motion of molecules of the water near the interface thus lowering convection.

The evaporation rates predicted for natural evaporation for water without surfactants for the current study conditions were: 0.015 g/hr if mass transfer occurred by diffusion alone, 0.34 g/hr if mass transfer occurred by natural convection, and 1.7 g/hr if mass transfer occurred by forced convection. (See Appendix C for calculations.) The muslin gauze was expected to hinder most of both forced and natural convection. Therefore, the expected evaporation rate for the current study was higher than 0.015 g/hr but significantly lower than 0.34 g/hr. The average evaporation rate for water without surfactant over all tests was observed to be 0.062 g/hr.

3.3 Subcooled Boiling Evaporation Measurements

The mass loss measurements for SLS, EH-14, and SA-9 aqueous solutions during subcooled pool boiling evaporation tests are shown in Figures 3.26, 3.27, and 3.28 respectively.

3.3.1 Sodium Lauryl Sulfate

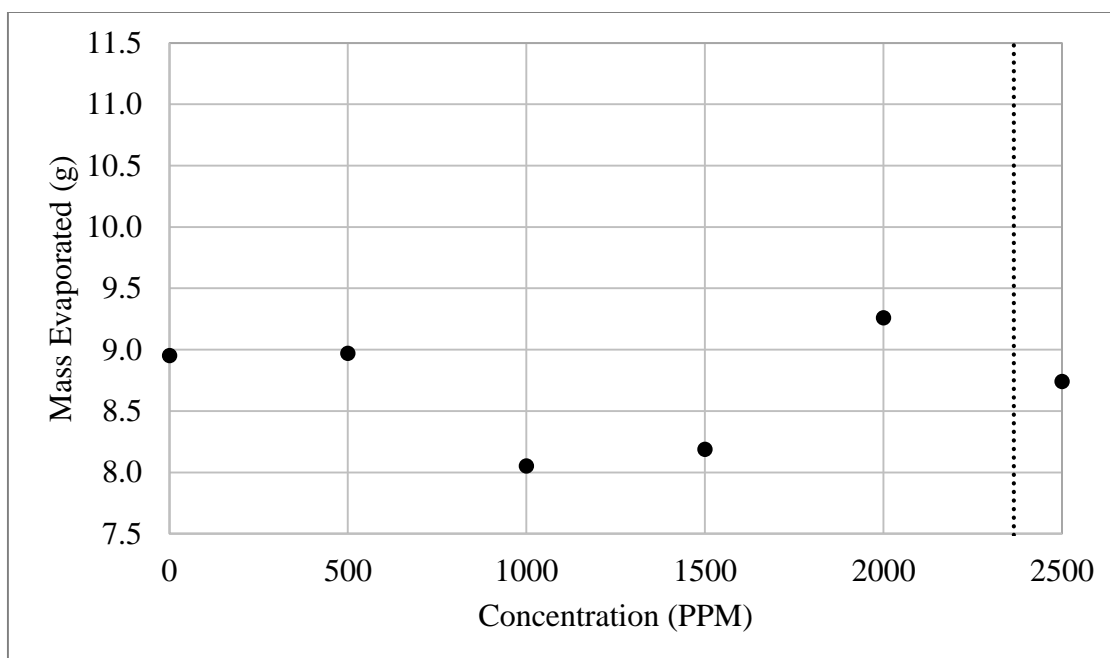


Figure 3.26 Subcooled boiling mass evaporation measurements for SLS solutions.

Figure 3.26 shows the mass evaporated at subcooled boiling versus the concentration of sodium lauryl sulfate. A 10% decrease of evaporation mass loss at the 1000 PPM concentration was observed. The subcooled boiling evaporation occurs at the heated surface as opposed to the evaporation occurring at the air-water interface in the natural evaporation tests. Thus, the effects seen for subcooled boiling may not be similar to the effects seen for natural evaporation. The SLS monolayer at the heated surface may

hinder motion at the heated surface during the boiling initiation and thus lower heat transfer for the subcooled boiling conditions.

3.3.2 ECOSURF™ EH-14

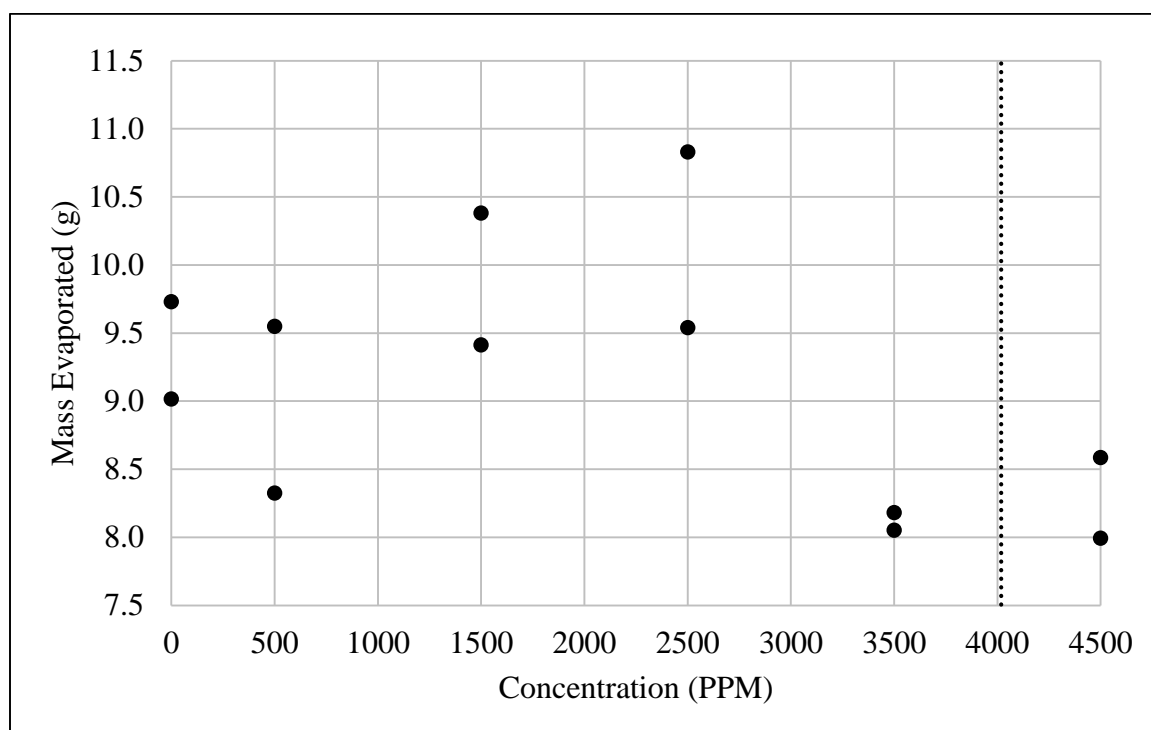


Figure 3.27 Subcooled boiling mass evaporation measurements for EH-14 solutions.

The mass loss measurements ECOSURF™ EH-14 aqueous solutions during subcooled pool boiling evaporation tests are shown in Figure 3.27. EH-14 had some effect on the subcooled boiling evaporation of water. The general trend was an increase in mass loss with increasing concentration up to 2500 PPM. The concentrations near the CMC of 4018 PPM decreased the mass loss during subcooled boiling. An average 8.7% increase of evaporation mass loss at 2500 PPM and an average 13.4% decrease of evaporation mass loss at 3500 PPM are observed. The lack of increase in evaporation for concentrations near

the CMC of 4018 PPM indicates that the EH-14 micelle formation adversely affects vapor formation for subcooled boiling. The micelles may negatively affect the re-adsorption rate of the surfactant molecules to the heated surface. The surfactants on the heated surface will be moved away from the surface by the vapor nuclei released from the heated surface.

3.3.3 ECOSURF™ SA-9

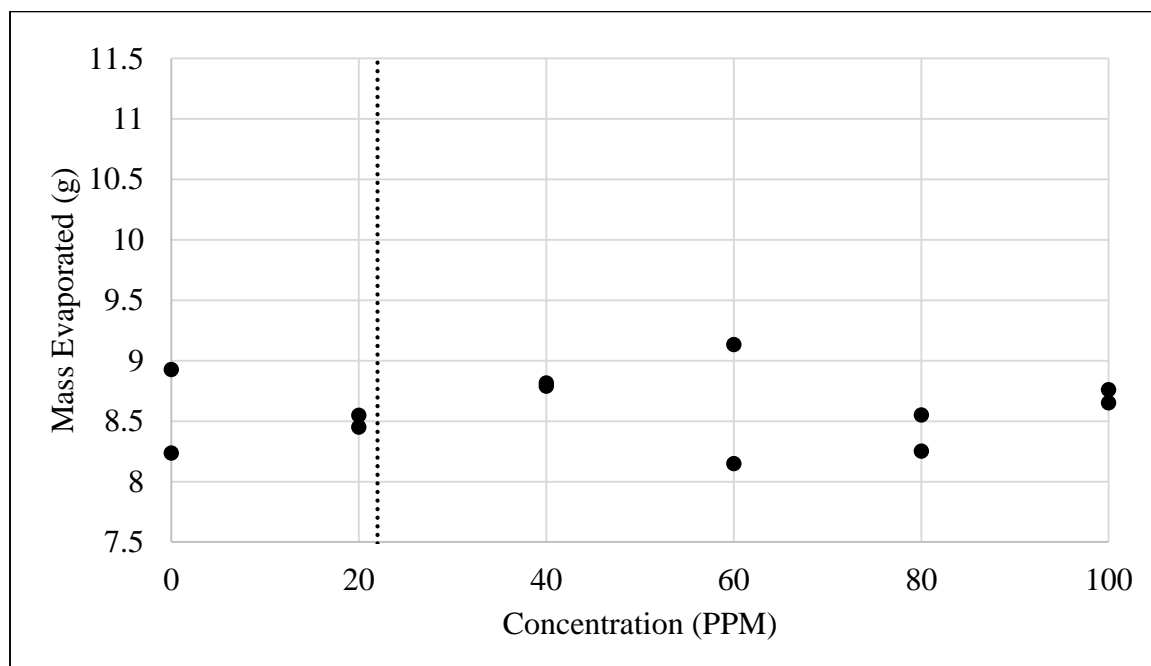


Figure 3.28 Subcooled mass evaporation measurements for SA-9 solutions.

The mass loss measurements for ECOSURF™ SA-9 aqueous solutions during subcooled pool boiling evaporation tests are shown in Figure 3.28. SA-9 did not significantly affect the evaporation mass loss of subcooled boiling water. The SA-9 lack of effect on evaporation may be due to the relative high concentrations tested. Concentrations for SLS and EH-14 near or above their respective CMCs showed little effect on subcooled boiling evaporation. SA-9 concentrations tested were all near or higher

than the CMC of 22 PPM. Thus, all three surfactants tested showed insignificant effect on subcooled boiling evaporation for concentrations near or above their respective CMC.

3.3.4 Further Discussion of Subcooled Boiling Evaporation Results

The relation, observed below CMC, between surface tension and evaporation suppression was opposite for SLS and ECOSURF™ EH-14. The trends under CMC seen in the current study were that the lowering of surface tension led to a decrease in evaporation by the anionic surfactant (SLS) and an increase in evaporation by the nonionic surfactant (EH-14). An explanation for the contrast may be that the SLS monolayer at the heated surface is lowering convective motion at the heated surface and the EH-14 monolayer is not. The two surfactants monolayers may have different effects because of the interaction between the surfactants and the heated surface, which is negatively, charged (Rosen, 2004). Thus, a negative charge on the SLS may cause a different effect from the neutral charge of the EH-14 on the sub-cooled boiling phenomena occurring at the negative surface.

The mass loss for boiling water without surfactants was calculated as 35.5 g/min for the current study conditions. The average mass loss for water without surfactants in current study tests is observed to be 1.79 g/min. The calculated value is higher than the observed values because Rohsenow correlation is used for nucleate boiling rather than subcooled boiling. Also, the assumed value for C_{sf} may be too low or the assumed value for surface temperature may be too high. See Appendix C for calculations.

Adding surfactants can lower the liquid-vapor surface tension and thereby increase the frequency of the bubble departure from the heated surface and thus increases heat

transfer. The increase of heat transfer by decreasing surface tension (σ) can be seen in the Rohsenow correlation (Cengel, 2011):

$$\dot{q}_{nucleate} = \mu_l h_{fg} \left[\frac{g(\rho_l - \rho_g)}{\sigma} \right]^{\frac{1}{2}} \left[\frac{c_{pl}(T_s - T_{sat})}{C_{sf} h_{fg} Pr_l^n} \right]^3 = h_{heat}(T_s - T_{sat}) = \frac{\dot{m}_b h_{fg}}{A} \quad (3-1)$$

Additionally, the increase in heat transfer will translate to an increase in boiling mass evaporation rate (\dot{m}_b). Under steady state conditions, all heat addition to boiling water will result in water evaporation (Cengel, 2011). The study of air-water surface tension will not have a direct relation to boiling at the heated surface but could be used as an indication of how much of the surfactant mass will be available to aggregate at the heated surface.

Dikici & Al-Sukaini (2016) found that SLS, ECOSURF™ EH-14, and ECOSURF™ SA-9 increased heat transfer and lowered wall temperatures at a given heat flux. The concentrations which had the highest effects on boiling were 400 PPM for SLS, 800 PPM for EH-14, and 200 PPM for SA-9. Increases in concentrations beyond these respective concentrations showed “no further improvement” (p.5). Up to 31%, 18%, and 10% lower wall superheats for SLS, EH-14, and SA-9 respectively were found as compared to water. Boiling heat transfer coefficients were observed to increase by up to 46% for SLS, 30% for EH-14, and 21% for SA-9. The heat flux in the current study is much higher than the max heat flux used in the Dikici & Al-Sukaini study. Thus, the results of the two studies are not compared.

Chapter 4

Conclusions and Recommendations

Sodium lauryl sulfate, ECOSURF™ EH-14, and ECOSURF™ SA-9 were tested in aqueous solutions for their effects on surface tension, natural evaporation, and subcooled boiling evaporation. The conclusions of the study and recommendations for future studies are presented in this section.

4.1 Conclusions

4.1.1 Surface Tension Suppression

Sodium lauryl sulfate, ECOSURF™ EH-14, ECOSURF™ SA-9 surfactants were shown to depress the surface tension of distilled water. The lowest respective concentration for each surfactant (500 PPM for SLS, 500 PPM for EH-14, and 20 PPM for SA-9) had the greatest effect on surface tension with some additional effect observed with increase of concentration up to critical micelle concentration. No significant change in surface tension was observed with increasing concentration above CMC. SLS had the highest surface tension for concentrations higher than CMC with values measured at 33.5 (mN/m). EH-14 and SA-9 both had minimum surface tensions measured near 30.0 (mN/m). SLS measurements were consistent with measurements found in literature concentrations from 0 to 500 PPM and from 2000 to 3500 PPM.

4.1.2 Natural Evaporation Suppression

Evaporation Suppression by Surfactants

SLS, SA-9, and EH-14 all lowered the natural evaporation of aqueous solutions. The application of a surfactant monolayer lowered evaporation of water by up to 35%. SLS was the most effective at lowering evaporation rates in these natural evaporation tests

with natural evaporation suppression ranging from 10% to 35%. EH-14 was more effective than SA-9 at evaporation suppression. The water saved by EH-14 ranged from 10% to 23% for the 5 day tests. The water saved by SA-9 over the 5 day tests ranged from 0% to 26%. The most consistently effective concentrations at natural evaporation suppression were all near but below the respective CMCs: 2000 PPM for SLS, 3500 PPM for EH-14, and 20 PPM for SA-9.

Natural Evaporation and Surface Tension

A consistent relation between natural evaporation suppression and surface tension suppression was not seen for any of the surfactants tested. The evaporation suppression decreased with decreasing surface tension for SLS. However, the natural evaporation suppression increased with decreasing surface tension for EH-14 and SA-9. These trends were only seen below CMC. Thus, the current study shows that surface tension is not the only parameter affecting the natural evaporation.

Natural Evaporation Suppression and CMC

Effect of CMC was difficult to ascertain for SA-9 because of its low CMC. For SLS and EH-14, the natural evaporation suppression for concentrations above these surfactants' respective CMCs were the lowest measured. The concentrations below CMC were more effective at lowering evaporation of water. The results of this study indicate that micelles may lower the effectiveness of natural evaporation suppression for both SLS and EH-14.

4.1.3 Subcooled Boiling Evaporation Suppression

The surfactants of this study had varying effects on subcooled aqueous solution evaporation. SLS was the only surfactant to lower evaporation at concentrations below

CMC. EH-14 increased evaporation below CMC and SA-9 had showed least effect on evaporation at all concentrations. SLS and EH-14 both showed a relation between CMC and the subcooled boiling evaporation effects. The SLS effects on evaporation were mitigated near CMC and the EH-14 effects were reversed near CMC (from increasing water loss to lowering water loss). The SA-9 solutions were all near or above CMC and all concentrations showed insignificant effects on evaporation losses.

The effects on subcooled boiling evaporation for all 3 surfactants generally stayed below 10% increases or decreases. Thus, the effect on subcooled boiling evaporation was minimal despite significant heat transfer coefficients observed by Dikici & Al-Sukaini (2016) for the current study surfactants. No relation was seen between evaporation and surface tension suppression. This is may be due to the vapor nuclei formation occurring at the heated surface and not the air-water interface. Pre-boiling evaporation may be affected by the monolayer at the air-water interface but this effect was not measured in the current study. Surface tension at the air-water interface may be used to indicate how much of the surfactant is active at the heated surface. However, the contact angle between the heated surface and the surfactant solutions may be a better indicator of surfactant effect on activity at the heated surface.

4.2 Recommendations

Several conclusions were drawn based on the current study of sodium lauryl sulfate, ECOSURF™ EH-14, and ECOSURF™ SA-9 effects on surface tension, natural evaporation, and subcooled boiling evaporation. Recommendations for future studies based on the conclusions of the current study follow.

4.2.1 Natural Evaporation Further Studies

The current study showed that SLS, EH-14, and SA-9 all suppress the natural evaporation of water. Experimenting should be done to determine the monolayers performance under wind shear. Wind shear increases the convection over the air-water interface. The ability of the monolayers to lower convection rates and not break up under wind shear is very important. Based on literature, monolayers may have more effects on lowering convection than on suppressing water to air diffusion. The effects of wind shear on the monolayers evaporation suppression effects is the next logical step to determine the potential of these surfactants to lower water reservoir evaporation losses.

4.2.2 Subcooled Boiling Evaporation Further Studies

The surfactants effect on subcooled pool boiling evaporation was minimal and variable. However, due to surfactants activity at interfaces, studies could be performed on subcooled flow boiling. Some caution would be warranted due to potential flash points if surfactant sediment were to build up on the heated surface.

References

- Australian Bureau of Meteorology. (2016, May 6). April Rainfall Reduces Deficiencies in Some Areas. Retrieved from <http://www.bom.gov.au/climate/drought/archive/20160505.shtml>
- Barnes, G. T. (1997). Permeation through monolayers. *Colloids and Surfaces A: Physicochemical and Engineering Aspects*, 126(2), 149-158.
- Barnes, G. T. (2008, January 18). The potential for monolayers to reduce the evaporation of water from large water storages. *Agricultural Water Management*, 95(4), 339-353.
- Biswal, R.R. (2012). Effect of Surfactant on Evaporation of Water. (Bachelor of Technology Thesis). Retrieved from National Institute of Technology, Rourkela website. URL: <http://ethesis.nitrkl.ac.in/3249/1/Thesis.pdf>
- Bower, S. M., & Saylor, J. R. (2011). The effects of surfactant monolayers on free surface natural convection. *International Journal of Heat and Mass Transfer*, 54(25), 5348-5358.
- C.R. (2004) Force tensiometry with ring and plate. (Report No. TN308e). Retrieved from www.Kruss.de: https://www.kruss.de/fileadmin/user_upload/website/literature/kruss-n308-en.pdf
- Çengel, Y. A., & Ghajar, A. J. (2011). *Heat and mass transfer: Fundamentals & applications* (Fourth ed.). New York: McGraw-Hill.
- Chen, Y.F., Yang, C.H., Chang, M.S., Ciou, Y.P., Huang, Y.C. (2010, November 4). Foam properties and detergent abilities of the saponins from *Camellia oleifera*. *International Journal of Molecular Sciences*, 11, 4417-4425.
- Cheng, L., Mewes, D., & Luke, A. (2007). Boiling phenomena with surfactants and polymeric additives: A state-of-the-art review. *International Journal of Heat and Mass Transfer*, 50(13), 2744-2771.
- Dawood, K.A., Rashid, F.L., Hashim, A. (2013). Reduce evaporation losses from water reservoirs. *International Journal of Energy and Environmental Research*, 1(1), 23-29.
- Daily Water Resources Update. (2016, June 24). Retrieved from http://www.cnrfc.noaa.gov/water_resources_update.php
- Dikici, B., Eno, E., & Compere, M. (2014). Pool boiling enhancement with environmentally friendly surfactant additives. *Journal of Thermal Analysis and Calorimetry*, 116(3), 1387-1394.

Dikici, B., Al-Sukaini, B.Q.A. (2016, June). Comparisons of Aqueous Surfactant solutions for Nucleate Pool Boiling. ASME 2016 Power and Energy Conference and Exhibition, Charlotte, North Carolina.

Di Liberto, T. (2016, February 17). A Not so Rainy Season: Drought in Southern Africa in January 2016. Retrieved from <https://www.climate.gov/news-features/event-tracker/not-so-rainy-season-drought-southern-africa-january-2016>

Doganci, M.D., Sesli, B.U., Erbil, H.Y. (2011). Diffusion-controlled evaporation of sodium dodecyl sulfate solution drops placed on a hydrophobic substrate. *Journal of Colloid and Interface Science*, 362, 524-531.

The Dow Chemical Company. (2013). ECOSURF™ EH-14 (90% Actives) Surfactant: Product Information. (Form No. 119-0316-5/13). Retrieved from http://msdssearch.dow.com/PublishedLiteratureDOWCOM/dh_08d3/0901b803808d367d.pdf?filepath=surfactants/pdfs/noreg/119-02316.pdf&fromPage=GetDoc

The Dow Chemical Company. (2012). ECOSURF™ SA-9 Surfactant: Product Information. (Form No. 119-02220-0112). Retrieved from http://msdssearch.dow.com/PublishedLiteratureDOWCOM/dh_088e/0901b8038088e25b.pdf?filepath=surfactants/pdfs/noreg/119-02220.pdf&fromPage=GetDoc

Elghanam, R. I., Fawal, M. M. E., Abdel Aziz, R., Skr, M. H., & Hamza Khalifa, A. (2011). Experimental study of nucleate boiling heat transfer enhancement by using surfactant. *Ain Shams Engineering Journal*, 2(3-4), 195-209.

Fellows, C. M., Coop, P. A., Lamb, D. W., Bradbury, R. C., Schiretz, H. F., & Woolley, A. J. (2015). Understanding the role of monolayers in retarding evaporation from water storage bodies. *Chemical Physics Letters*, 623, 37-41.

Frey Scientific. (2014, April 8). Sodium Lauryl Sulfate Safety Data Sheet. (SDS No. SS0650). Retrieved from https://store.schoolspecialty.com/OA_HTML/xxssi_ibeGetWCCFile.jsp?docName=F2817484

Gray, E. (2016, March 1). NASA Finds Drought in Eastern Mediterranean Worst of Past 900 Years. Retrieved from <http://www.nasa.gov/feature/goddard/2016/nasafindsdroughtineasternmediterraneanworstofpast900years>

Hightower, M., Brown, G. (2004, April 21-22) Evaporation Suppression Research and Applications for Water Management. *Identifying Technologies to Improve Regional Water Stewardship: North-Middle Rio Grand Corridor*, 76-78.

Kino. (2005) Method of Surface Tensiometer and Interfacial Tensiometry for Measurement of Surface Tension and Interface Tension. Retrieved from <http://www.surface-tension.org/news/55.html>

Kou, J., Judd, K. P., & Saylor, J. R. (2011). The temperature statistics of a surfactant-covered air/water interface during mixed convection heat transfer and evaporation. *International Journal of Heat and Mass Transfer*, 54(15), 3394-3405.

Kyowa. (2015, September 10). Fundamental of Surface Tension. Kyowa Interface Science Co., Ltd. Technical Presentation. Retrieved from <http://www.slideshare.net/scientificgear/fundamental-of-surface-tension>

L.G. (1999) Characterization of Cationic Surfactants (Report No. AR210e). Retrieved from www.kruss.de: https://www.kruss.de/fileadmin/user_upload/website/literature/kruss-ar210-en.pdf

Magin, G.B., Randall, L.E. (1960). *Review of Literature on Evaporation Suppression*. United States Department of the Interior Geological Survey. (Report No. 272C.) Retrieved from <http://pubs.usgs.gov/pp/0272c/report.pdf>

Manges, H., Crow, F.R. (1965). Evaporation Suppression by Chemical and Mechanical Treatments. *Proceedings of the Oklahoma Academy of Science for 1965*, 251-254.

Myers, D. (2006) *Surfactant Science and Technology*. Hoboken, NJ: John Wiley & Sons, Inc.

Prime, E., Leung, A., Tran, D., Gill, H., Solomon, D., Qiao, G., Dagley, I. (2012, June). *New technology to reduce evaporation from large water storages*. Canberra, Australia: National Water Commission.

Prime, E. L., Tran, D. N. H., Plazzer, M., Sunartio, D., Leung, A. H. M., Yiapanis, G., Solomon, D. H. (2012). Rational design of monolayers for improved water evaporation mitigation. *Colloids and Surfaces A: Physicochemical and Engineering Aspects*, 415, 47-58.

Roberts, W.J. (1957). Evaporation Suppression from Water Surfaces. *Transaction, American Geophysical Union*, 38(5), 740-744.

Rosen M.J. (2004) *Surfactants and interfacial phenomena*. Hoboken, NJ: John Wiley & Sons, Inc.

Salager, J-L. (2002). Surfactants types and uses. Retrieved March 8, 2015, from <http://www.nanoparticles.org/pdf/Salager-E300A.pdf>

Schramm, L.L., Stasiuk, E.N., Marangoni, D.G. (2003). Surfactants and their applications. *Annual Reports on the Progress of Chemistry, Section C*, 99, 3-48

Seager, R., Hoerling, M., Schubert, S., Wang, H., Lyon, B., Kumar, A. Henderson, N. (2015). Causes of the 2011-14 California drought. *Journal of Climate*, 28(18), 6997-7024.
Shah, M.M. (2014). Methods for calculation of evaporation from swimming pools and other water surfaces. *ASHRAE Transactions*, 120(2), 1-15

Sulek, M.W., Wasilewski, T., Kurzydowski, K., J. (2010). The Effect of Concentration on Lubricating Properties of Sodium Lauryl Sulfate and Ethoxylated Sodium Lauryl Sulfate. *Tribology Letters*, 40(3), 337-345

Time and Date AS. (2016). Past Weather in Daytona Beach, Florida, USA – July 2016. Retrieved from <http://www.timeanddate.com/weather/usa/daytona-beach/historic?month=7&year=2016>

Vargaftik, N. B., Volkob, B. N., Voljak, L.D. (1983). International Tables of the Surface Tension of Water. *Journal of Physical and Chemical Reference Data*, 12(3), 817-820.

Vuglinsky, V.S. (2009). Evaporation from open water surface and groundwater. *Hydrological Cycle Volume II, Encyclopedia of Water Sciences, Engineering and Technology Resources*. Paris, France: EOLSS Publications.

Wasekar, V. M., & Manglik, R. M. (2000). Pool boiling heat transfer in aqueous solutions of an anionic surfactant. *Journal of Heat Transfer*, 122(4), 708-715.

Yang, C., Wu, Y., Yuan, X., Ma, C. (1999). Study on bubble dynamics for nucleate pool boiling. *International Journal of Heat and Mass Transfer*, 43(2000), 203-208.

Zhang, J. T., & Wang, B. X. (2003). Study on the interfacial evaporation of aqueous solution of SDS surfactant self-assembly monolayer. *International Journal of Heat and Mass Transfer*, 46(26), 5059-5064.

Appendix A

Measured Values

Table A.1 Surface tension measurements of aqueous SLS solutions.

Concentration (PPM)	Reading (mN/m)	Repeat (mN/m)	Reading (mN/m)	Repeat (mN/m)
0	69	68.9	71.2	71.2
500	35.1	35.1	33.1	33.1
1000	28.9	28.9	28	28
1500	31.7	31.7	30.6	30.6
2000	33.6	33.6	33.1	33.1
2500	33.7	33.8	33.9	33.9
3000	33.4	33.5	-	-
3500	33.5	33.5	-	-

Table A.2 Surface tension measurements of aqueous EH-14 solutions

Concentration (PPM)	Reading (mN/m)	Repeat (mN/m)	Reading (mN/m)	Repeat (mN/m)
0	69.9	70	70.2	70.3
500	37.8	37.7	37.8	37.7
1500	32.1	32	32.4	32.4
2500	30	30.1	30.7	30.7
3500	30.2	30.3	30.2	30.2
4500	30.3	30.2	30.2	30.4
5500	29.8	29.9	-	-
6500	30.2	30.2	-	-

Table A.3 Surface tension measurements of aqueous SA-9 solutions

Concentration (PPM)	Reading (mN/m)	Repeat (mN/m)	Reading (mN/m)	Repeat (mN/m)
0	68.3	68.2	71.4	71.4
20	33.2	33.3	29.6	29.6
40	32.2	31.6	29.7	29.7
60	30.5	30	29.8	29.8
80	30.8	30.3	29.6	29.6
100	30.5	30.2	29.7	29.7

Table A.4 Natural evaporation mass loss measurements for aqueous SLS: Test 1

SLS Concentration (PPM)	After 24 hrs (g)	After 48 hrs (g)	After 72 hrs (g)	After 96 hrs (g)	After 120 hrs (g)
0	2.305	4.488	6.130	8.097	9.792
500	1.479	2.879	4.048	5.336	6.575
1000	1.757	3.424	4.734	6.250	7.613
1500	1.494	2.826	4.061	5.418	6.657
2000	1.486	2.801	4.079	5.438	6.656
2500	1.520	3.006	3.980	5.252	6.420

Table A.4 Natural evaporation mass loss measurements for aqueous SLS: Test 2

SLS Concentration (PPM)	After 24 hrs (g)	After 48 hrs (g)	After 72 hrs (g)	After 96 hrs (g)	After 120 hrs (g)
0	1.701	3.354	4.741	5.934	7.186
500	1.397	2.764	3.925	5.082	6.225
1000	1.436	2.812	3.957	5.077	6.232
1500	1.384	2.724	3.856	4.978	6.138
2000	1.367	2.635	3.714	4.793	5.899
2500	1.374	2.728	4.212	5.482	6.810

Table A.5 Natural evaporation mass loss measurements for aqueous SLS: Test 3

SLS Concentration (PPM)	After 24 hrs (g)	After 48 hrs (g)	After 72 hrs (g)	After 96 hrs (g)	After 120 hrs (g)
0	1.350	2.703	3.789	4.927	6.147
3000	1.212	2.424	3.396	4.484	5.604
3500	1.419	2.722	3.734	4.847	6.083

Table A.6 Natural evaporation mass loss measurements for aqueous SLS: Test 4

SLS Concentration (PPM)	After 24 hrs (g)	After 48 hrs (g)	After 72 hrs (g)	After 96 hrs (g)	After 120 hrs (g)
0	1.643	3.016	4.367	5.642	6.952
3000	1.238	2.242	3.487	4.560	5.599
3500	1.186	2.221	3.408	4.448	5.505

Table A.7 Natural evaporation mass loss measurements for aqueous EH-14: Test 1

EH-14 Concentration (PPM)	After 24 hrs (g)	After 48 hrs (g)	After 72 hrs (g)	After 96 hrs (g)	After 120 hrs (g)
0	-	3.283	-	7.277	8.920
500	-	3.595	-	6.215	7.600
1500	-	3.084	-	5.707	7.049
2500	-	3.050	-	5.590	6.849
3500	-	3.175	-	5.811	7.079
4500	-	3.254	-	5.899	7.213

Table A.8 Natural evaporation mass loss measurements for aqueous EH-14: Test 2

EH-14 Concentration (PPM)	After 24 hrs (g)	After 48 hrs (g)	After 72 hrs (g)	After 96 hrs (g)	After 120 hrs (g)
0	1.697	3.023	4.328	5.743	7.064
500	1.258	2.422	3.597	4.889	5.961
1500	1.238	2.386	3.521	4.762	5.829
2500	1.263	2.416	3.538	4.779	5.855
3500	1.250	2.406	3.529	4.765	5.857
4500	1.299	2.511	3.724	5.050	6.148

Table A.9 Natural evaporation mass loss measurements for aqueous EH-14: Test 3

EH-14 Concentration (PPM)	After 24 hrs (g)	After 48 hrs (g)	After 72 hrs (g)	After 96 hrs (g)	After 120 hrs (g)
0	2.009	3.515	5.906	7.511	9.324
500	1.727	3.313	4.905	6.568	8.227
1500	1.516	2.873	4.361	5.836	7.165
2500	1.596	3.028	4.531	6.223	7.725
3500	1.533	2.931	4.445	5.975	7.459
4500	1.487	2.878	4.355	5.897	7.167

Table A.10 Natural evaporation mass loss measurements for aqueous EH-14: Test 4

EH-14 Concentration (PPM)	After 24 hrs (g)	After 48 hrs (g)	After 72 hrs (g)	After 96 hrs (g)	After 120 hrs (g)
0	1.565	2.927	4.010	5.659	6.935
5500	1.325	2.771	3.807	4.859	5.989
6500	1.379	2.691	3.804	5.057	6.159

Table A.11 Natural evaporation mass loss measurements for aqueous EH-14: Test 5

EH-14 Concentration (PPM)	After 24 hrs (g)	After 48 hrs (g)	After 72 hrs (g)	After 96 hrs (g)	After 120 hrs (g)
0	1.415	3.002	4.156	5.290	6.434
5500	1.346	2.457	3.658	4.742	5.779
6500	1.234	2.421	3.604	4.717	5.803

Table A.12 Natural evaporation mass loss measurements for aqueous SA-9: Test 1

SA-9 Concentration (PPM)	After 24 hrs (g)	After 48 hrs (g)	After 72 hrs (g)	After 96 hrs (g)	After 120 hrs (g)
0	1.675	3.195	4.796	6.348	7.919
20	1.301	2.550	3.851	5.323	6.534
40	1.280	2.523	3.702	4.930	6.053
60	1.269	2.516	3.707	4.942	6.108
80	1.241	2.460	3.654	4.883	6.075
100	1.238	2.453	3.609	4.785	5.877

Table A.13 Natural evaporation mass loss measurements for aqueous SA-9: Test 2

SA-9 Concentration (PPM)	After 24 hrs (g)	After 48 hrs (g)	After 72 hrs (g)	After 96 hrs (g)	After 120 hrs (g)
0	1.485	3.096	4.372	5.582	6.803
20	1.265	2.487	3.630	4.785	5.922
40	1.423	2.839	4.156	5.452	6.722
60	1.357	2.668	3.932	5.196	6.448
80	1.240	2.444	3.592	4.774	5.941
100	1.294	2.583	4.025	5.377	6.810

Table A.14 Subcooled boiling evaporation measurements for aqueous SLS: Test 1

SLS Concentration (PPM)	Initial Mass* (g)	Final Mass* (g)	Mass Evaporated (g)
0	152.038	143.087	8.951
500	151.621	142.651	8.97
1000	151.635	143.583	8.052
1500	152.488	144.301	8.187
2000	151.32	142.061	9.259
2500	151.186	142.447	8.739

*Includes beaker dry mass.

Table A.15 Subcooled boiling evaporation measurements for aqueous EH-14: Test 1

EH-14 Concentration (PPM)	Initial Mass* (g)	Final Mass* (g)	Mass Evaporated (g)
0	151.914	142.9	9.014
500	151.649	142.1	9.549
1500	151.741	141.36	10.381
2500	152.257	141.428	10.829
3500	151.661	143.609	8.052
4500	151.447	143.455	7.992

*Includes beaker dry mass.

Table A.14 Subcooled boiling evaporation measurements for aqueous EH-14: Test 2

EH-14 Concentration (PPM)	Initial Mass* (g)	Final Mass* (g)	Mass Evaporated (g)
0	151.900	142.17	9.730
500	151.674	143.35	8.324
1500	151.755	142.343	9.412
2500	152.253	142.715	9.538
3500	151.653	143.472	8.181
4500	151.474	142.89	8.584

*Includes beaker dry mass.

Table A.15 Subcooled boiling evaporation measurements for aqueous SA-9: Test 1

SA-9 Concentration (PPM)	Initial Mass* (g)	Final Mass* (g)	Mass Evaporated (g)
0	154.447	146.210	8.237
20	154.095	145.643	8.452
40	152.973	144.182	8.791
60	154.448	145.313	9.135
80	154.639	146.087	8.552
100	153.611	144.851	8.760

*Includes beaker dry mass.

Table A.15 Subcooled boiling evaporation measurements for aqueous SA-9: Test 2

SA-9 Concentration (PPM)	Initial Mass* (g)	Final Mass* (g)	Mass Evaporated (g)
0	154.469	145.54	8.929
20	154.183	145.635	8.548
40	154.487	145.67	8.817
60	154.554	146.404	8.150
80	154.967	146.714	8.253
100	154.058	145.405	8.653

*Includes beaker dry mass.

Appendix B

Subcooled Boiling Phenomena Visualization

Turbidity and violent vapor release in the subcooled boiling tests were photographed. The EH-14 aqueous solutions became turbid as temperature approached its cloud point of 84 Celsius. The solution reversed the turbidity and became clear as the temperature cooled below 84 Celsius after completion of a boiling test. Figure B.1 shows an EH-14 aqueous solution above its cloud point.



Figure B.1 Aqueous EH-14 1000 PPM solution at 98 Celsius.

Some violent vapor release was seen with SLS and SA-9 solutions. The sudden eruption of vapor from the heated surface was caught with high speed photography as seen below for a 1000 PPM SLS solution in subcooled boiling. Two tests had to be repeated due to these types of vapor formation pushing liquid out of the beaker due to the high speed and force with which the vapor nuclei left the heated surface.



Figure B.2 Violent vapor release sequence of subcooled boiling 1000 PPM SLS solution.

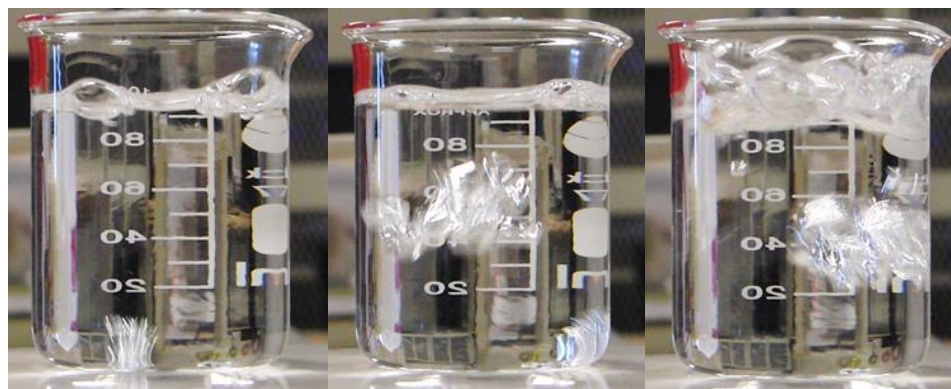


Figure B.3 Violent vapor release sequence of subcooled boiling 1000 PPM SLS solution.

The cause of this eruption, seen originating in the far images on the left of Figures B.2 and B.3 may be flash point. Flash point is the temperature at which the surfactant will ignite (Rosen, 2004). The flash point may be reached because of boiling hysteresis which is a thermal overshoot on the surface. The SLS and SA-9 monolayers may cause this hysteresis behavior by hindering convection near the heated surface.

Appendix C

Evaporation Rate Calculations

Natural Evaporation Calculations

Evaporation rate of water into air from a 100 mL beaker is calculated for three scenarios: still water and air at the interface with the air and water at the same temperature, convection of air over the water surface due to buoyancy caused by a temperature difference between the air and water, and forced convection over the water surface. Thermodynamic values for water vapor and air are taken from Cengel & Ghajar (2011) Table A-9: Properties of saturated water and Table A-15: Properties of air at 1 atm. The following conditions are used:

$T_{\infty} = 20^{\circ}\text{C}$, equilibrium room temperature as measured

Relative humidity = 50%, standard relative humidity in air conditioned room

$d = 0.05\text{m}$, diameter of the beaker as measured

$A = 0.00196\text{m}^2$, from diameter of the beaker

$P = 1$ atmosphere, reasonable assumption for laboratory

$C_{\text{vapor_at_surface}} = 0.0173 \text{ kg/m}^3$, density of saturated water vapor at 20°C

$C_{\text{water_vapor}_{\infty}} = 0.00865 \text{ g/m}^3$, density of water at 20°C and 50% relative humidity

Still water and air at interface: Diffusion

Using Equation 1-10, the mass diffusion coefficient is:

$$D_{H_2O-Air} = (1.87 * 10^{-10}) * \frac{T^{2.072}}{P} \text{ (m}^2/\text{s)}$$

$$D_{H_2O-Air} = (1.87 * 10^{-10}) * \frac{(293 \text{ K})^{2.072}}{(1 \text{ atm})} \text{ (m}^2/\text{s)}$$

$$D_{H_2O-Air} = 0.000024 \text{ (m}^2/\text{s)}$$

The concentration gradient is assumed to be linear and dx is assumed to be 0.1 m. Then plugging into Equation 1-9:

$$\begin{aligned}\dot{m}_{diff} &= D_{H_2O-Air} * A * \frac{dC_A}{dx} \\ \dot{m}_{diff} &= 0.000024 \left(\frac{m^2}{s}\right) * 0.00196(m^2) * \frac{0.0173 \left(\frac{kg}{m^3}\right) - 0.00865 \left(\frac{kg}{m^3}\right)}{0.1 (m)} \\ \dot{m}_{diff} &= 4.1 * 10^{-9} \left(\frac{kg}{s}\right) = \mathbf{0.015 \left(\frac{g}{hr}\right)}\end{aligned}$$

Thus, the expected evaporation rate for distilled water (without surfactant) if both the air and water are still at the interface is 0.015 g/hr.

Air movement due to buoyancy: Natural convective evaporation

Convection due to buoyancy will only occur if the water temperature is above the air temperature (Cengel & Ghajar, 2011). For the current study, the room temperature was measured at 20°C. Thus, a water temperature (T_s) of 27°C (300 K) was chosen as a practical maximum temperature the water may reach if the laboratory doors were opened to the Florida climate. The T_∞ was chosen to be a minimum of 20°C (293 K) as the temperature the room would return to after doors were closed. Starting with Equation 1-15:

$$Ra_L = \frac{g\beta(T_s - T_\infty)L_c^3}{\nu\alpha}$$

Where, $g = 9.81 \text{ m/s}^2$, $T_f = (T_s + T_\infty)/2 = (300 + 293)/2 = 297 \text{ K}$, $\beta = 1/T_f = 0.0034 \text{ (1/K)}$, $L_c = d/4 = 0.0125 \text{ (m)}$, $\nu = 0.000015 \text{ (m}^2/\text{s)}$, and $\alpha = 0.000021 \text{ (m}^2/\text{s)}$.

$$Ra_L = \frac{9.81 * 0.0034 * (300 - 293) * 0.0125^3}{0.000015 * 0.000021} = 1450$$

Then, for $k = 0.025$ (W/m*K) and assuming $n = 0.25$ and $C = 0.54$ for laminar natural convection over a horizontal surface (Cengel & Ghajar, 528), the natural convection heat transfer coefficient is found using Equation 1-14:

$$h_{heat,natural\ convection} = \frac{kCRa_L^n}{L_C}$$

$$h_{heat,natural\ convection} = \frac{0.025 \left(\frac{W}{m * K}\right) * 0.54 * 1450^{0.25}}{0.0125 (m)}$$

$$h_{heat,natural\ convection} = 6.7 \left(\frac{W}{m^2 * K}\right)$$

For air at 20°C, $c_p = 1007$ (J/kg) and $\rho = 1.204$ (kg/m³). Then the mass transfer coefficient is found with Equation 1-12:

$$h_{mass} = \frac{h_{heat}}{\rho c_p}$$

$$h_{mass} = \frac{6.7 \left(\frac{W}{m^2 * K}\right)}{1.204 \left(\frac{kg}{m^3}\right) * 1007 \left(\frac{J}{kg * K}\right)}$$

$$h_{mass} = 0.0055 \left(\frac{m}{s}\right)$$

The density at the surface is the that of 100% water vapor, $\rho_{A,s} = 0.0173$ (kg/m³). The density of water vapor in air at relative humidity of 50% is $\rho_{A,\infty} = 0.009$ (kg/m³) and $A_s = 0.00196$ (m²). Then, Equation 1-13 yields

$$\dot{m}_{conv} = h_{mass} A_s (\rho_{A,s} - \rho_{A,\infty}) \left(\frac{kg}{s}\right)$$

$$\dot{m}_{natural\ convection} = 0.0055 \left(\frac{m}{s}\right) * 0.00196 (m^2) * \left(0.0173 \left(\frac{kg}{m^3}\right) - 0.00865 \left(\frac{kg}{m^3}\right)\right)$$

$$\dot{m}_{natural\ convection} = 9.3 * 10^{-8} \left(\frac{kg}{s}\right)$$

$$\dot{m}_{natural\ convection} = \mathbf{0.34} \left(\frac{g}{hr}\right)$$

Air movement due to currents: Forced convective evaporation

For forced convection from the air conditioning currents in the room, the temperature of the air and water was assumed to both be 20°C. The velocity of the air generated by air conditioning over the beakers located in the corner of the laboratory was given a conservative estimate of 1 m/s. For T=20°C, $L_c = d/4 = 0.0125$ (m), $\nu = 0.000015$ (m²/s), and $\alpha = 0.000021$ (m²/s). Then,

$$Re_L = \frac{L_c * V}{\nu} = \frac{0.0125 \text{ (m)} * 1 \left(\frac{\text{m}}{\text{s}}\right)}{0.000015 \left(\frac{\text{m}^2}{\text{s}}\right)} = 833$$

$$Pr = \frac{\nu}{\alpha} = \frac{0.000015 \left(\frac{\text{m}^2}{\text{s}}\right)}{0.000021 \left(\frac{\text{m}^2}{\text{s}}\right)} = 0.71$$

Plugging Re_L and Pr into Equation 1-16

$$h_{heat,forced\ convection} = 0.664 Re_L^{0.5} Pr^{\frac{1}{3}} \frac{k}{L_c}$$

$$h_{heat,forced\ convection} = 0.664 * 833^{0.5} * 0.71^{\frac{1}{3}} * \frac{0.025 \left(\frac{\text{W}}{\text{m} * \text{K}}\right)}{0.0125 \text{ (m)}}$$

$$h_{heat,forced\ convection} = 34.2 \left(\frac{\text{W}}{\text{m}^2 * \text{K}}\right)$$

Using the Chilton-Colburn Analogy (Equation 1-12):

$$h_{mass} = \frac{h_{heat}}{\rho c_p} \left(\frac{\text{m}}{\text{s}}\right)$$

$$h_{mass,forced\ convection} = \frac{34.2 \left(\frac{\text{W}}{\text{m}^2 * \text{K}}\right)}{1.204 \left(\frac{\text{kg}}{\text{m}^3}\right) * 1007 \left(\frac{\text{J}}{\text{kg} * \text{K}}\right)}$$

$$h_{mass} = 0.028 \left(\frac{\text{m}}{\text{s}}\right)$$

Then Equation 1-13 yields,

$$\dot{m}_{conv} = h_{mass} A_s (\rho_{A,s} - \rho_{A,\infty}) \left(\frac{kg}{s} \right)$$

$$\dot{m}_{forced_convection} = 0.028 \left(\frac{m}{s} \right) * 0.00196 (m^2) * \left(0.0173 \left(\frac{kg}{m^3} \right) - 0.00865 \left(\frac{kg}{m^3} \right) \right)$$

$$\dot{m}_{forced_convection} = 4.7 * 10^{-7} \left(\frac{kg}{s} \right) = 1.7 \left(\frac{g}{hr} \right)$$

Summary

The values calculated for mass flux by diffusion, buoyancy (natural convection), or air currents (forced convection) are respectively: 0.015 g/hr, 0.34 g/hr, and 1.7 g/hr.

The effects from forced and natural convection on the current study should be lowered significantly but not eliminated by the muslin gauze covering. Thus, the actual mass flux from the solutions should be higher than the 0.015 g/hr and significantly lower than 0.34 g/hr.

Subcooled Boiling Evaporation Calculations

The heat flux and evaporation rate for boiling distilled water without surfactants is calculated here as an estimate for the current study subcooled boiling experiments.

Thermodynamic values for water vapor and air are taken from Cengel & Ghajar (2011)

Table A-9: Properties of saturated water. For pure water at saturation temperature: $T_{sat} =$

100 C, $\sigma = 0.0589$ N/m, $\rho_l = 957.9$ kg/m³, $\rho_v = 0.6$ kg/m³, $Pr_l = 1.75$, $h_{fg} = 2257000$ J/kg,

$\mu_l = 0.000282$ kg/m*s, and $c_{pl} = 4217$ J/kg*K. For the current study with the hotplate set

at its highest setting and glass beaker as the heated surface, the $T_s = 116.91$ C. The $C_{s,f}$

and n are assumed to be 0.013 and 1 respectively (Cengel & Ghajar, 2011). Plugging these values into Equation 1-20:

$$\dot{q}_{nucleate} = 0.282 * 2257 * \left[\frac{9.81 * (957.9 - 0.6)}{0.0589} \right]^{\frac{1}{2}} * \left[\frac{4217 * (16.91)}{0.013 * 2257000 * 1.75^1} \right]^3$$

Yields,

$$\dot{q}_{nucleate} = 6.8 * 10^5 \text{ W/m}^2$$

The diameter of the glass beaker is 0.05 m. Thus, $A = \pi d^2/4 = 0.00196 \text{ m}^2$ and using

Equation 1-21:

$$\dot{m}_{evaporation} = \frac{0.00196 * 6.8 * 10^5}{2257000} = 5.9 * 10^{-4} \frac{kg}{s} = 35.5 \frac{g}{min}$$

This value is a general estimate of the evaporation rate because this study deals with subcooled boiling.